



Linking microbial populations and geochemical processes in soils, mine tailings, and geothermal environments

by Richard Eugene Macur

A dissertation submitted in partial fulfillment of the requirements for the degree of Doctor of Philosophy in Land Resources and Environmental Sciences MONTANA STATE UNIVERSITY  
Bozeman, Montana

Montana State University

© Copyright by Richard Eugene Macur (2004)

Abstract:

The primary goal of this work was to identify and characterize the microbial populations responsible for transformations of As and 2,4-D in soils and waters. Chemical, spectroscopic, and microscopic techniques were used to characterize the aqueous and solid phase geochemistry of soils, mine tailings, and a geothermal spring. The role of specific microbial populations in these systems was examined using cultivation-independent molecular methods [total DNA extraction, 16S rDNA amplification, denaturing gradient gel electrophoresis (DGGE), and sequence analysis] coupled with either characterization of microorganisms isolated from the same systems, or inference of physiological characteristics from (i) closely related (16S rDNA sequence) cultured microorganisms and (ii) the geochemical environments in which they were detected.

The microbial reduction of As(V) to As(III) and the subsequent effects on As mobilization in contaminated mine tailings was examined under transport conditions. Enhanced elution of As from mine tailings apparently resulted from the enrichment of aerobic As(V)-reducing *Caulobacter leidyi*, *Sphingomonas yanoikuyae*, and *Rhizobium loti* -like populations after liming.

Arsenite was rapidly oxidized to As(V) via microbial activity in unsaturated Madison River Valley soil columns. Eight aerobic heterotrophic bacteria with varying As redox phenotypes were isolated from these columns. Three isolates, identified as *Agrobacterium tumefaciens*, *Pseudomonas fluorescens*, and *Variovorax paradoxus* -like organisms, were As(III) oxidizers and all were apparently important members of the soil microbial community responsible for net As(III) oxidation.

Successional changes in microbial communities colonizing an As-rich acid-sulfate-chloride geothermal spring stream channel in Norris Geyser Basin of Yellowstone National Park were examined. Enhanced As(III) oxidation correlated in time and space with the appearance of three *Hydrogenobaculum* -like populations. The formation of an As(V)-rich hydrous-ferric-oxide mat correlated with the detection of *Thiomonas*, *Acidimicrobium*, and *Metallosphaera* —like populations whose nearest cultivated relatives (based on 16S rDNA sequence) were Fe-oxidizers.

Fingerprints of microbial communities (DGGE) established under increasing concentrations of 2,4-D (0 - 500 mg kg<sup>-1</sup>) in batch soil microcosms showed that at least 100 mg kg<sup>-1</sup> 2,4-D was required to obtain apparent shifts in community structure. The microbial community selected at high 2,4-D concentrations was predominantly composed of *Burkholderia* -like populations, which harbored homologs of *tfdA* genes.

LINKING MICROBIAL POPULATIONS AND GEOCHEMICAL PROCESSES  
IN SOILS, MINE TAILINGS, AND GEOTHERMAL ENVIRONMENTS

by

Richard Eugene Macur

A dissertation submitted in partial fulfillment  
of the requirements for the degree

of

Doctor of Philosophy

in

Land Resources and Environmental Sciences

MONTANA STATE UNIVERSITY  
Bozeman, Montana

January 2004

0378  
M1193

APPROVAL

of a dissertation submitted by

Richard Eugene Macur

This dissertation has been read by each member of the dissertation committee and has been found to be satisfactory regarding content, English usage, format, citations, bibliographic style, and consistency, and is ready for submission to the College of Graduate Studies.

William P. Inskeep, Ph.D. William P. Inskeep 1/13/04  
(Signature) Date

Approved for the Department Land Resources and Environmental Sciences

Jon M. Wraith, Ph.D. Jon M. Wraith 1-14-04  
(Signature) Date

Approved for the College of Graduate Studies

Bruce R. McLeod, Ph.D. Bruce R. McLeod 1-14-04  
(Signature) Date

## STATEMENT OF PERMISSION TO USE

In presenting this dissertation in partial fulfillment of the requirements for a doctoral degree at Montana State University, I agree that the Library shall make it available to borrowers under rules of the Library. I further agree that copying of this dissertation is allowable only for scholarly purposes, consistent with "fair use" as prescribed in the U.S. Copyright Law. Requests for extensive copying or reproduction of this dissertation should be referred to Bell & Howell Information and Learning, 300 North Zeeb Road, Ann Arbor, Michigan 48106, to whom I have granted "the exclusive right to reproduce and distribute my dissertation in and from microform along with the non-exclusive right to reproduce and distribute my abstract in any format in whole or in part".

Signature



Date

1/12/04

## ACKNOWLEDGEMENTS

Foremost, I give praise and thanks to my Lord and Savior, Jesus Christ, the Maker of heaven and earth. I owe Him my all.

I also express my deep gratitude to my mentor Dr. Bill Inskeep. His guidance, patience, and extensive help have enabled me to attain my goal of becoming a Ph.D. I thank Dr. Tim McDermott and Dr. Dave Ward whose guidance and instruction have also contributed to my success. My sincere appreciation also goes to my committee members Dr. Jon Wraith and Dr. Warren Jones. I greatly appreciate the help and friendship of the many co-workers that have been my daily companions during the last five years. These include Dr. Heiko Langner, Dr. Greg Colores, Dr. Mark Burr, Dr. Colin Jackson and many others.

I express deep appreciation to my dear wife Debbie, and two sons, David and Daniel, who have made many sacrifices so I could pursue a doctorate. I also thank all my other family members, Tata, Mama, Chrissy, Juliet, Dad, Mom, Dave, Cindy, Dave, Pam, Nick, and Cheyenne for their love. In addition, I thank all my brothers and sisters in the Lord who have loved me and prayed for me over the years.

## TABLE OF CONTENTS

	Page
LIST OF TABLES .....	viii
LIST OF FIGURES .....	ix
ABSTRACT.....	xi
1. INTRODUCTION .....	1
REFERENCES CITED.....	7
2. MICROBIAL POPULATIONS ASSOCIATED WITH THE REDUCTION AND ENHANCED MOBILIZATION OF ARSENIC IN MINE TAILINGS .....	8
Introduction.....	8
Materials and Methods.....	10
Sample Collection and Chemical Characterization .....	10
Column Experiments .....	11
As(V) Reducing Isolates.....	13
DNA Extraction and Purification.....	14
Partial 16S rDNA Amplification and Denaturing Gradient Gel Electrophoresis (DGGE).....	15
PCR Amplification and DNA Sequencing of DGGE Bands .....	16
Full Length 16S rDNA Amplification and Sequencing.....	16
Results and Discussion .....	17
Column Experiments .....	17
Molecular Analysis.....	22
Isolates .....	23
As(V) Reduction Kinetics of Isolates .....	25
Mechanisms of As(V) Reduction and Implications for As Cycling.....	28
REFERENCES CITED.....	31
3. BACTERIAL POPULATIONS ASSOCIATED WITH THE OXIDATION AND REDUCTION OF ARSENIC IN AN UNSATURATED.....	35
Introduction.....	35
Materials and Methods.....	37
Column Experiments .....	37
Isolation and Characterization of As-Transforming Aerobic Heterotrophs.....	39
DNA Extraction, PCR, and DGGE Analysis.....	41

## TABLE OF CONTENTS - CONTINUED

	Page
Full Length 16S rDNA Amplification and Sequencing of Isolates .....	43
Amplification, Hybridization, and Phylogeny of <i>ArsC</i> genes .....	43
Results and Discussion .....	45
Column Experiments .....	45
Molecular Analysis .....	45
Isolates .....	49
Correlating Isolates with Column Populations .....	51
Rates of As Transformation by Bacteria .....	52
Mechanisms of As Oxidation/Reduction .....	54
Implications for As Cycling in Soils .....	57
REFERENCES CITED .....	60
 4. LINKING GEOCHEMICAL PROCESSES WITH MICROBIAL COMMUNITY ANALYSIS: SUCCESSIONAL DYNAMICS IN AN ARSENIC-RICH ACID-SULFATE-CHLORIDE GEOTHERMAL SPRING .....	 65
Introduction .....	65
Materials and Methods .....	68
Site Description and Sampling Procedures .....	68
Aqueous Phase Chemistry .....	69
Characterization of Solid Phases .....	70
Molecular Analysis of Microbial Communities .....	71
Thermodynamic Calculations .....	73
Results and Discussion .....	74
Aqueous Temperature and Chemistry .....	74
Aqueous Chemistry of Arsenic .....	77
Sulfur Species .....	79
Dissolved Inorganic C .....	80
Soluble Fe, H <sub>2</sub> , and O <sub>2</sub> Profiles .....	80
Characterization of Microbial Mats and Associated Solid Phases .....	81
Fe Successional Changes .....	85
Microbial Populations Detected in Parent Material .....	88
Initial Colonization by Hydrogenobaculum-like Organisms .....	88
Hyperthermophiles .....	94
Formation of HFO Microbial Mats .....	96
Novel Organisms .....	97

## TABLE OF CONTENTS - CONTINUED

	Page
Microbially Mediated As(III) Oxidation .....	99
Energetics and Primary Production .....	100
Microbial Species Distribution and Community Development .....	103
REFERENCES CITED.....	105
5. 2,4-D CONCENTRATION DRIVEN SHIFTS IN SOIL MICROBIAL POPULATIONS ASSOCIATED WITH 2,4-D DEGRADATION UNDER BATCH AND TRANSPORT CONDITIONS	
Introduction.....	111
Materials and Methods.....	113
Soil .....	113
Enrichment of 2,4-D Degrading Microorganisms Under Batch Conditions.....	114
Enrichment of 2,4-D Degrading Microorganisms Under Transport Conditions .....	115
Enumeration and Isolation of 2,4-D Degrading Microorganisms .....	116
Nucleic Acid Extraction and 16S rDNA Sequence Analysis .....	117
PCR Amplification and Sequencing of Near-Full Length 16S rRNA Genes.....	118
PCR Amplification and Sequencing of <i>tfdA</i> Genes .....	119
Results and Discussion .....	119
2,4-D Degradation Under Batch and Transport Conditions .....	119
MPN Determinations .....	121
2,4-D Degrading Isolates .....	123
Molecular Analysis of Bacteria Selected Under Batch Conditions.....	125
Molecular Analysis of Bacteria Selected Under Transport Conditions .....	129
<i>tfdA</i> Harboring Isolates .....	130
Diversity of 2,4-D Degrading Bacteria.....	131
REFERENCES CITED.....	134
6. SUMMARY .....	137
REFERENCES CITED.....	146

## LIST OF TABLES

Table	Page
2.1 Chemistry of Effluent from RT Columns .....	18
2.2 Phylogenetic Affiliation and Characteristics of Isolates Obtained from RT .....	24
3.1 Characteristics of Isolates Obtained from Madison River Soil .....	50
4.1 Chemical Composition of Succession Spring Source Water .....	76
4.2 Microorganisms Detected in Succession Spring.....	91
4.3 Energetics of Possible Chemical Reactions in Succession Spring Source Water .....	102
5.1 Microorganisms Detected and Isolates Obtained from 2,4-D Treated Soil.....	124

## LIST OF FIGURES

Figure	Page
2.1 Redox Potentials and As Concentrations in Aerobic RT Columns .....	19
2.2 Redox Potentials and As Concentrations in an Anaerobic RT Column .....	21
2.3 Denaturing Gradient Gel of RT Treatments .....	21
2.4 As Transforming Characteristics of Isolates Obtained from RT .....	27
3.1 As Concentrations in Effluent from Madison River Soil Columns .....	46
3.2 Denaturing Gradient Gel of Madison River Soil Treatments .....	47
3.3 As Transforming Characteristics of Isolates Obtained from Madison River Soil .....	53
3.4 <i>ArsC</i> Hybridizations to Isolate DNA .....	56
4.1 Aqueous Chemistry of Succession Spring Source Water .....	75
4.2 As(III) Oxidation Rate Constants as a Function of Time and Position in Succession Spring .....	78
4.3 Progression of Microbial Mats in Succession Spring .....	78
4.4 Photographs of Microbial Mats in Succession Spring .....	82
4.5 SEM Images of Yellow Mat .....	83
4.6 SEM Images of As-Rich HFO Mat .....	86
4.7 Denaturing Gradient Gels of PCR Products Obtained from Succession Spring Using Bacterial Primers .....	89
4.8 Denaturing Gradient Gels of PCR Products Obtained from Succession Spring Using Archaeal Primers .....	90

## LIST OF FIGURES - CONTINUED

Figure	Page
5.1 Application and Degradation of 2,4-D in Soil Batch Treatments.....	120
5.2 Application and Degradation of 2,4-D in Soil Column Treatments .....	122
5.3 Most Probable Numbers of 2,4-D Degrading Bacteria in Soil Batch Treatments .....	122
5.4 Denaturing Gradient Gels of PCR Products Obtained from 2,4-D Treated Soil Batches .....	126
5.5 Denaturing Gradient Gels of PCR Products Obtained from 2,4-D Treated Soil Columns and Batches .....	128

## ABSTRACT

The primary goal of this work was to identify and characterize the microbial populations responsible for transformations of As and 2,4-D in soils and waters. Chemical, spectroscopic, and microscopic techniques were used to characterize the aqueous and solid phase geochemistry of soils, mine tailings, and a geothermal spring. The role of specific microbial populations in these systems was examined using cultivation-independent molecular methods [total DNA extraction, 16S rDNA amplification, denaturing gradient gel electrophoresis (DGGE), and sequence analysis] coupled with either characterization of microorganisms isolated from the same systems, or inference of physiological characteristics from (i) closely related (16S rDNA sequence) cultured microorganisms and (ii) the geochemical environments in which they were detected.

The microbial reduction of As(V) to As(III) and the subsequent effects on As mobilization in contaminated mine tailings was examined under transport conditions. Enhanced elution of As from mine tailings apparently resulted from the enrichment of aerobic As(V)-reducing *Caulobacter leidyi*, *Sphingomonas yanoikuyae*, and *Rhizobium loti*-like populations after liming.

Arsenite was rapidly oxidized to As(V) via microbial activity in unsaturated Madison River Valley soil columns. Eight aerobic heterotrophic bacteria with varying As redox phenotypes were isolated from these columns. Three isolates, identified as *Agrobacterium tumefaciens*, *Pseudomonas fluorescens*, and *Variovorax paradoxus*-like organisms, were As(III) oxidizers and all were apparently important members of the soil microbial community responsible for net As(III) oxidation.

Successional changes in microbial communities colonizing an As-rich acid-sulfate-chloride geothermal spring stream channel in Norris Geyser Basin of Yellowstone National Park were examined. Enhanced As(III) oxidation correlated in time and space with the appearance of three *Hydrogenobaculum*-like populations. The formation of an As(V)-rich hydrous-ferric-oxide mat correlated with the detection of *Thiomonas*, *Acidimicrobium*, and *Metallosphaera*-like populations whose nearest cultivated relatives (based on 16S rDNA sequence) were Fe-oxidizers.

Fingerprints of microbial communities (DGGE) established under increasing concentrations of 2,4-D ( $0 - 500 \text{ mg kg}^{-1}$ ) in batch soil microcosms showed that at least  $100 \text{ mg kg}^{-1}$  2,4-D was required to obtain apparent shifts in community structure. The microbial community selected at high 2,4-D concentrations was predominantly composed of *Burkholderia*-like populations, which harbored homologs of *tfdA* genes.

## CHAPTER 1

## INTRODUCTION

Geochemical processes are often inextricably linked with the activity of microbial communities in soil and water environments. The geochemical environment controls which microorganisms may grow or survive by defining the bioavailability of specific chemical constituents including essential nutrients and toxic elements. Conversely, microorganisms alter their surrounding chemical environment as they carry out metabolic and physiologic functions necessary for growth and survival. At a minimum, microbial activity involves the uptake of nutrients, the release of cellular by-products, and the exchange of compounds associated with energy conservation. Microorganisms influence their microenvironment in many other significant ways including the release of siderophores that mobilize metals (e.g., 1), detoxification reactions which result in transformation of toxic compounds (e.g., 2), exudation of organic chemicals including biofilm formation (e.g., 3) and release of protons. In essence, the geochemical environment is a primary factor controlling microbial species distribution while simultaneously the resident microorganisms are important mediators of the geochemical environment.

The role of specific microbial populations must be considered to accurately predict speciation and fate of many chemical constituents in soils and waters. The use of traditional cultivation methods to identify dominant microbial populations has been problematic since cultivation approaches may not capture the organisms important in the

actual physical-chemical environments (4). With the advent of molecular techniques (e.g., amplification and sequencing of 16S rRNA genes), it is now possible to assess the predominant microbial populations in natural samples without cultivation bias. Coupling traditional cultivation with molecular approaches can be used to more accurately describe the distribution and function of microorganisms in soils and natural waters. In some cases, 16S rDNA sequence analysis of environmental samples can be used to suggest the function of uncultured organisms by inferring physiological attributes from phylogenetically related characterized organisms. However, examples exist where such phylogenetic inference is inadequate for defining the physiology of naturally occurring microorganisms. For example, closely related *Thiomonas* strains exhibit different arsenic (As) transforming capabilities under the same conditions (5). Moreover, numerous 16S rDNA sequences identified in soil-water systems do not have closely related cultivated organisms from which to infer microbial properties (6, 7, also see Chapter 4, Novel Organisms section).

The primary goal of the research conducted during my Ph.D. program was to identify microbial populations responsible for observed chemical transformations of contaminants in soils, mine tailings, and geothermal springs using a combination of molecular, cultivation, and chemical characterization tools. The function of specific populations detected using cultivation-independent 16S rDNA sequence analysis was determined by cultivating microorganisms with identical 16S rDNA sequences and characterizing their chemical transforming properties. In the geothermal spring study, function of populations detected with 16S analysis was inferred from the co-occurrence

of specific geochemical processes with the appearance of specific microbial populations. The use of these strategies to identify microbial populations associated with chemical processes occurring *in situ* has provided an important methodological approach for unraveling the complex biological interactions that govern the distribution of important chemical species in soil-water environments.

The research presented in this thesis demonstrates the application of this conceptual approach to understanding several microbially mediated chemical processes in soil and water systems. Specifically, this work was focused on the behavior of arsenic (As) and 2,4-dichlorophenoxyacetic acid (2,4-D) in soil-water systems, two very different, yet important priority environmental pollutants. Arsenic is a highly toxic metalloid, ubiquitous in the environment and often concentrated in mine tailings and geothermal systems. Potentially harmful levels have also been detected in many drinking water sources throughout the world. Currently, the largest mass poisoning in human history is taking place in Bangladesh and surrounding areas, where As laden ground waters are being consumed by millions of people (8). 2,4-D is a chlorinated organic herbicide utilized extensively for broadleaf control throughout the world. The Montana Department of Agriculture and the U.S. Geological Survey have conducted several monitoring programs and have found significant amounts of 2,4-D in ground waters throughout the U.S., including Montana (9, 10). Both As and 2,4-D are subject to microbial interactions that mediate their chemical speciation and subsequent behavior in soils and waters. Understanding processes that control the fate and transport of these important types of contaminants is critical for successfully managing impacted

ecosystems. In addition, understanding the behavior of these compounds may help us to predict the behavior of other inorganic and chlorinated aromatic contaminants in the environment.

Increased interest in the biogeochemical pathways controlling As distribution has resulted from epidemiological studies indicating that relatively low levels of As can impair human health (11). These findings have caused the U.S. EPA to decrease the maximum contaminant level in drinking water from 50 ppb to 10 ppb. The role of microorganisms in As cycling in the environment has received considerable attention because it is thought that microbially mediated transformations of As may be the most important factor controlling As speciation. The speciation of As is important because different As species exhibit variation in solubility, mobility, bioavailability, and toxicity. Chapters two, three, and four of this dissertation describe three separate studies focused largely on the microbial populations important in As oxidation-reduction reactions in three different geochemical environments: mine tailings, unsaturated agricultural soils, and geothermal springs. Although each individual study has provided meaningful insight about microbial processes important in As-cycling, observations across different environments provides necessary data for exploring similarities and patterns useful for predictive purposes.

My initial research effort, fully described in chapter two, was to characterize the As redox activity of aerobic microbial populations residing in mine tailings. This was accomplished by utilizing both molecular and traditional isolation techniques to identify dominant microbial populations present in the mine tailings, and then, correlating these

populations to observed As transformations. The results demonstrated that microbially mediated arsenate [As(V)] reduction was important under aerobic conditions and that this process enhanced the leaching potential of As. In the study presented in chapter three, I examined the diversity and relevance of As-transforming microbial populations resident in an As-contaminated agricultural soil. This work showed that bacteria capable of either oxidizing arsenite [As(III)] or reducing As(V) for apparent detoxification purposes coexist in soils, and that identification of microorganisms based solely on 16S rDNA sequence may not be sufficient for predicting the As transforming capabilities of specific bacterial populations.

The goal of the study described in chapter four was to monitor changes in aqueous and solid phase geochemistry, and microbial community structure associated with initial colonization of an acid-sulfate-chloride geothermal spring in Norris Geyser Basin, Yellowstone National Park. The co-occurrence of specific geochemical processes with the appearance of specific microbial populations was used to infer the physiology and ecological role of microorganisms detected using molecular methods. Dr. Heiko Langner, a postdoctoral fellow in Dr. Inskeep's laboratory, initiated this project and led much of the effort to collect aqueous chemical field data. During this time, my work focused on molecular characterization of the spring. With his departure after the field season, I assumed the responsibilities of leading and completing the project. The objectives of this study were to; (i) correlate the distribution of bacterial and archaeal sequences in time and space with changes in temperature and geochemical energy gradients, (ii) identify microorganisms responsible for rapid rates of *in situ* As(III) oxidation, and (iii) determine

the microorganisms and processes responsible for the formation of As-rich hydrous ferric oxide (HFO) mats. Understanding microbial processes associated with the formation of HFO phases is important primarily due to their extremely high capacity to sequester As, and the fact that HFO phases are important in controlling the mobility of As in many natural water systems. The suite of complementary analyses included the 16S rDNA molecular fingerprinting technique, denaturing gradient gel electrophoresis (DGGE) coupled with sequence analysis, and a variety of chemical, microscopic, and spectroscopic techniques.

Microorganisms also play a crucial role in the degradation of chlorinated organic compounds in soils and waters. In the study presented in chapter five, I examined the effects of 2,4-D application rate and hydrodynamic environment on the diversity of microbial populations associated with 2,4-D degradation in an agricultural soil. Molecular techniques were used in combination with traditional isolation and characterization to describe the activity of the dominant 2,4-D degrading microbial populations. The role of specific functional genes associated with 2,4-D degradation in these organisms was also investigated.

These studies serve as significant contributions to our understanding of microbial processes controlling the chemical speciation of important contaminants in various environments. Coupling 16S rDNA based molecular techniques with traditional methods was shown to be effective in most cases for elucidating the role of specific microbial populations involved in geochemical transformations of As and the degradation of 2,4-D.

## REFERENCES CITED

1. Cornelis, P., and S. Matthihs. 2002. Diversity of siderophore-mediated iron uptake systems in fluorescent pseudomonads: not only pyoverdines. *Environ. Microbiol.* 4:787-798.
2. Silver, S., 1996. Bacterial resistances to toxic metal ions-a review. *Gene.* 179:9-19.
3. Abraham, W.R., B. Nogales, P.N. Golyshin, D.H. Pieper, and K.N. Timmis. 2002. Polychlorinated biphenyl-degrading microbial communities in soils and sediments. *Curr. Opin. Microbiol.* 5:246-253.
4. Dunbar, J., S. White, and L. Forney. 1997. Genetic diversity through the looking glass: effect of enrichment bias. *Appl. Environ. Microbiol.* 63:1326-1331.
5. Bruneel, O., J.C. Personne, C. Casiot, M. Leblanc, F. Elbaz-Poulichet, B.J. Mahler, A. Le Fleche, and P.A.D. Grimont. 2003. Mediation of arsenic oxidation by *Thiomonas* sp. in acid-mine drainage (Carnoules, France). *J. Appl. Microbiol.* 95:492-499.
6. Inskeep, W.P., R.E. Macur, G. Harrison, B.C. Bostick, and S. Fendorf. 2003. Microbial mineralization of As(V)-hydrous ferric oxyhydroxide mats in an acid-sulfate-chloride geothermal spring of Norris Geyser Basin, Yellowstone National Park. *Geochim. Cosmochim. Acta.* (in press).
7. Jackson, C.R., H.W. Langner, J. Donahoe-Christiansen, T.R. McDermott, and W.P. Inskeep, 2001. Molecular analysis of microbial community structure in an arsenite-oxidizing acidic thermal spring. *Environ. Microbiol.* 3:532-542.
8. Betts, K.S. 2001. Developing a good solution for arsenic. *Environ. Sci. Technol.* 35:415A-416A.
9. DeLuca, T., J. Larson, L. Torma, and G. Algard. 1989. A survey of pesticide residues in ground water in Montana. Tech. Report 89-1. Montana Dept. of Agric., Helena, MT.
10. Clark, D.W. 1990. Pesticides in soils and groundwater in selected irrigated agricultural areas near Havre, Ronan, and Huntley, Montana, U.S.G.S. Water Resources Report 90-4023, Helena, MT.
11. Smith, A.H., M.L. Biggs, L. Moore, R. Haque, C. Steinmaus, J. Chung, A. Hernandez, and P. Lopipero. 1999. Cancer risks from arsenic in drinking water: Implications for drinking water standards. p. 191-200. In *Arsenic Exposure and Health Effects*. Chappell W., Abernathy C.O. and Calderon R.L. (Ed's.), Elsevier, NY.

## CHAPTER 2

MICROBIAL POPULATIONS ASSOCIATED WITH THE REDUCTION AND  
ENHANCED MOBILIZATION OF ARSENIC IN MINE TAILINGSIntroduction

Microorganisms possess a variety of mechanisms for reducing As(V) and oxidizing As(III) (1-4). Transformation of As by microorganisms has important environmental implications because As(V) and As(III) have different sorption and toxicological characteristics; As(III) is often considered the more mobile and toxic species and thus more problematic regarding contamination of natural waters (5-7). Reduction of As(V) to As(III) in anoxic environments is thought to occur primarily by dissimilatory reduction where microorganisms utilize As(V) as a terminal electron acceptor for anaerobic respiration (8, 9). To date, dissimilatory reduction has been characterized in at least seven bacteria; *Sulfurospirillum barnesii*, *Bacillus arsenicoselenatis*, *B. selenitireducens*, *S. arsenophilum*, *Desulfotomaculum auripigmentum*, *Chrysiogenes arsenatis*, and *Desulfomicrobium* strain Ben-RB (1, 10, 11), which represent genera scattered throughout the bacterial domain. In addition, dissimilatory reduction of As(V) has been observed in two hyperthermophilic archaea; *Pyrobaculum arsenaticum* and *P. aerophilum* (12). Microorganisms may also possess reduction mechanisms that are not coupled to respiration, but instead are thought to impart As resistance (2, 13, 14). Enzymes involved in the detoxification pathway are transcribed by the *ars* operon. Homologues of the *ars* operon have been discovered in the *Pseudomonas*, *Bacillus*, *Klebsiella*, *Enterobacter*, *Citrobacter*, *Staphylococcus*,

*Salmonella*, *Thiobacillus*, *Yersinia* and *Escherichia* genera (13-18); genotypes that also are scattered throughout the bacterial domain. Microorganisms which express As resistance genes are able to withstand higher concentrations of As through the intracellular reduction of As(V) and the subsequent excretion of As(III) into the surrounding media. It is thought that this pathway may function in aerobic as well as anaerobic environments (10, 11), and may contribute to apparent nonequilibrium conditions where As(III) has been often observed in oxic surface waters (19, 20). Although it is likely that bacteria in soil, especially at As-contaminated sites, possess As detoxification pathways, to our knowledge, the effect of aerobic As(V) reducing bacteria on As behavior in soils has not yet been presented in the literature.

Liming of acidic mine tailings is recognized as an effective method for immobilizing trace metals and promoting plant establishment (21). However, as demonstrated by Jones et al. (22), liming may also result in enhanced As mobilization due to the pH dependence of As sorption reactions. The work presented here is an extension of the study conducted by Jones et al. (22), wherein our primary objective was to examine the effect of microbial processes on As behavior in mine tailings. We hypothesized that microbial reduction of As(V) may enhance As mobilization in mine tailings and that liming may impact the populations and activities of As(V)-reducing microorganisms. These hypotheses were tested by: (i) examining the affect of microbial As(V) reduction on mobilization of As in mine tailings under column transport conditions, and by (ii) using molecular and traditional cultivation techniques to identify microorganisms responsible for As(V) reduction in the mine tailings. Column transport experiments were designed to observe relationships among pH (limed vs unlimed

treatments), redox potential (Pt-electrode), dissolved As species, and corresponding shifts in microbial populations. Several microbial populations enriched after liming were identified using molecular and phylogenetic analysis of 16S rDNA fragments, and through traditional methods of bacterial cultivation. Several isolates matching 16S fragments observed in the environmental samples were shown to reduce As(V) under aerobic conditions, suggesting a potential role of aerobic heterotrophs in As cycling.

### Materials and Methods

#### Sample Collection and Chemical Characterization

Arsenic contaminated reprocessed mine tailings (RT) were collected near an abandoned copper smelter in Anaconda, Montana (EPA Superfund Site # MTD093291656). Extensive characterization of this sample by Jones et al. (22) included sequential extractions of As fractions, scanning electron microscopy (SEM)/energy dispersive analysis of X-rays (EDAX), and total metal concentrations as determined by x-ray fluorescence. Briefly, Fe represented 15-21 % (w/w) of the RT, primarily in the form of Fe-oxyhydroxides. Total As accounted for approximately 0.3 % (w/w) of the RT, with about 32 % of the As sorbed to the Fe-oxyhydroxide phases (quantified by the 0.1 M NaOH sequential extraction step which has been correlated with As surficially bound to Fe-oxyhydroxide). The largest fraction of As, approximately 60 %, was in the "nonlabile" pool, extracted only after a four acid heat treatment. Extensive analysis of the RT with SEM-EDAX revealed no discrete solid phases concentrated in As.

### Column Experiments

Mobilization of As under transport conditions was studied using polycarbonate columns (length = 54 mm, diam. = 32 mm) packed with a mixture of 20 % RT and 80 % acid-purified, autoclaved quartz sand (50-70 mesh, Sigma Chemical, St. Louis, MO) for a total mass of 62 g (bulk density  $\sim 1.43 \text{ g cm}^{-3}$ ). Limed treatments included a mix of 60 %  $\text{CaCO}_3$ /40 %  $\text{Ca(OH)}_2$  at a concentration of  $25.6 \text{ g kg}^{-1}$  (23). The column apparatus was either autoclaved or fumigated with chloroform prior to packing. Sterilized treatments used RT that was either autoclaved (12 g RT portions for 1 h x 2) or exposed to chloroform ( $\sim 5 \text{ mm}$  layer RT in a vacuum evacuated dessicator with chloroform for  $\sim 250 \text{ h}$ ). The alternate chloroform sterilization treatment was used to circumvent potential alteration of solid phases during autoclaving, however, our results showed no apparent differences between the two sterilization methods (e.g., steady-state values of pH, Fe and As measured in the effluent of chloroform-treated limed columns bracketed values for the autoclaved columns). Autoclaved influent was supplied to the bottom of the columns with a continuous flow pump set to deliver  $0.88 \text{ mL h}^{-1}$  (1.1 pore volume  $\text{d}^{-1}$ , pore water velocity =  $0.24 \text{ cm h}^{-1}$ ). The influent, formulated to simulate a "typical" soil solution (SSE) was modified from Angle et al. (24) and contained  $\text{NH}_4\text{NO}_3$  (1.25 mM),  $\text{CaSO}_4$  (2 mM),  $\text{MgCl}_2$  (2 mM),  $\text{KH}_2\text{PO}_4$  (10  $\mu\text{M}$ ), KOH (1.25 mM),  $\text{FeCl}_2$  (5  $\mu\text{M}$ ), supplemented with  $100 \mu\text{L L}^{-1}$  of micronutrient solution (25). The pH of the influent was adjusted with HCl to pH 3.6 for unlimed columns and with NaOH to pH 7.0 for limed columns. Effluent pH values in the limed treatments near 7.7 were due to liming amendments as opposed to affects of the unbuffered, pH-adjusted influent solution. Because organic amendments and topsoils rich in organic C are routinely added to mine tailings in

reclamation efforts, an additional treatment simulating these high C environments included 0.5 mM glucose and 1.0 mM lactate in the influent. For several specific columns, air was continuously pumped through a port in the bottom end cap at a rate of 10 mL min<sup>-1</sup> to insure that oxic conditions were present and to disrupt potential redox gradients.

An effluent collection system was devised to minimize microbial and abiotic transformations of As mobilized from the columns. Solution exiting the top of the columns was plumbed directly into 50 mL glass syringes whose pistons were allowed to freely extend as effluent flowed in. The syringes were housed within a N<sub>2</sub>(g)-purged temperature-controlled chamber set at 2 ± 1 °C. To allow for expulsion of air from aerated columns, tubing exiting the top endcap was open to the atmosphere and effluent flowing from the tube was collected with a fraction collector rather than syringes. During the column transport experiments, samples were removed periodically, filtered (0.22 μm) and analyzed for As(V), As(Total), Fe(II), Fe(Total), sulfide and pH. The method used for quantifying As species was modified from Masscheleyn et al. (26). Specifically, 5 mL aliquots of effluent or standard were added to each of two 15 mL polyethylene bottles and analyzed separately for total As and As(V), with As(III) determined by difference. Arsenite was liberated from one sample by selectively reducing As(III) to arsine gas and subsequent purging of the arsine gas. This was accomplished by adding 1 mL of 0.25 M NaOH and 0.79 M NaBH<sub>4</sub> (over a period of 3 min) to a sample buffered with 1 mL of 2 M Tris (pH 6.5) while sparging with N<sub>2</sub>(g). The sample was then sparged for 7 additional min. Total As was analyzed with hydride generation-atomic absorption spectrophotometry as described in Jones et al. (22). The phenanthroline method was used

to determine Fe(II) and Fe(total) concentrations, and sulfide was measured colorimetrically using methylene blue (27). Redox potential within the columns was measured using a Pt-wire inserted into the center of the column midway between the top and bottom endcaps and sealed prior to starting the experiments (surface area =  $0.5 \text{ cm}^2$ ), and a reference electrode connected to the top endcap. The Pt-electrodes were interfaced to a computer that collected voltage data at prescribed intervals. Prior to the experiments, the Pt-electrodes were calibrated in accordance with ASTM method D1498-76 (28) using Fe(II)/Fe(III) reference solutions. All column transport experiments were conducted in triplicate unless otherwise noted. At the conclusion of the experiments, columns were dismantled and the RT/sand mixture was used for isolation of As(V) reducing microorganisms and for molecular analysis.

#### As(V) Reducing Isolates

Bacteria were isolated by adding 1 g of post-experimental RT-sand mixture to 10 mM NaCl and shaking @  $100 \text{ cycles min}^{-1}$  for 5 min. The slurry was serially diluted and 0.1 mL aliquots of each dilution were plated onto various media designed to culture aerobic and anaerobic bacteria, and specifically, bacteria capable of anaerobic As(V) respiration. Bacteria were isolated using yeast-extract peptone-glucose (YEPG) agar media and SSE agar media supplemented with 1 mM glucose and 2 mM lactate (SSE+C). Both media also contained  $13 \text{ } \mu\text{M}$  As(V). These plates were incubated under both aerobic and anaerobic conditions. To specifically isolate As(V) respiring bacteria, SSE agar media was prepared with  $500 \text{ } \mu\text{M}$  As(V) and  $250 \text{ } \mu\text{M}$  cysteine;  $\text{NH}_4\text{NO}_3$  was replaced with  $2.5 \text{ mM}$   $\text{NH}_4\text{Cl}$ . Anaerobic plates were degassed for several days, inoculated, then

incubated in a chamber containing a GasPak Plus generator (Becton Dickinson, Sparks, MD). Isolated colonies were restreaked several times to obtain pure cultures.

Isolates obtained from the post-experimental RT/sand were screened for their ability to reduce As(V) in serum bottles containing 50 mL SSE+C media and 13  $\mu\text{M}$  As(V). Aerobic treatments were maintained by continuously purging the solution with filter-sterilized air ( $> 5 \text{ mL min}^{-1}$ ). Anaerobic treatments were conducted using  $\text{N}_{2(\text{g})}$ -purged serum bottles containing 13  $\mu\text{M}$  As(V). The potential for isolates to respire on As(V) was tested in  $\text{N}_{2(\text{g})}$ -purged serum bottles containing SSE media supplemented with 500  $\mu\text{M}$  As(V) and 250  $\mu\text{M}$  cysteine;  $\text{NH}_4\text{NO}_3$  was replaced with 2.5 mM  $\text{NH}_4\text{Cl}$ . Aerobic isolates that were capable of reducing As(V) were further characterized using serum bottles containing SSE media plus 5 mM MOPS buffer, 20 mM glucose, 50  $\mu\text{M}$   $\text{NaH}_2\text{PO}_4$ , and 200  $\mu\text{M}$   $\text{Na}_2\text{HAsO}_4$ . Serum bottle experiments with isolates obtained from the C supplemented columns utilized the same media with exception of 10  $\mu\text{M}$  P and 1.4 or 156  $\mu\text{M}$  As(V). Serum bottles were inoculated to attain an initial cell density of  $10^6$  cells  $\text{mL}^{-1}$ , as determined using an empirically-developed relationship between cell enumeration with epifluorescence microscopy of DAPI stained cells and optical density (OD) measurements ( $A_{500}$ ) of cell suspensions. At each sampling interval, 3.5 mL of suspension was removed for determination of OD ( $A_{500}$ ), As(V) and As(Total) concentrations as described above.

#### DNA Extraction and Purification

Total sample DNA was extracted using the FastDNA SPIN Kit for Soil (Bio 101, Vista, CA) following the manufacturer's instructions. The extracted DNA was

electrophoresed in a 1 % SeaKem GTG agarose gel (FMC BioProducts, Rockland, ME); and stained with ethidium bromide.

Partial 16S rDNA Amplification and Denaturing Gradient Gel Electrophoresis (DGGE)

DNA extracts were used as template for polymerase chain reaction (PCR) that targeted a 322 bp region within the 16S rRNA gene. The 1070 forward primer (Integrated DNA Technologies, Coralville, IA) targeted the domain *Bacteria* (*E. coli* positions 1055-1070) and the 1392 reverse-GC primer targeted a universally conserved region (*E. coli* positions 1392-1406). The reverse primer contained a 40 bp GC-rich clamp used in DGGE (5'-CGC CCG CCG CGC CCC GCG CCC GGC CCG CCG CCC CCG CCC CAC GGG CGG TGT GTA C-3'; 29). PCR reaction mixtures (50  $\mu$ L) contained 1-5  $\mu$ L template DNA (2-20 ng), 2 mM Tris-HCl (pH 8), 10 mM KCl, 10  $\mu$ M EDTA, 2.5 mM MgCl<sub>2</sub>, 800  $\mu$ M dNTP's, 0.5  $\mu$ M of each primer, and 1.25 U *Taq* DNA polymerase (Promega, Madison, WI). PCR reactions were run on a 9700 GeneAmp PCR System (Perkin-Elmer, Foster City, CA). The protocol was 94 °C for 4 min, 30 cycles of 94 °C, 55 °C and 72 °C each for 45 sec, and a final 7 min extension period at 72 °C. DNA was quantified by electrophoresis on a 3 % SeaKem GTG agarose gel (FMC BioProducts, Rockland, ME) run with a Low DNA Mass Ladder (Gibco BRL, Grand Island, NY) and stained with ethidium bromide.

PCR products were separated and visualized using DGGE as described by Muyzer et al. (30) with the following modifications. A DCode Universal Mutation Detection System (Bio-Rad, Hercules, CA) was used to resolve the PCR products. The gel consisted of 8 % acrylamide and a 35-70 % gradient of urea/formamide increasing in

the direction of electrophoresis (running buffer = 1X TAE [40 mM Tris, 20 mM acetic acid, and 2 mM EDTA at pH 8.5]; 60 V at 60 °C for 17 h). DGGE gels were stained with SYBR Green II (Molecular Probes, Eugene, OR) in 1X TAE for 30 min and photographed using UV transillumination. DGGE bands of interest were stabbed with a sterile pipet tip, rinsed in sterile molecular biology grade water and used as template for PCR amplification and subsequent sequencing reactions.

#### PCR Amplification and DNA Sequencing of DGGE Bands

Template for sequencing of DGGE bands was amplified using primers 1114 forward and 1392 reverse (without the GC clamp; 31) as described above. The product was purified with a QIAquick PCR Purification Kit (Qiagen Inc., Valencia, CA) and the sequencing reaction was carried out using an ABI Prism BigDye Terminator Cycle Sequencing Ready Reaction Kit as described by the manufacturer (Perkin-Elmer). The samples were processed on an ABI Prism 310 capillary sequencer (Perkin-Elmer) and the resultant sequences were aligned using Sequencher 3.1.1 software (Gene Codes Corporation, Ann Arbor, MI). Phylogenetic information was obtained by using BLAST to compare the sequences with sequences found in the GenBank database (32).

#### Full Length 16S rDNA Amplification and Sequencing

DNA from each of the isolates was amplified using primers that amplify nearly the entire 16S rRNA gene. Template for the reactions was obtained by scraping several colonies with a sterile pipet tip and swirling the tip in 50 µL of DNase free water. The suspension was heated at 98 °C for 10 min. and 1.0 or 5.0 µL was used as template for

PCR. Primers for the initial PCR consisted of the *Bacteria*-specific primer Bac8 forward (5'-AGAGTTTGATCCTGGCTCAG-3') and the universal primer Univ1492 reverse (5'-GGTTACCTTGTTACGACTT-3'). The products were purified with a QIAquick PCR Purification Kit. All primers for the full-length sequence reactions were derived from the probes described by Amann et al. (33). Sequencing conditions and sequence analysis were conducted as described above.

## Results and Discussion

### Column Experiments

The mean steady-state effluent pH increased from 3.85 in unlimed treatments to 7.75 after liming (Table 2.1), consistent with lime requirement calculations for this acid mine soil (23). Iron eluted from unlimed columns was predominantly Fe(II), which is consistent with thermodynamic predictions of Fe speciation at  $\text{pH} < 4$  and  $E_H < 530$  mV (Table 2.1; 34). As expected, the pH increase after liming resulted in undetectable concentrations of Fe in the effluent ( $< 0.8 \mu\text{M}$ ), and thus confirmed the use of liming as an effective method for immobilizing Fe in RT. No detectable sulfide ( $> 3.0 \mu\text{M}$ ) was released from either unlimed or limed columns. Estimates of redox potential using Pt-electrodes suggested that limed columns not supplemented with C were too oxidized to support significant concentrations of As(III) (Figure 2.1; Table 2.1). At pH 7.75, thermodynamic predictions suggest that redox potential values must be less than -23 mV to support significant concentrations of As(III) ( $> 1$  % of total; 35); observed Pt- $E_H$  values at steady-state were never less than 380 mV (Table 2.1). In limed columns that

Table 2.1. Mean steady-state pH values and Fe and As concentrations in effluent from reprocessed tailing (RT) columns. Influent for these treatments was not supplemented with C.

Treatments	pH	$E_H$ (mV)	$Fe(II)$ $Fe(Total)$		$As(III)$	$As(Total)$
			( $\mu M$ )		(nM)	
Unlimed Sterile <sup>a</sup>	3.9 (0.1) <sup>b</sup>	473.2 (12.3)	158.6 (9.9)	162.5 (12.4)	8.3 (5.0)	16.7 (8.4)
Unlimed Nonsterile	3.8 (0.03)	522.5 (19.6)	78.3 (42.5)	76.4 (43.7)	16.3 (7.9)	24.5 (5.9)
Limed Sterile	7.8 (0.07)	418.3 (38.6)	0.0 (0.0)	0.0 (0.0)	3.0 (3.0)	99.3 (14.3)
Limed Nonsterile	7.7 (0.06)	412.9 (17.4)	0.0 (0.0)	0.0 (0.0)	252.1 (52.8)	300.3 (61.4)
Limed-Aerated-Nonsterile	7.8	393	0.0	0.0	299.5	340.0

<sup>a</sup>Values for sterilized treatments are means of three replicate columns experiments; two of the experiments used RT pretreated with chloroform, and the third used RT that was autoclaved.

<sup>b</sup>Standard errors of three replicate column experiments in parenthesis.

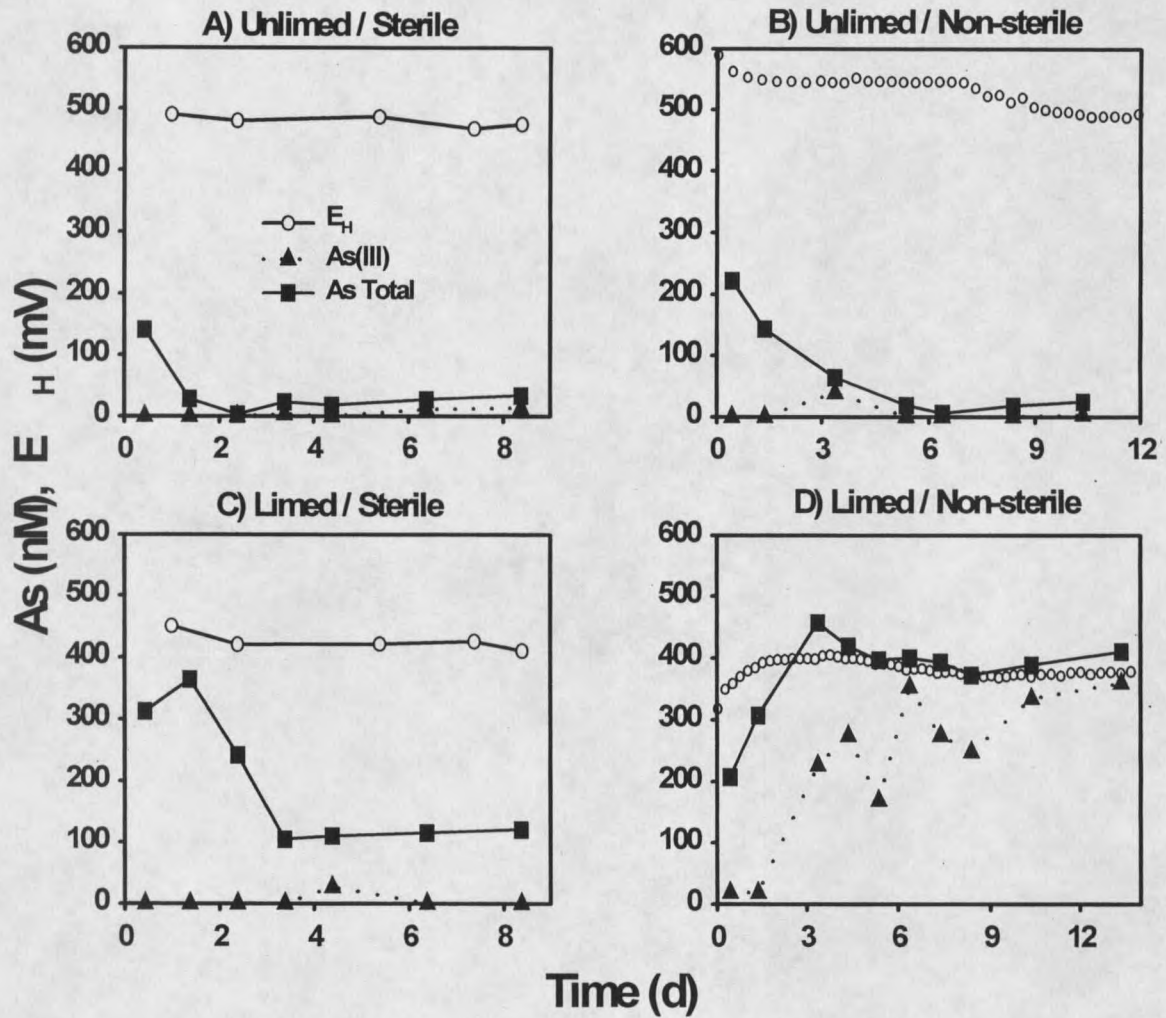


Figure 2.1. Total As and As(III) concentrations in the effluent from unlimed and limed, sterile (autoclaved) and non-sterile RT columns. Influent was not supplemented with C. The As(V) concentration is the difference between total As and As(III) concentrations. The  $E_H$  was measured with a Pt-electrode positioned in the center of the columns.

received influent containing 0.5 mM glucose and 1.0 mM lactate, redox potential values that theoretically favored the presence of As(III) were attained after 5 d (Figure 2.2).

In unlimed columns, both the sterilized and nonsterilized treatments released an initial pulse of As which ranged from 100 to 250 nM, then gradually declined to approximately 20 nM As after 1 to 5 d (Figure 2.1A, B). After liming, steady-state concentrations of total As mobilized from sterile columns increased significantly to about 100 nM (Figure 2.1C; Table 2.1). In nonsterile treatments, mean steady-state As concentrations increased further to approximately 300 nM (Figure 2.1D, Table 2.1). In the absence of microbial activity, As(V) was the predominant species mobilized after liming. Conversely, in the limed, nonsterile treatments, As(III) was the predominant species mobilized after 3 d, and the increased mobilization of As was associated with the reduction of As(V) to As(III). To verify that As(V) reduction and enhanced As mobilization occurred under oxic conditions, an additional experiment was conducted during which air was continuously pumped through a limed nonsterile column. Steady-state effluent As(III) and total As concentrations for the aerated treatment were essentially identical to concentrations in the nonaerated-limed treatments (Table 2.1), supporting the conclusion that microbial As(V) reduction within these limed columns occurred under redox conditions considered oxic as determined using Pt-electrode measurements and  $\text{Fe}^{2+}$  concentrations (34). Limed columns that received influent supplemented with C released about 450 nM total As after 3 d; nearly all as As(III) (Figure 2.2).

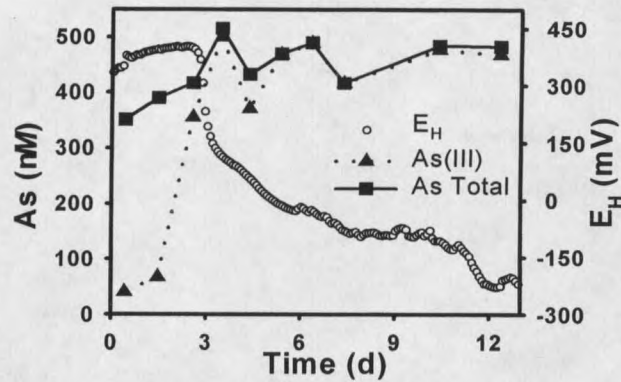


Figure 2.2. Total As and As(III) concentrations in the effluent from limed non-sterile RT column that received influent containing 1.0 mM lactate and 0.5 mM glucose. The As(V) concentration is the difference between total As and As(III) concentrations. The  $E_H$  was measured with a Pt-electrode positioned in the center of the columns.

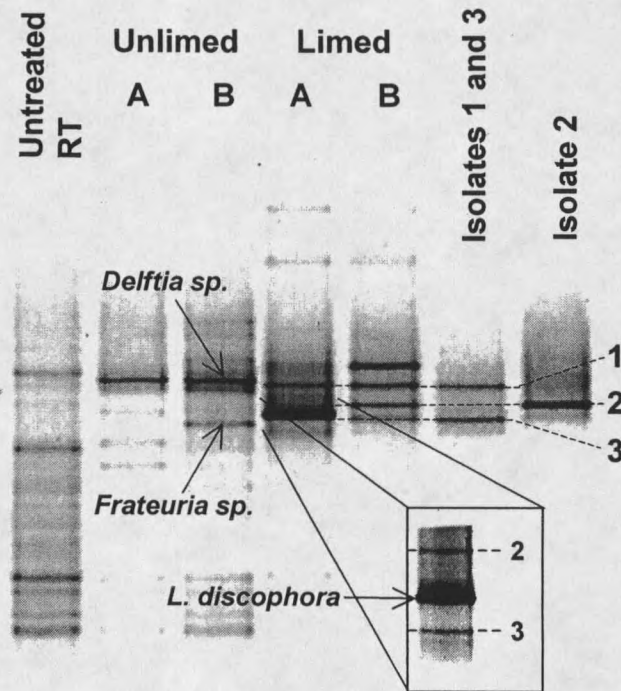


Figure 2.3. Denaturing gradient gel (35 - 70 %) of PCR-amplified 16S rDNA fragments from untreated RT, unlimed RT columns (replicates A and B), limed RT columns (replicates A and B) and *C. leidyi* (1), *S. yanoikuyae* (2), and *R. loti* (3)-like isolates. To resolve the *S. yanoikuyae* and *R. loti* bands in the limed RT column (replication A), the sample was run with a narrower (40 - 60 %) denaturing gradient (inset). Comigration of isolate bands with bands from limed RT columns is indicated with dashed lines.

### Molecular Analysis

DNA fingerprints of the microbial populations present in untreated (preexperimental) RT and in two of the three unlimed and limed column replicates were obtained using DGGE. Distinct banding patterns, representing different microbial assemblages, were associated with the different treatments (Figure 2.3). The presence of many bands in the untreated RT suggested that a relatively diverse microbial community resided in the RT prior to treatment. Significant differences in the banding patterns of unlimed versus limed treatments demonstrated that pH and its consequent impacts on solution chemistry are strong determinants of microbial selection. Comparisons between the banding patterns from column replicates revealed the comigration of many bands and suggested that similar microbial populations were stimulated in the replicate experiments (compare unlimed lanes A vs B and limed lanes A vs B); however, some differences between the replicates were observed, indicating potential variation in inoculum or subsequent column conditions, or during DNA extraction and amplification of 16S rDNA segments.

Sequence analysis of prominent bands in the denaturing gradient gels and comparison with sequences in the GenBank database revealed that diverse bacterial populations were selected in the column environments. Prominent bands in unlimed column lane B represent populations that were 100 % identical to a *Delftia* species and 100% identical to a *Frateuria* species within the region of the rRNA gene analyzed (~ 322 bp; Figure 2.3). Prominent bands in the limed column lanes represent *Caulobacter leidyi*, *Sphingomonas yanoikuyae*, *Rhizobium* species, and *Leptothrix discophora* (99.1 % identical) -like populations based on the ~ 322 bp region analyzed (Figure 2.3). The

prominent upper band in limed column B represented at least two populations that were not easily resolved and therefore were not sequenced.

### Isolates

We cultivated and characterized several bacterial populations that may have been responsible for As(V) reduction in the limed RT columns. Bacteria were isolated from two of the three limed (no C supplement) RT column replicates and screened for their ability to reduce As(V). No microorganisms capable of anaerobic growth (under these conditions), including anaerobic respiration using As(V), were isolated during this study. However, three microorganisms capable of aerobic As(V) reduction were isolated from each of these replicate limed columns. Near full-length sequence analysis of the 16S rRNA genes of these three bacteria and comparison with sequences in the GenBank database revealed that their closest phylogenetic neighbors were *Caulobacter leidyi*, *Sphingomonas yanoikuyae*, and *Rhizobium loti* (Table 2.2).

The relevance of these cultivated organisms in the column environment was examined by comparing DGGE band migration and sequences of bands detected in the column environment to those of each isolate. Bands representing the *C. leidyi*, *S. yanoikuyae*, and *R. loti*-like populations in RT had the same mobility in the DGGE gels as isolate bands and sequence analysis verified that they were 100 % identical (Figure 2.3). These observations suggest that our isolates represented at least three of the bacterial populations that were stimulated by the liming treatment.

Three additional microorganisms capable of reducing As(V) in aerated serum bottles were isolated from replicate limed RT columns that received supplemental C in

Table 2.2. Phylogenetic affiliation and As(V) reduction rate parameters of isolates cultivated from limed columns containing reprocessed tailings (RT). Measured optical density (OD) values and As(V) concentrations were used to fit a second-order rate expression (Eqn. 1) to obtain values for an apparent second-order rate constant (k).

Isolate	GenBank accession no.	-----Nearest GenBank relative <sup>a</sup> -----			-----As(V) reduction parameters <sup>b</sup> -----			
		Species	Phylogenetic group	Percent similarity	k <sup>c</sup> (AU <sup>-1</sup> d <sup>-1</sup> )	r <sup>2</sup>	Max rate (mM d <sup>-1</sup> )	Half-life <sup>c</sup> (d)
1	AF331660	<i>Caulobacter leidyi</i>	$\alpha$ proteobacteria	100	0.037	0.93	0.054	2.6
2	AF331661	<i>Sphingomonas yanoikuyae</i>	$\alpha$ proteobacteria	100	0.073	0.88	0.401	0.4
3	AF331662	<i>Rhizobium loti</i>	$\alpha$ proteobacteria	98.3	0.033	0.88	0.293	0.5
4	AF331663	<i>Pseudomonas aeruginosa</i>	$\gamma$ proteobacteria	99.9	0.939	0.97	0.118	0.9
5	AF331665	<i>Pseudomonas fluorescens</i>	$\gamma$ proteobacteria	99.0	0.224	0.98	0.066	1.7
6	AF331664	<i>Sphingomonas echinoides</i>	$\alpha$ proteobacteria	99.4	0.469	0.82	0.0004	2.4

<sup>a</sup> Phylogenetic affiliations were determined by comparing near full-length 16S rDNA sequences of these isolates to sequences in the GenBank database. <sup>b</sup> Initial As (V) concentrations were 160-200  $\mu$ M for isolates 1-5; and only 1.4  $\mu$ M for isolate 6.

<sup>c</sup> Apparent rate constants and half-lives ( $t_{1/2}$ ) dependent on experimental conditions and limited to optical density values achieved in current experiment; half-lives estimated based on maximum rates assuming pseudo first-order reaction dependent on As(V).

the influent. This treatment was specifically designed to enrich for microorganisms that may be important under the elevated C levels resulting from remediation treatments that incorporate C amendments. Although the conditions within these columns may have been conducive to the growth of anaerobic bacteria, no bacteria were isolated under anaerobic conditions; the three bacteria obtained from this treatment were all isolated under aerobic conditions. Near full-length sequences of the 16S rRNA genes of these isolates were compared with sequences in the GenBank database; the nearest phylogenetic neighbors were *Pseudomonas fluorescens*, *P. aeruginosa*, and *Sphingomonas echinoides* (Table 2.2). All six of the As(V) reducing bacteria isolated from the mine tailings were members of either the  $\alpha$  or  $\gamma$  proteobacteria subdivisions (Table 2.2). The 16S rDNA sequences of these isolates were deposited in GenBank under the accession numbers AF331660 - AF331665 (Table 2.2).

#### As(V) Reduction Kinetics of Isolates

The kinetics of As(V) reduction were measured in continuously aerated serum bottles for each of the six isolates cultivated from limed tailings (Figure 2.4). The dependence of As(V) reduction rate on As(V) concentration and optical density (OD) during the growth phase of the isolates was modeled using the following second-order rate equation (36):

$$- d[As(V)] / dt = k[As(V)]X \quad (1)$$

where X represents OD in absorbance units (AU) and k is the apparent As(V) reduction rate constant in units of  $AU^{-1} h^{-1}$ . Measured values of OD and As(V) as a function of time

were used as inputs to Equation 1 to obtain fitted values of  $k$  for each isolate (Table 2.2). Predicted concentrations of As(V) obtained using the fitted  $k$  values and measured OD values correlated well with measured data for all isolates ( $r^2 > 0.8$ ; Table 2.2; Figure 2.4). The apparent rate constants ( $k$ ) for isolates 1, 2, and 3 were significantly lower compared to isolates 4, 5, and 6, due in part to the different growth characteristics of the isolates and the composition of the media used in these experiments. For example, the P nutritional status and the P:As ratio may be very important to the growth rates and As(V) reduction kinetics observed in these experiments (14). Isolates 1, 2, and 3 received 50  $\mu\text{M}$  P and achieved much higher OD values than isolates 4, 5, and 6 which received only 10  $\mu\text{M}$  P. Because the fitted second-order rate constants ( $k$ ) depend on both As(V) concentration and OD, variation in growth kinetics among isolates under the culture conditions employed influences the magnitude of  $k$ . Although we are interested in the affect of P:As ratio on the reduction kinetics of As(V), the current objectives were focused on establishing that these isolates may be responsible for As(V) reduction observed in the limed columns under aerobic conditions. Towards this end, the serum bottle experiments clearly showed that the reduction of As(V) was coincident with microbial growth under aerobic conditions. Moreover, maximum OD values were not significantly different in the absence of As(V) (data not shown) suggesting that growth was not coupled to reduction of As(V) and that growth was not inhibited by the presence of As(V) at these levels. Maximum rates of As(V) reduction by these isolates ranged from about 0.4  $\text{mM d}^{-1}$  for *S. yanoikuyae* to about 0.4  $\mu\text{M d}^{-1}$  for *S. echinoides* (Table 2.2). Since the maximum concentration of As(III) eluted from the limed columns was about 0.4  $\mu\text{M}$  (at a flow rate of 21  $\text{mL d}^{-1}$ ), it is reasonable that these isolates could have been responsible for the

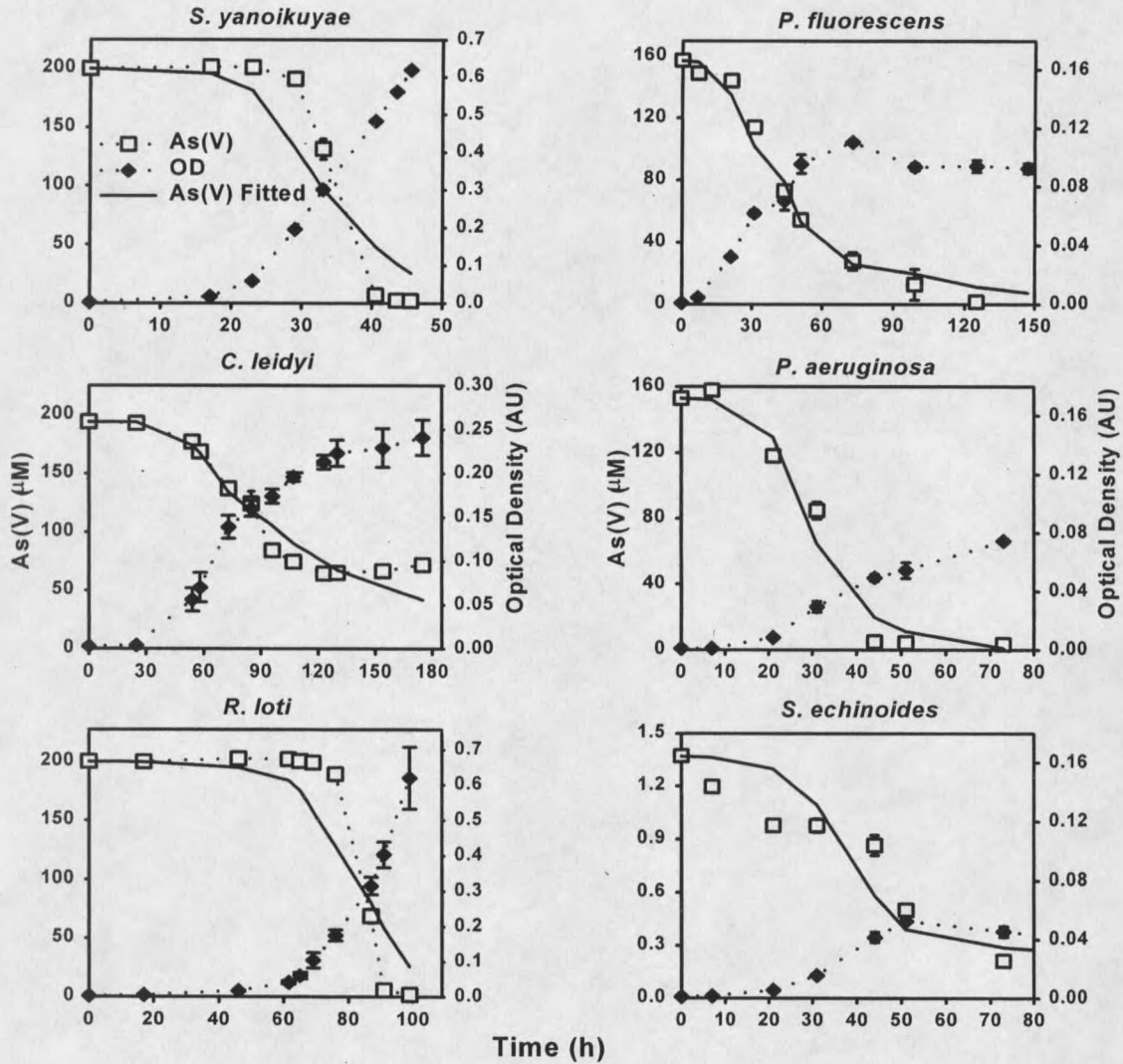


Figure 2.4. Microbial biomass (as optical density, OD) and As(V) concentrations as a function of time for six As(V) reducing isolates incubated under aerated conditions. Isolates are named after their nearest phylogenetic neighbor found in the GenBank database. Serum bottles inoculated with *S. yanoikuyae*, *C. leidyi*, and *R. loti* contained 50  $\mu\text{M}$  P and 200 mM As(V). Serum bottles inoculated with *P. fluorescens* and *P. aeruginosa* contained 10  $\mu\text{M}$  P and 157  $\mu\text{M}$  As(V). Because *S. echinoides* did not reduce any As(V) at an initial As(V) concentration of 157  $\mu\text{M}$ , reduction experiments with this isolate were conducted using and 1.4  $\mu\text{M}$  As(V) (10  $\mu\text{M}$  P). Error bars represent standard errors of three replicate serum bottle experiments conducted for each of the isolates.

reduction of As(V) that was observed during transport. Nevertheless, the As(V) reduction rates demonstrated by several of these isolates are comparable to rates measured for other bacteria. For example, researchers have reported dissimilatory As(V) reduction rates as high as  $7 \text{ mM d}^{-1}$  (37) while As(V) reduction rates attributed to detoxification have been observed to be as high as  $1 \text{ mM d}^{-1}$  (11, 36).

#### Mechanisms of As Reduction and Implications for As Cycling

In the reprocessed mine-tailings used in the current study, liming enhanced the mobilization of As due to both chemical (pH dependent sorption; 38) and microbiological processes (Table 2.1). A combination of cultivation and cultivation-independent methods were used to evaluate specific bacterial populations responsible for the reduction of As(V) in mine-tailings after liming. Six different microbial populations representing *Sphingomonas*, *Caulobacter*, *Rhizobium*, and *Pseudomonas* genera were isolated from limed reprocessed tailings, and all were capable of rapidly reducing As(V) in aerated serum bottles. The appearance of 16S rDNA bands representing these bacteria in denaturing gradient gels revealed that several of these populations were present in the limed columns, and in some cases appeared to be dominant members of the microbial community. The reduction of As(V) to As(III) by these microorganisms was associated with the enhanced mobility of As in column transport experiments. However, reductive dissolution of the Fe-oxide phase was not a significant factor in mobilizing As as judged by the absence of detectable Fe(II) or Fe(III) in column effluent. Conversely, the pH change from 4 to 7.7 resulting from lime amendment would be expected to cause

significant precipitation of Fe-oxyhydroxides and measured dissolved Fe concentrations before and after liming were consistent with this expectation.

Several lines of evidence suggest that the microbial reduction of As(V) in these column transport experiments occurred via a process other than As(V) respiration. The fact that aeration had little effect on As(V) reduction rates (Table 2.1) suggests that reduction of As(V) was not coupled to anaerobic respiration. Furthermore, the bacterial isolates shown to be relevant members of the microbial community did not demonstrate growth under anaerobic conditions with As(V) as an electron acceptor, but rather, were able to grow and rapidly reduce As(V) under oxic conditions. These data suggest that As(V) reduction in the mine tailings occurred via a detoxification process which is functional under oxic conditions. Cai et al. (17) demonstrated that strains of *P. aeruginosa* and *P. fluorescens*, which are closely related to two of our isolates, carry *ars* operon homologues which confer increased resistance to As. This pathway results in intracellular reduction of As(V) and the subsequent efflux of As(III) via a transmembrane pump. DNA sequence homologues of As detoxification genes have also been detected in *Thiobacillus ferrooxidans*, an obligately chemolithotrophic bacterium common in pyritic mine tailings (13). Although we recognize that anaerobic microsites within soil aggregates may have contributed to dissimilatory As(V) reduction, the molecular analysis and cultivation techniques employed in the current study did not reveal any potential As(V) respiring bacteria. It is certainly possible that these microorganisms may have been present in our columns, but were not detected due to limitations of the techniques, including (i) the inability to extract or amplify DNA from these bacteria, (ii) the inability to identify and/or sequence less prominent DGGE bands representing organisms capable

of dissimilatory As(V) reduction, and (iii) the inability to successfully simulate the column environment during attempts to cultivate these microorganisms. However, while dissimilatory reduction of As(V) may be an important process in strict anaerobic environments, the results from this study suggest that rapid reduction of As(V) in limed mine tailings, and potentially in other soils and natural waters may be facilitated by microorganisms under aerobic conditions. Consequently, the prediction of As valence, and thus, the behavior of As based solely on redox status may be problematic. Because the ability to reduce As(V) via detoxification pathways may be a widely distributed trait in soil and aquatic microorganisms, these processes need to be taken into account in order to fully understand As cycling in natural systems.

## REFERENCES CITED

1. Stolz, J.F., and R.S. Oremland. 1999. Bacterial respiration of arsenic and selenium. *FEMS Microbiol. Rev.* 23:615-627.
2. Silver, S., 1996. Bacterial resistances to toxic metal ions-a review. *Gene.* 179:9-19.
3. Anderson, G.L., J. Williams, and R. J. Hille. 1992. The purification and characterization of arsenite oxidase from *Alcaligenes faecalis*, a molybdenum-containing hydroxylase. *Biol. Chem.* 267:23674-23682.
4. Santini, J.M., L.I. Sly, R.D. Schnagl, and J.M. Macy. 2000. A new chemolithotrophic arsenite-oxidizing bacterium isolated from a gold mine: phylogenetic, physiological, and preliminary biochemical studies. *Appl. Environ. Microbiol.* 66:92-97.
5. Pierce, M.L., and C.B. Moore. 1982. Adsorption of arsenite and arsenate on amorphous iron hydroxide. *Water Res.* 16:1247-1253.
6. Masscheleyn, P.H., R.D. Delaune, and W.H.Jr. Patrick. 1991. Effect of redox potential and pH on arsenic speciation and solubility in a contaminate soil. *Environ. Sci. Technol.* 25:1414-1419.
7. Tamaki, S., and W.T.Jr. Frankenberger. 1992. Environmental biochemistry of arsenic. *Rev. Environ. Contam. Tox.* 124:79-110.
8. Ahmann, D., A.L. Roberts, L.R. Krumholz, and F.M.M. Morel. 1994. Microbe grows by reducing arsenic. *Nature* 371:750.
9. Dowdle, P.R., A.M. Laverman, and R.S. Oremland. 1996. Bacterial dissimilatory reduction of arsenic(V) to arsenic(III) in anoxic sediments. *Appl. Environ. Microbiol.* 62:1664-1669.
10. Newman, D.K., D. Ahmann, and F.M.M. Morel. 1998. A brief review of dissimilatory arsenate reduction. *Geomicrobiol. J.* 15:255-268.
11. Macy, J.M., J.M. Santini, B.V. Pauling, A.H. O'Neill, and L.I. Sly. 2000. Two new arsenate/sulfate reducing bacteria: mechanisms of arsenate reduction. *Arch. Microbiol.* 173:49-57.
12. Huber, R., M. Sacher, A. Vollmann, H. Huber, and D. Rose. 2000. Respiration of arsenate and selenate by hyperthermophilic archaea. *System. Appl. Microbiol.* 23:305-314.

13. Butcher, B.G., S.M. Deane, and D.E. Rawlings. The chromosomal arsenic resistance genes of *Thiobacillus ferrooxidans* have an unusual arrangement and confer increased arsenic and antimony resistance to *Escherichia coli*. Appl. Environ. Microbiol. 66:1826-1833.
14. Cervantes, C., G. Ji, J.L. Ramirez, and S. Silver. 1994. Resistance to arsenic compounds in microorganisms. FEMS Microbiol. Rev. 15:355-367.
15. Diorio, C., J. Cai, J. Marmor, R. Shinder, and M.S. DuBow. 1995. An *Escherichia coli* chromosomal *ars* operon homolog is functional in arsenic detoxification and is conserved in gram-negative bacteria. J. Bacteriol. 177:2050-2056.
16. Neyt, C., M. Iriarte, V.H. Thi, and G.R. Cornelis. 1997. Virulence and arsenic resistance in *Yersinia*. J. Bacteriol. 179:612-619.
17. Cai, J., K. Salmon, and M.S. DuBow. 1998. A chromosomal *ars* operon homologue of *Pseudomonas aeruginosa* confers increased resistance of to arsenic and antimony I *Escherichia coli*. Microbiol. 144:2705-2713.
18. Sato, T., and Y. Kobayashi. 1998. The *ars* operon in the skin element of *Bacillus subtilis* confers resistance to arsenate and arsenite. J. Bacteriol. 180:1655-1661.
19. Cullen, W.R., and K.J. Reimer. 1989. Arsenic speciation in the environment. Chem. Rev. 89:713-764.
20. Sohrin, Y., M. Matsui, M. Kawashima, M. Hojo, and H. Hasegawa. 1997. Arsenic biogeochemistry affected by eutrophication in Lake Biwa, Japan. Environ. Sci. Technol. 31:2712-2720.
21. Neuman, D.R., F.F. Munshower, and D.J. Dollhopf. 1993. ARTS phase I final report, Anaconda revegetation treatability studies, Anaconda smelter superfund site; Document no. ASSS-Arts-I-FR-RI-102293; Montana State Univ: Bozeman.
22. Jones, C.A., W.P. Inskeep, and D.R. Neuman. 1997. Arsenic transport in contaminated mine tailings following liming. J. Environ. Qual. 26:433-439.
23. Schafer, W., D.R. Neuman, F.F. Munshower, D.J. Dollhopf, and CH2M Hill Inc. 1989. Final summary report-STARs phase II: Field scale treatability study plot construction; Reclamation Research Unit, Montana State Univ: Bozeman.
24. Angle, J.S., S.P. McGrath, and R.L. Chaney, 1991. New culture medium containing ionic concentrations of nutrients similar to concentrations found in the soil solution. Appl. Environ. Microbiol. 57:3674-3676.

25. Skerman, V.B.D. 1967. A guide to the identification of the genera of bacteria. The Williams and Wilkins Co.: Baltimore, MD.
26. Masscheleyn, P.H., R.D. Delaune, and W.H.Jr. Patrick. 1991. A hydride generation atomic absorption technique for arsenic speciation. *J. Environ. Qual.* 20:96-100.
27. American Public Health Association. Ch. 3: Iron and Ch. 4: Sulfide. In: Standard methods for the examination of water and wastewater; Clesceri, L.S., Greenberg, A.E., Eaton, A.D., Eds.; APHA: Washington, DC, 1998; pp 76-78 and 165-166.
28. American Society for Testing and Materials. Standard practice for oxidation-reduction potential of water. In: Annual book of ASTM standards, water and environmental technology; ASTM, Ed.: Philadelphia, PA, 1993; pp 319-323.
29. Ferris, M.J., G. Muyzer, and D.M. Ward. 1996. Denaturing gradient gel electrophoresis profiles of 16S rRNA-defined populations inhabiting a hot spring microbial mat community. *Appl. Environ. Microbiol.* 62:340-346.
30. Muyzer, G.; E.C. de Waal, A.G. Uitterlinden. 1993. Profiling of complex microbial populations by denaturing gradient gel electrophoresis analysis of polymerase chain reaction-amplified genes coding for 16S rRNA. *Appl. Environ. Microbiol.* 59:695-700.
31. Ferris, M.J., and D.M. Ward. 1997. Seasonal distributions of dominant 16S rRNA-defined populations in a hot spring microbial mat examined by denaturing gradient gel electrophoresis. *Appl. Environ. Microbiol.* 63:1375-1381.
32. Altschul, S.F., T.L. Madden, A.A. Schaffer, J. Zhang, Z. Zhang, W. Miller, and D.J. Lipman. 1997. Gapped BLAST and PSI-BLAST: a new generation of protein database search programs. *Nucleic Acid Res.* 25:3389-3402.
33. Amann, R.I., W. Ludwig, and K.H. Schleifer. 1995. Phylogenetic identification and in situ detection of individual cells without cultivation. *Microbiol. Rev.* 59:143-169.
34. Stumm, W.; Morgan, J.J. *Aquatic Chemistry*; John Wiley & Sons: New York, 1996; pp 425-515.
35. Holm, T.R., and C.D. Curtiss. 1989. A comparison of oxidation-reduction potentials calculated from the As(V)/As(III) and Fe(III)/Fe(II) couples with measured platinum-electrode potentials in groundwater. *J. Contam. Hydro.* 5:67-81.
36. Jones, C.A., H.W. Langner, K. Anderson, T.R. McDermott, and W.P. Inskeep. 2000. Rates of microbially mediated arsenate reduction and solubilization. *Soil Sci. Soc. Am. J.* 64:600-608.

37. Ahmann, D., L.R. Krumholz, H.F. Hemond, D.R. Lovley, F.M.M. Morel. 1997. Microbial mobilization of arsenic from sediments of the Aberjona watershed. *Environ. Sci. Technol.* 31:2923-2930.
38. Goldberg, S. 1986. Chemical modeling of arsenate adsorption on aluminum and iron oxide minerals. *Soil Sci. Soc. Am. J.* 50:1154-1157.

## CHAPTER 3

BACTERIAL POPULATIONS ASSOCIATED WITH THE OXIDATION AND  
REDUCTION OF ARSENIC IN AN UNSATURATED SOILIntroduction

The activity of As transforming microorganisms in soils and natural waters has significant implications for the behavior of As because different As species exhibit variation in solubility, mobility, bioavailability, and toxicity (1-4). Of the dominant inorganic species, arsenite ( $\text{H}_3\text{AsO}_3^0$ ) is generally considered to be more mobile and more toxic than arsenate ( $\text{H}_2\text{AsO}_4^-$ ,  $\text{HAsO}_4^{2-}$ ) (1-4). Known As transforming bacteria possess diverse mechanisms for either oxidizing As(III) or reducing As(V), including energy generation and detoxification (e.g., 5-10). For example, an As(III) oxidizing *Agrobacterium/Rhizobium* -like bacterium isolated from a gold mine in Australia can grow chemolithoautotrophically, utilizing As(III) as the sole electron donor (8). Conversely, *Alcaligenes* sp. and *Agrobacterium albertimagni* strains grow heterotrophically, but can rapidly oxidize As(III) using a mechanism consistent with As detoxification rather than energy generation (7, 11). The crystal structure of arsenite oxidase in *Alcaligenes* sp. has recently been elucidated (12).

Dissimilatory reduction of As(V) has been shown to occur in at least nine different genera scattered throughout the domain *Bacteria* (10, 13-15), and has also been observed in two hyperthermophilic *Archaea* (16). These microorganisms are either strict anaerobes, facultative anaerobes, or microaerophiles capable of utilizing arsenate as a

terminal electron acceptor. Interestingly, *Thermus* strain HR13 apparently has the capability to both reduce As(V) via respiration under anaerobic conditions and oxidize As(III) via a detoxification mechanism in the presence of oxygen (13). Dissimilatory reduction is often considered the primary mechanism responsible for the rapid reduction of As(V) observed in anaerobic environments. However, work also suggests that a variety of soil microorganisms, both anaerobic and aerobic, may reduce As(V) to As(III) via As detoxification (17-19). Significant prior work has shown that As(V) reduction activity by numerous bacteria is encoded by a variably organized *ars* operon, which may either be plasmid borne or chromosomal (e.g., 20-22). The *ars* genes are inducible by either As(V) or As(III), resulting in the intracellular reduction of As(V) by ArsC, a cytoplasmic reductase, and subsequent excretion of As(III) into the surrounding media (ArsB, A). Homologues of the *ars* operon have been identified in diverse bacteria including *Pseudomonas*, *Bacillus*, *Klebsiella*, *Staphylococcus*, *Salmonella*, *Acidithiobacillus*, *Yersinia* and *Escherichia* (21, 23-26). In addition, putative *ars* homologues have been detected in many of the bacteria and archaea whose genomes have recently been sequenced, suggesting that *ars* genes are relatively common among prokaryotes (27).

The reduction of As(V) via detoxification may contribute to apparent nonequilibrium conditions where As(III) has been observed in oxic soils and surface waters (e.g., 18, 28, 29). For example, several As(V)-reducing bacteria have been found to mediate the reduction of As(V) under highly aerobic conditions resulting in enhanced mobilization of As from limed mine tailings (18). The characterization of several aerobic heterotrophs isolated from these tailings suggested that the probable mechanism of As(V)

reduction was As(V) detoxification. Other investigators have also isolated apparent As detoxifying bacteria from soil, although the relevance of these populations to As redox cycling actually occurring in the environment was not studied (17, 19, 30). Given the importance of As(V)-As(III) redox cycling in soil-water systems, very little is known regarding the potential role of various As detoxification strategies versus metabolisms capitalizing on As for energy conservation. Consequently, one of the goals of the current study was to improve our understanding of the possible mechanisms and associated microbial diversity responsible for As (III)/(V) cycling in soil systems. Specifically, the objectives of this study were to (i) utilize cultivation-independent 16S rDNA sequence analysis to identify microbial populations associated with observed As redox transformations occurring in a soil environment, (ii) cultivate As(III) oxidizing and As(V) reducing aerobic heterotrophic bacteria from the same soil systems, and (iii) determine if isolates with demonstrated As redox activity correspond to those populations detected with molecular methods. These objectives were addressed by conducting unsaturated flow column transport experiments where micromolar concentrations of either As(III) or As(V) were used as influent to enrich for microorganisms capable of transforming As under aerobic conditions.

## Materials and Methods

### Column Experiments

The upper 20 cm of a well-drained, fine loamy, frigid Typic Calciaquoll that contained 2.6  $\mu\text{M}$  soluble As (saturated paste extraction using deionized  $\text{H}_2\text{O}$  equilibrated

for 0.5 h, 31) was collected from an irrigated pasture in the Madison River Valley (Gallatin County, Montana), and used as inocula for column studies. Measurements of soluble As concentrations in Madison River Valley soils typically range from 0.2 to 35  $\mu\text{M}$  (31). The fate of As in irrigated Madison River water containing 1 – 4  $\mu\text{M}$  As originating from Yellowstone National Park (32), has been an important regional water quality problem regarding As contamination of soils and shallow ground waters (31, 32). Redox transformations of As within this soil were studied under unsaturated flow conditions using autoclaved polycarbonate columns (length = 100 mm, diam. = 35 mm) packed with a mixture of 5 % soil and 95 % acid-washed, autoclaved quartz sand (50-70 mesh, Sigma Chemical, St. Louis, Missouri, USA) for a total mass of 115 g (bulk density  $\sim 1.2 \text{ g cm}^{-3}$ ). The columns received autoclaved influent supplied to the top of the columns with a continuous-flow pump set at  $1.8 \text{ mL h}^{-1}$  ( $1.9 \text{ pore volume d}^{-1}$ , pore water velocity  $\sim 0.77 \text{ cm h}^{-1}$ ). To insure thorough aeration and create unsaturated flow within the columns, filter sterilized air was drawn through the column via a nylon screen at the bottom endcap using a peristaltic pump at a rate of  $100 \text{ mL h}^{-1}$ . Solution applied to the columns drained through the soil/sand matrix via gravimetric flow and exited the bottom of the columns along with the air stream. The volumetric water content ( $\theta_v$ ) of the soil/sand mixture was maintained at  $0.24 \text{ cm}^3 \text{ cm}^{-3}$  ( $\sim 53 \%$  of saturation). The influent was formulated to enrich for aerobic heterotrophs capable of transforming As and contained  $\text{NH}_4\text{NO}_3$  (1.25 mM),  $\text{CaSO}_4$  (2 mM),  $\text{MgCl}_2$  (2 mM),  $\text{KH}_2\text{PO}_4$  (10  $\mu\text{M}$ ), KOH (1.25 mM),  $\text{FeCl}_2$  (5  $\mu\text{M}$ ) (33), supplemented with micronutrients (34), vitamins (35), 5 mM glucose (added to enrich for heterotrophic organisms), and either 75  $\mu\text{M}$   $\text{NaH}_2\text{AsO}_3$

or 250  $\mu\text{M}$   $\text{NaH}_2\text{AsO}_4$ . These concentrations of As were significantly higher than concentrations shown to induce genes involved in As detoxification (21), but lower than those normally employed for As(III) chemolithotrophic growth or for anaerobic respiration on As(V) (8, 35). The pH of the influent was adjusted to 7.0 with NaOH. Column experiments were conducted in duplicate and sterile controls were performed using autoclaved soil (30 g portions of soil autoclaved for three 1 h cycles).

Arsenic transformations within all columns were monitored periodically during the 14 to 16 d experiments by collecting 2 mL samples of column effluent, which were then filtered (0.22  $\mu\text{m}$ ) and analyzed for As(V) and As(Total) using hydride generation - atomic absorption spectrometry (HG-AAS) and  $\text{NaBH}_4$  speciation, where arsenite is determined by difference (17). Upon termination, all columns were dismantled and subsamples of the soil/sand mixture were used for isolation of As(III)-oxidizing and As(V)-reducing microorganisms and for molecular analysis.

#### Isolation and Characterization of As-Transforming Aerobic Heterotrophs

Bacteria were isolated from the unsaturated columns by homogenizing the entire soil/sand mixture and adding 1 g to 10 mL of 10 mM NaCl and shaking @ 100 cycles  $\text{min}^{-1}$  for 5 min. The slurry was serially diluted and 0.1 mL aliquots of each dilution were plated onto R2A nutrient agar (Difco Laboratories, Detroit, MI), a medium designed to maximize culturability of stressed cells. This plating protocol was used to isolate aerobic heterotrophs consistent with the soil column enrichment conditions and was not intended

to cultivate dissimilatory As(V) reducers, which are generally anaerobic or microaerophilic (10).

Isolates obtained from the soil/sand mixture were tested for their ability to oxidize or reduce As during growth in 25 mL bottles containing 5 mL column influent media (described above) modified to include 5 mM MOPS buffer (pH = 7.0), 50  $\mu\text{M}$   $\text{NaH}_2\text{PO}_4$ , 1 mg  $\text{L}^{-1}$  yeast extract (added to enhance growth in pure culture), and either 75  $\mu\text{M}$   $\text{NaH}_2\text{AsO}_3$  or 250  $\mu\text{M}$   $\text{NaH}_2\text{AsO}_4$ . Bottles were agitated on a shaker table and were aseptically vented daily to maintain aerobic conditions. The As transforming isolates were grouped based on comigration of PCR amplified 16S rDNA fragments in denaturing gradient gel electrophoresis (DGGE) (described below), and finally, by near-full length sequencing of their 16S rRNA gene (described below). Rates of either As(III) oxidation or As(V) reduction by each isolate were characterized in continuously aerated serum bottles (5 mL  $\text{min}^{-1}$  filter sterilized air) containing 50 mL of the same liquid media used for initial testing (discussed above) with the exception that 50  $\mu\text{M}$   $\text{NaH}_2\text{AsO}_3$  was used for isolate 3. Prior to inoculation, all isolates were grown in the same liquid media without As. Serum bottles were inoculated to attain an initial cell density of  $10^6$  cells per mL based on optical density (OD) measurements ( $A_{500}$ ) of cell suspensions. At each sampling interval, 3.0 mL of suspension was removed for determination of OD and concentrations of As(V) and As(III) as described above. Arsenic oxidation and reduction rates were determined from maximum slopes of As concentration curves versus time and normalized to cell number (OD correlating to position of maximum slope) using an

empirically-developed relationship between cell enumeration with phase contrast microscopy and optical density (OD) measurements ( $A_{500}$ ) of cell suspensions.

To confirm that As(III) oxidation was dependent on the presence of microbial cells, culture filtrates from As(III) oxidizing isolates were tested for oxidization of As(III) (5) by spiking 3 mL of filtrate (0.22  $\mu\text{m}$ ) from actively oxidizing cell suspensions (inoculated similarly and grown in the same media described for the oxidation rate experiments) with 200  $\mu\text{M}$  As(III) and measuring oxidation after 3 h. The ability of the As(III) oxidizing isolates to grow chemolithoautotrophically with As(III) as the sole electron donor and  $\text{CO}_2$  as the primary C source was tested using the serum bottle method described above with 25 mL of column influent media (described above) supplemented with 50  $\mu\text{M}$   $\text{NaH}_2\text{PO}_4$ , 30 mM  $\text{NaHCO}_3$  (added to replace glucose as the C source) and 5 mM As(III) (modified from reference 8). The serum bottles were sealed to maintain the partial pressure of  $\text{CO}_2$ . The potential for the As(V)-reducing isolates to respire on As(V) was tested in  $\text{N}_2$ (gas)-purged serum bottles containing column influent media modified to contain 5 mM MOPS buffer (pH = 7.0), 50  $\mu\text{M}$   $\text{NaH}_2\text{PO}_4$ , 1 mg  $\text{L}^{-1}$  yeast extract, 4 mM As(V), and 1 mM cysteine;  $\text{NH}_4\text{NO}_3$  and glucose were replaced with 2.5 mM  $\text{NH}_4\text{Cl}$  and 20 mM lactate, respectively, based on past reports of media used to culture As(V) dissimilatory reducers (35).

#### DNA Extraction, PCR, and DGGE Analysis

Total DNA was extracted from the homogenized soil/sand mixture using the FastDNA SPIN Kit for Soil (Bio 101, Vista, CA). DNA extracts were used as template for polymerase chain reaction (PCR) which targeted a specific 322 bp segment within the

16S rRNA gene. The 1070 forward primer targeted the domain *Bacteria* (*E. coli* positions 1055-1070) and the 1392 reverse-GC primer targeted a universally conserved region (*E. coli* positions 1392-1406; 36). The reverse primer was modified to contain a 40 bp GC-rich clamp to facilitate analysis by DGGE (37). PCR mixtures (50  $\mu$ L) contained 1-5  $\mu$ L template DNA (2-20 ng), 10 mM Tris-HCl (pH 8), 50 mM KCl, 0.1 % Triton X-100, 4.0 mM MgCl<sub>2</sub>, 800  $\mu$ M dNTP's, 0.5  $\mu$ M of each primer, and 1.25 U *Taq* DNA polymerase (Promega, Madison, WI). The protocol was 94 °C for 4 min, 30 cycles of 94 °C, 55 °C and 72 °C each for 45 sec, and a final 7 min extension period at 72 °C.

PCR products were separated by DGGE as described by Ferris et al. (37) with the following modifications. A DCode System (Bio-Rad, Hercules, CA) was used to resolve the PCR products in gels consisting of 8% acrylamide and a 40 - 70% gradient of urea/formamide. Electrophoresis was performed at 60 V at 60 °C for 17 h. DGGE gels were stained with SYBR Green II (Molecular Probes, Eugene, OR) for 30 min and photographed using UV transillumination. DGGE bands of interest were stabbed with a sterile pipet tip and used as template for PCR amplification, purification (repeated PCR amplification and DGGE until a pure band was obtained), and subsequent sequencing reactions. The templates were amplified using primers 1070 forward and 1392 reverse (without the GC clamp) as described above. The product was purified with a QIAquick PCR Purification Kit (Qiagen Inc., Valencia, CA) and the sequencing reaction was carried out using an ABI Prism BigDye Terminator Cycle Sequencing Ready Reaction Kit (Perkin-Elmer, Foster City, CA). The samples were processed on an ABI Prism 310 capillary sequencer (Perkin-Elmer) and the resultant sequences were aligned and edited

using Sequencher 3.1.1 software (Gene Codes Corporation, Ann Arbor, MI). The sequences were then compared with those found in the GenBank database using BLAST (38).

#### Full Length 16S rDNA Amplification and Sequencing of Isolates

Total DNA from each of the isolates was used as template to amplify nearly the entire 16S rRNA gene. Template for PCR was obtained by scraping several colonies with a sterile pipet tip and swirling the tip in 50  $\mu$ L of DNase free water. The suspension was heated at 98 °C for 10 min. and 1.0  $\mu$ L was used as template for PCR. Primers for the initial PCR consisted of the *Bacteria*-specific primer Bac8 forward (5'-AGAGTTTGATCCTGGCTCAG-3') and the universal primer Univ1492 reverse (5'-GGTTACCTTGTTACGACTT-3'). The PCR products were purified with a QIAquick PCR Purification Kit. All primers for the full length sequence reactions were derived from the probes described by Amann et al. (36). Sequencing reactions and analysis were conducted as described above. The near-full length 16S rDNA sequences for the isolates obtained in this study have been submitted to GenBank and have been assigned the accession numbers AF388027 - AF388034.

#### Amplification, Hybridization, and Phylogeny of *arsC* Genes

Three sets of primers for *arsC* genes were designed based on different groupings of *arsC* sequences (23). Sequences of 17 characterized and putative *arsC* genes were obtained from GenBank, and aligned using the ArbEdit Fast Aligner function in the ARB

software package (W. Ludwig and O. Strunk, Technical University of Munich). Primer set 1 was derived from the *arsC* genes of enteric bacteria (5'-ATGAGCAACATYACCAT-3' forward and 5'-TTATTTTCAGYCGTTTACC-3' reverse; corresponding to positions 1-426 of *Escherichia coli arsC*). Primer set 2 was derived from the *arsC* genes of Gram-positive bacteria (5'-ATTTAYTTTATATGYACAG-3' forward and 5'-GATCATCAAACCCCAAT-3' reverse; corresponding to positions 16-317 of the *Bacillus subtilis arsC*). Primer set 3 was derived from the *arsC* genes of *Pseudomonas aeruginosa* and *P. putida* (5'-AGTCCTGTTCATGTGYAC-3' forward and 5'-TGGCGTSGAAYGCCG-3' reverse; corresponding to positions 6-365 of the *P. aeruginosa arsC*). The *arsC* genes of *E. coli* (strain K-12, 21), a *Geobacillus sp.* (isolate from a Yellowstone National Park geothermal soil, accession number for 16S rDNA - AF391973), and *P. aeruginosa* (strain PAO1, 24), were used as controls in amplification reactions using each set of primers. PCR conditions were as described for 16S rRNA gene amplification except for annealing temperature, which was reduced to 37 °C for primer sets 1 and 2, and to 42 °C for primer set 3, and cycle number, which was increased to 35. Attempts were made to amplify *arsC* genes from DNA extracted from each isolate with each primer set. PCR products of positive controls were confirmed as *arsC* genes by sequencing. *E. coli*, and *P. aeruginosa arsC* genes corresponded to previously reported *arsC* sequences in GenBank (accession nos. X80057 and AF010234, respectively). The putative *Geobacillus sp. arsC* gene was novel and was submitted to GenBank (AF393651). PCR products of all three were used as probes for dot-blot hybridizations. Probes were labeled with <sup>32</sup>P using the Megaprime DNA Labeling System (RPN 1606,

Amersham Pharmacia Biotech, Piscataway, NJ). Total DNA from each of the isolates was applied to nylon membranes (GeneScreen Plus, NEN Life Sciences, Boston, MA) using the Bio-Dot Microfiltration Apparatus (BioRad, Hercules, CA), and hybridizations with each probe performed according to the manufacturer's instructions. Probed membranes were visualized using autoradiography with Kodak BioMax MS film (Rochester, NY).

## Results and Discussion

### Column Experiments

Arsenate was the predominant species of As eluted from nonsterile unsaturated columns after three days, regardless of whether they received As(III) or As(V) (Fig. 3.1). The value of the column derived first-order rate constant ( $k$ ) for As(III) oxidation in treatments receiving 75  $\mu\text{M}$  As(III) was determined to be  $> 0.60 \text{ h}^{-1}$  ( $t_{1/2} < 1.2 \text{ h}$ ) using an analytical solution to the advection dispersion equation (equation 9 in ref. 41), assuming that all As(III) was converted to As(V) (detection limit = 0.05  $\mu\text{M}$ ). Although the oxidation of As(III) to As(V) is thermodynamically favored under oxic conditions (42), sterilized treatments did not result in detectable conversion of As(III) to As(V). Consequently, the rapid oxidation of As(III) observed in the nonsterile columns was mediated by microbial processes.

### Molecular Analyses

DGGE was used to obtain DNA fingerprints of microbial populations present in the original soil inoculum and in each of the column enrichments. Replicate DGGE profiles of the untreated soil appeared identical, exhibited numerous bands, and suggested

that numerous microorganisms were present in the original soil inoculum (Fig. 3.2). The As(III) and As(V) treatments produced somewhat different banding patterns, indicating that enrichment conditions, including As speciation and/or concentration, influenced the selection of soil microbial populations. Replicate columns of each As treatment yielded similar DGGE banding patterns, however, differences in band intensity between the

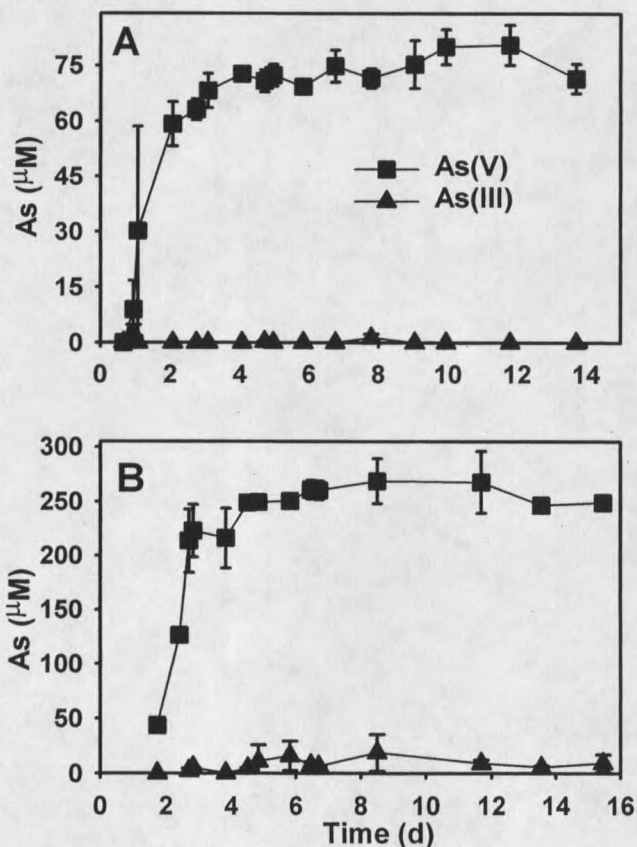


Figure 3.1. Concentrations of As(V) and As(III) in the effluent from unsaturated soil columns receiving either (A) 75  $\mu\text{M}$  As(III) or (B) 250  $\mu\text{M}$  As(V). Error bars are standard errors of duplicate column experiments.

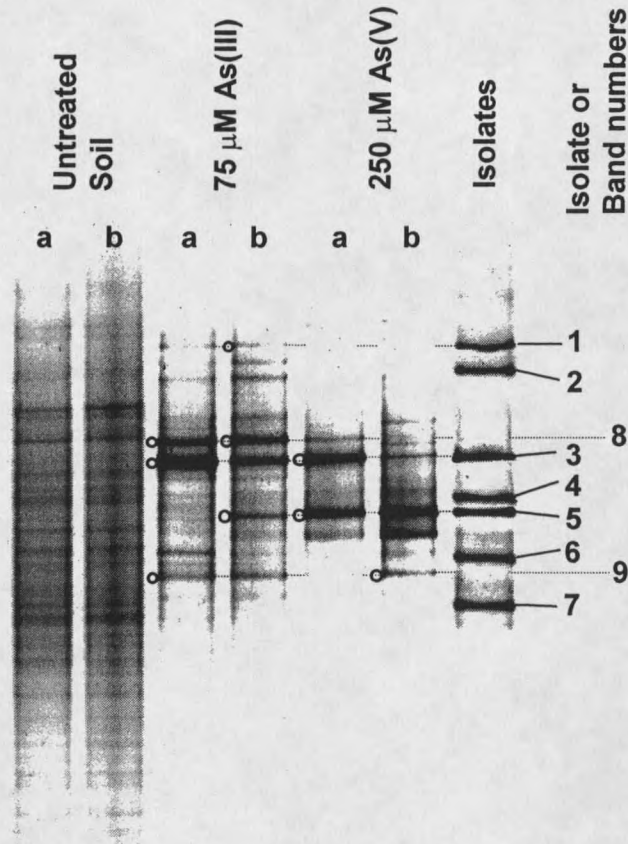


Figure 3.2. Separation of PCR-amplified 16S rDNA fragments using denaturing gradient gel electrophoresis (40–70 %). DNA was derived from either the untreated soil, soil columns (replicates a and b) that had received either 75  $\mu\text{M}$  As(III) (14 d treatment) or 250  $\mu\text{M}$  As(V) (16 d treatment) and As transforming isolates obtained from the columns. Band numbers labeled on the right side of gel correspond to 1) *Variovorax paradoxus*, 2) *Flavobacterium heparinum*, 3) *Pseudomonas fluorescens*, 4) *Microbacterium sp.*, 5) *Agrobacterium tumefaciens*, 6) *Arthrobacter aureescens*, and 7) *Arthrobacter sp.*-like organisms. Bands observed in the soil columns that did not correspond to any isolates represent 8) *Alcaligenes sp.* and 9) *Agrobacterium vitis*-like populations based on comparison of band sequences to entries in the GenBank database. Dashed lines show comigrating bands and open circles indicate bands that were purified and sequenced.

replicates were observed, indicating potential variation in inoculum and/or subsequent column conditions. As with all defined enrichment environments, the chemical and physical attributes of the media select for organisms that are competitive or highly adapted to such conditions. Consequently, use of glucose as a potential C and energy source and the relatively high As concentrations used in these experiments does not necessarily enrich for organisms that may predominate in natural soil environments containing other C substrates and lower As concentrations.

Purification and sequencing of selected bands in the DGGE gels and comparison with sequences in GenBank revealed that the two most prominent bands in the columns supplemented with As(III) represented populations that were 99.4 % similar to *Pseudomonas fluorescens* (band 3) and 99.6 % similar to *Alcaligenes sp.* (band 8, accession no. AF536820) (Fig. 3.2). Less conspicuous bands in this treatment that were successfully purified and sequenced most closely matched *Variovorax paradoxus* (99.5 % identity, band 1), *Agrobacterium tumefaciens* (100 % identity, band 5), and *Agrobacterium vitis* (100 % identity, band 9, accession no. AF536821) populations. Major bands in columns supplemented with As(V) represented *P. fluorescens* (band 3) and *A. tumefaciens* (band 5), while minor bands represented *Alcaligenes sp.* (band 8) and *A. vitis* (band 9) -like populations. Thus, all of the sequenced bands were found in each of the two treatments, with exception of *V. paradoxus*, which was only observed in the As(III)-supplemented columns. The most apparent differences between treatments were decreased intensity of the *Alcaligenes sp.* band (No. 8) and increased intensity of the *A. tumefaciens* band (No. 5) in the As(V) treated columns relative to the As(III) treated

columns. These differences in band intensity suggested that the *Alcaligenes sp.* -like population may have been favored in the presence of As(III) and conversely, the *A. tumefaciens* -like population was favored in the presence of As(V).

### Isolates

Traditional cultivation methods were used to isolate microorganisms from the As treated columns. Serial dilutions of the soil/sand mixture obtained after column enrichment were plated on R2A media and after 72 h, 24 colonies representing 10 different colony morphologies were picked from the most dilute plates ( $10^{-5}$  -  $10^{-4}$  dilutions), and tested for their ability to either oxidize As(III) or reduce As(V). Because all of these isolates were obtained from plates inoculated with dilute serial suspensions, they represented the cultivatable organisms that were enriched as a result of the As(III) or As(V) treatments. As with any cultivation method, the microorganisms selected under specific enrichment conditions, in this case, on R2A media, do not necessarily represent all the populations that were important in the soil columns. Of the 24 bacteria isolated from plates, ten were capable of oxidizing As(III) and ten were capable of reducing As(V). Four others grew poorly in the solution media and were therefore dropped from the experiment. Both the As(III) oxidizing and the As(V) reducing isolates were obtained from columns that received either As(III) or As(V) indicating that As oxidizers or reducers were not limited to a specific treatment (Table 3.1). The fact that both oxidizers and reducers were obtained from the same treatments suggests that As oxidation and reduction may have been occurring simultaneously. These organisms were identified by near-full length sequencing of their 16S rRNA genes, revealing that a total of three

Table 3.1. Closest GenBank neighbors and sequence similarities (16S rDNA) of isolates cultivated from unsaturated soil columns. Isolates were obtained from treatments indicated with checkmark and detection of their 16S rDNA sequences in soil columns is indicated. Rates of As(III) oxidation and As(V) reduction demonstrated by isolates were measured during logarithmic growth under aerated serum bottle conditions.

Isolate or DGGE band number	Isolate Accession Number	Closest GenBank neighbor (% Similarity) <sup>a</sup>	DNA sequences detected in columns <sup>b</sup>	Column treatment from which isolates were obtained		As(III) oxidation / As(V) reduction parameters	
				As(III)	As(V)	Rate <sup>c</sup> ( $\mu\text{mol d}^{-1} \text{cell}^{-9}$ )	Half-life <sup>d</sup> (d)
<u>As(III) Oxidizing Isolates</u>							
1	AF388028	<i>Variovorax paradoxus</i> (99.3)	yes	√		1.7	0.5
3	AF388027	<i>Pseudomonas fluorescens</i> (99.1)	yes	√	√	1.4	0.2
5A	AF388033	<i>Agrobacterium tumefaciens</i> (99.9)	yes		√	0.7	0.3
<u>As(V) Reducing Isolates</u>							
2	AF388029	<i>Flavobacterium heparinum</i> (94.9)	no	√		0.5	0.6
4	AF388031	<i>Microbacterium sp</i> (98.1)	no		√	2.4	0.2
5B	AF388030	<i>Agrobacterium tumefaciens</i> (99.9)	yes	√	√	3.3	0.1
6	AF388032	<i>Arthrobacter aureescens</i> (99.6)	no	√	√	2.9	0.1
7	AF388034	<i>Arthrobacter sp.</i> (97.8)	no		√	1.6	0.2

<sup>a</sup> Closest GenBank neighbors and similarities of near full-length 16S rDNA sequences of isolates were determined using BLAST (38). <sup>b</sup> 16S rDNA sequences in columns were analyzed by purifying and sequencing DGGE bands derived from PCR amplification of DNA extracts. <sup>c</sup> Rates normalized to cell number using an empirically-developed relationship between cell enumeration with phase contrast microscopy and optical density (OD) measurements (A500) of cell suspensions. <sup>d</sup> Apparent half-lives ( $t_{1/2}$ ) are dependent on experimental conditions and are estimated based on rates assuming pseudo first-order reaction dependent on As(III) (oxidizing isolates) or As(V) (reducing isolates).

different As(III) oxidizing populations and five different As(V) reducing populations were represented by these isolates (Table 3.1). BLAST searches showed that the closest matches to the three As(III) oxidizers were *Pseudomonas fluorescens*, *Variovorax paradoxus*, and *Agrobacterium tumefaciens*. The closest GenBank matches to the five As(V) reducing isolates were *Flavobacterium heparinum*, *A. tumefaciens*, *Microbacterium sp.*, *Arthrobacter aureescens*, and *Arthrobacter sp.* The *Pseudomonas* and *Agrobacterium* genera contain members that were previously shown to have As transforming capabilities (11, 21). Interestingly, the two *A. tumefaciens* isolates that exhibited opposite As redox phenotype have identical 16S rDNA sequences (across ~1400 bp). Further discussion regarding these two strains follows below. The similarity in colony morphology between the *A. tumefaciens* isolates as well as among other isolates prevented attempts to enumerate specific populations from either column based on colony forming units (CFU).

#### Correlating Isolates with Column Populations

Sequences of 16S rDNA fragments amplified from nucleic acid extracts of column samples were compared to sequences of As transforming isolates described above. These comparisons showed that three DGGE bands present in the column treatments represented 16S rDNA sequences that were 100 % identical to the *V. paradoxus* (band 1), *P. fluorescens* (band 3), and *A. tumefaciens* (band 5)-like isolates (Fig. 3.2), all of which were As(III) oxidizers. However, with exception of the *A. tumefaciens* band (No. 5), no DGGE bands corresponding to other As(V) reducing isolates were observed in DGGE profiles. The direct identification of As(III) oxidizing

populations in the column environments using molecular methods was consistent with the microbial oxidation of As(III) observed during solute transport. However, the fact that two strains of *A. tumefaciens* [an As(III) oxidizer and an As(V) reducer] could not be differentiated by DGGE, and that other As(V) reducers were isolated from these columns precludes a conclusion that only As(III) oxidizing microorganisms were relevant to the net As redox output observed in these columns. Template bias (43) may have reduced the sensitivity of the molecular approach, and may explain the lack of detection of As(V) reducing populations using PCR-DGGE. Furthermore, detection of the As(V) reducing populations using DGGE was potentially limited by the addition of ~ 100 ng total DNA per lane; it is possible that higher quantities of DNA may have allowed detection of these bands, although overall band resolution may have suffered. Regardless of the actual population size of As(V) reducing organisms in the soil columns, the combined metabolic activity of the As(V) reducers failed to dominate the net As redox activity in the column communities.

#### Rates of As Transformation by Bacteria

Rates of As(III) oxidation or As(V) reduction by each of the eight isolates cultivated from the column environments were measured in continuously aerated serum bottles (Fig. 3.3). Rates of As(III) oxidation during logarithmic growth of the three As(III) oxidizing isolates varied from 0.7 to 1.7  $\mu\text{mol d}^{-1}$  per  $10^9$  cell with corresponding As(III) half-lives ranging from 0.2 to 0.5 d (Table 3.1). In comparison, rates of As(V) reduction by the five As(V) reducing isolates ranged from 0.5 to 3.3  $\mu\text{mol d}^{-1}$  per  $10^9$  cell (half-lives of 0.1 – 0.6 d; Table 3.1). Assuming that As(III) oxidation was the only transformation

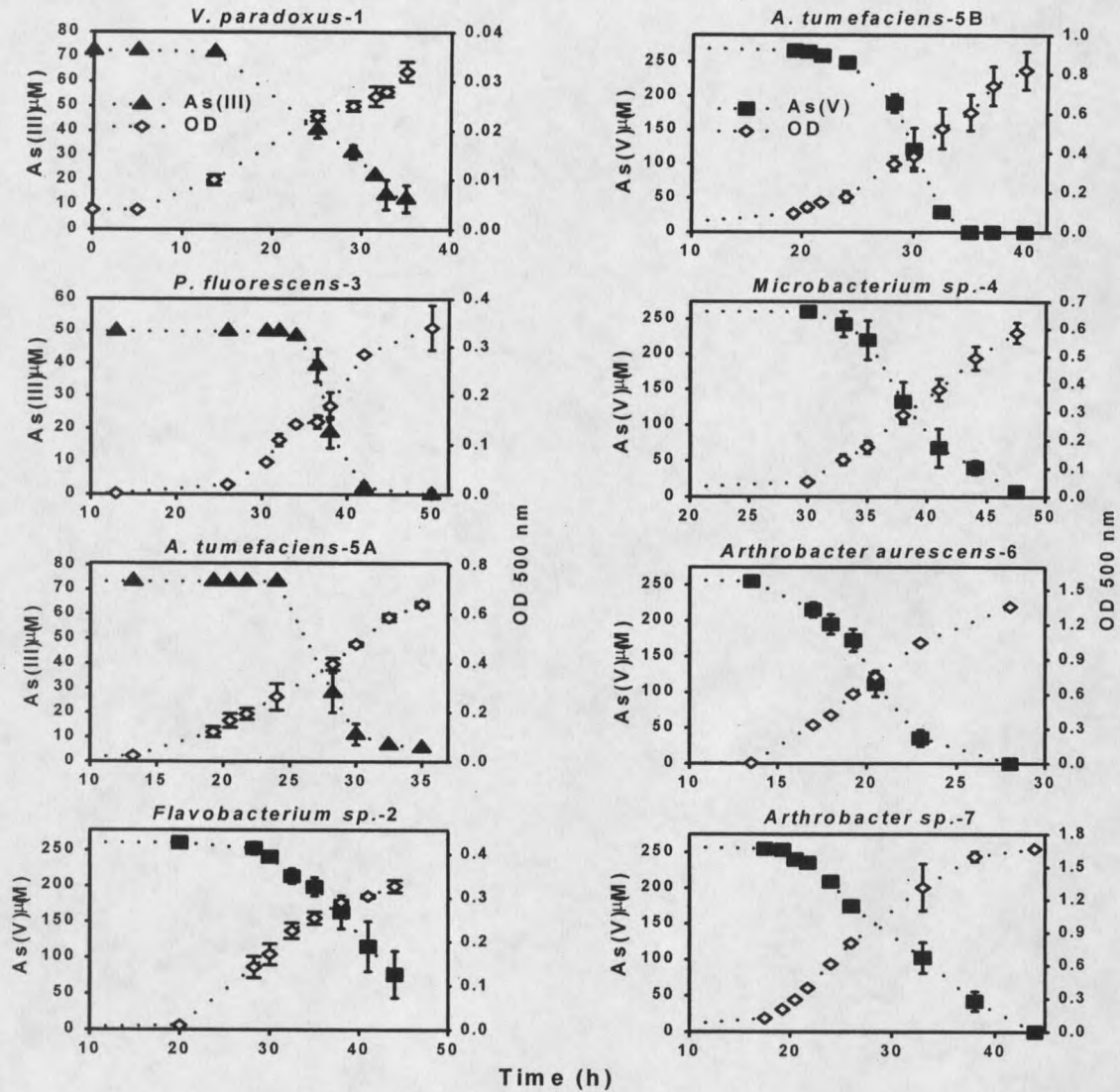


Figure 3.3. Microbial biomass (as OD 500 nm,  $\diamond$ ) and As(III) [ $\blacktriangle$ ] or As(V) [ $\blacksquare$ ] concentrations as a function of time for three As(III)-oxidizing isolates and five As(V)-reducing isolates incubated under aerated serum bottle conditions. Total concentrations of As in solution ( $[\text{Total As}] = [\text{As(III)}] + [\text{As(V)}]$ ) remained nearly constant during each experiment. Isolates are named after their nearest match found in the GenBank database. Error bars represent standard errors of three replicate serum bottle experiments for *P. fluorescens* and two replicate serum bottle experiments for all other isolates.

process in the soil column experiments, the number of As(III)-oxidizing organisms required to support the column-derived As(III) oxidation rates was estimated to range from  $1 - 3 \times 10^8$  cells/g soil, based on the As(III) oxidation rates obtained for each of the As(III)-oxidizing isolates (Table 3.1). Although this estimate assumes that the physiological status of the isolates was similar in pure culture to that under column conditions, it suggests that either of the three oxidizing isolates would be capable of supporting the oxidation of As(III) observed in the soil columns, either acting individually or in concert.

#### Mechanisms of As Oxidation/Reduction

No oxidation of As(III) was observed in sterile controls or in experiments using cell-free filtrate taken from isolate suspensions that were actively oxidizing As(III), indicating the observed As(III) oxidation required the presence of microbial cells. In addition, none of the As(III) oxidizing isolates grew in media designed for chemolithotrophic metabolism using As(III) as the sole electron donor (same medium as used during column enrichment except glucose was replaced by  $\text{CO}_2$  and As(III) was increased to provide adequate energy source). This result, taken together with the fact that As(III) oxidation profiles for each isolate corresponded with microbial growth (Fig. 3.3) suggests that the mechanism of As(III) oxidation by these isolates was related to As detoxification rather than energy generation. Likewise, none of the As(V)-reducing isolates could grow in media designed for dissimilatory As(V) reduction, where lactate served as the primary C and energy source and As(V) was present as the primary electron acceptor. This result was not surprising considering that the isolated organisms were

enriched under aerobic conditions. Although these findings must be tempered with the possibility that some or even all of these bacteria may utilize As for energy metabolism in different media, under the conditions tested here, none of these organisms demonstrated energy conserving reactions with As. Thus, all of the bacteria isolated from the As supplemented columns demonstrated the capacity to either oxidize As(III) or reduce As(V), apparently for detoxification purposes.

Hybridization experiments using *arsC* probes derived from *P. aeruginosa*, *Geobacillus*, and *E. coli*, for dot blots of DNA obtained from the soil isolates did not reveal significant homology under low stringency wash conditions (65 °C, 2X SSC; Fig. 3.4). Conversely, positive controls using total DNA extracts from *P. aeruginosa*, *Geobacillus*, and *E. coli* produced strong hybridization signals with their respective probes. The failure of these *arsC* probes to hybridize with DNA from the soil isolates is consistent with the enormous diversity of known *arsC* sequences (e.g., 9, 23-27), and the fact that this diversity may preclude detection of *arsC* homologs using probes designed from phylogenetically different organisms.

Recent hybridization experiments by Dr. Timothy McDermott and Lina Botero using an *arsC* probe derived from *arsC* annotated in the genome of *A. tumefaciens* strain C58, revealed significant homology between the *A. tumefaciens arsC* probe and the DNA from the *A. tumefaciens* isolates (5A and 5B). They further characterized the apparent *arsC* homologs in these *A. tumefaciens* isolates by PCR amplification and sequencing (accession nos.: AY286230 for isolate 5B, AY286231 for isolate 5A). The nucleotide sequences of these putative *arsC* genes (375 nucleotides) were 99.2% identical to each

other, and their inferred amino acid sequences were 80% identical and 88% similar to the annotated *arsC* in *A. tumefaciens* (across 124 amino acids). Amino acid alignments showed the cloned *A. tumefaciens arsC* genes shared extensive homology with the well characterized *arsC* from *E. coli*, including the highly conserved amino acids Cys12, Ser15, Arg60, Arg94, and Arg107 (*E. coli* p773 *arsC* numbering) found to be essential for activity in several ArsCs (44). Phylogenetic analysis of the cloned partial *arsC* genes unambiguously placed both as sharing a common node with the *A. tumefaciens* strain C58 *arsC* and separate from the other closely related *arsC* genes.

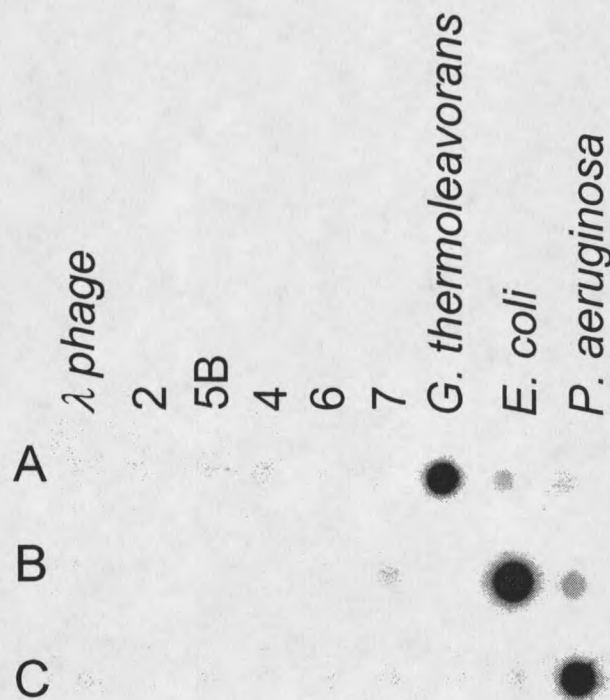


Figure 3.4. Hybridization of  $^{32}\text{P}$ -labeled probes prepared from *B. thermoleavorans*, *E. coli*, and *P. aeruginosa arsC* genes (rows A, B, and C, respectively) to dot blots of  $\lambda$  phage *Hind*III digested DNA (negative control), and genomic DNA extracted from each As(V) reducing isolate (2-*F. heparinum*, 5B- *A. tumefaciens*, 4-*Microbacterium* sp., 6-*Arthrobacter aurescens*, and 7-*Arthrobacter* sp.) and from *B. thermoleavorans*, *E. coli*, and *P. aeruginosa* (positive controls) are labeled at the top.

Interestingly, both of the *A. tumefaciens* isolates were shown to contain a putative *arsC*, despite the fact that isolate 5A did not exhibit As(V) reduction. The apparent lack of As(V) reduction in the As(III) oxidizing *A. tumefaciens* isolate may be due to a variety of reasons including point mutations in *arsC* or separation of *arsC* from its As derepressible promoter. Given that the two *arsC* genes cloned from the different *A. tumefaciens* isolates shared 100% amino acid identity across that portion of the gene amplified and sequenced in this study, any putative mutation would have to be external to this part of the *arsC* coding region. An alternative explanation may be that the *arsC* gene in the As(III) oxidizing isolate became separated from an As derepressible promoter due to a genomic rearrangement event that are now known to be common in bacteria (45, 46), including the Rhizobiaceae (47, 48). It is also possible that the opposite As redox activity of the two *A. tumefaciens* strains is due to the presence, absence, or differential expression of an As(III) oxidase gene. The As(V) reducing strain either may lack the genes required for As(III) oxidation, or may not have significantly expressed these genes under the conditions studied herein. Studies are currently under way in the McDermott laboratory to examine the genetic differences between these *A. tumefaciens* strains, and to assess whether mutation, lateral gene transfer events, or other factors may explain the different As phenotypes.

#### Implications for As Cycling in Soils

Eight heterotrophic, aerobic As-transforming bacteria representing diverse genera in the gram-positive, flavobacteria, and proteobacteria kingdoms were isolated from soil column enrichments and characterized. None of the five As(V)-reducing isolates grew on

media designed for dissimilatory As(V) reduction, and the three As(III)-oxidizing isolates did not grow in media with As(III) as the primary electron donor for chemolithotrophic metabolism. Based on reported mechanisms of As oxidation-reduction activity among microorganisms (44, 49), these results suggest that both the As(V)-reducing and As(III)-oxidizing isolates were transforming As via detoxification mechanisms as opposed to energy generation. Although we were able to cultivate both As(V)-reducing and As(III)-oxidizing bacteria from the column environments, As(III) oxidizing populations apparently dominated the observed net As redox activity and represented the primary 16S rDNA sequences that were detected in column samples using molecular methods.

The coexistence of both As(III) oxidizing and As(V) reducing aerobic populations in the same soil suggests that the relative numerical and or metabolic dominance of these populations will influence the predominant As valence state. The isolation of both As(III) oxidizing and As(V) reducing *A. tumefaciens* strains from the same column enrichment (Table 3.1) shows that the ability to either oxidize As(III) or reduce As(V) is variable even among strains that proliferate under the same environmental conditions. Because of such variation in phenotype within similar organisms, phylogenetic identification of microorganisms based on 16S rRNA sequence analysis is not sufficient to predict the redox transforming capabilities of specific bacterial populations. Further, As contamination in oxic environments may not select for microorganisms capable of utilizing As in energy metabolism, but rather, may shift the microbial community structure to favor organisms capable of detoxification either via As oxidation or reduction. Specifically, the broad phylogenetic distribution of *arsC* genes suggests that

the importance of nondissimilatory As(V) reduction may be underestimated as a mechanism of As redox cycling in natural systems. Results from the current study, as well as other recent examples (17, 18), support the hypothesis that the oxidization and reduction of As occurs in phylogenetically diverse soil bacteria via mechanisms that are not directly associated with respiration or chemolithotrophic metabolism.

## REFERENCES CITED

1. Masscheleyn, P.H., R.D. Delaune, and W.H.Jr. Patrick. 1991. Effect of redox potential and pH on arsenic speciation and solubility in a contaminate soil. *Environ. Sci. Technol.* 25:1414-1419.
2. Nriagu, J. O. 1994. *Arsenic in the Environment. Part II: Human Health and Ecosystem Effects.* Wiley: New York.
3. Pierce, M.L., and C.B. Moore. 1982. Adsorption of arsenite and arsenate on amorphous iron hydroxide. *Water Res.* 16:1247-1253.
4. Tamaki, S., and W.T.Jr. Frankenberger. 1992. Environmental biochemistry of arsenic. *Rev. Environ. Contam. Tox.* 124:79-110.
5. Abdrashitova, S.A., B.N. Mynbaeva, B.B. Aidarkhanov, and A.N. Ilyaletdinov. 1990. *Mikrobiologiya* 59:234-240.
6. Ahmann, D., A.L. Roberts, L.R. Krumholz, and F.M.M. Morel. 1994. Microbe grows by reducing arsenic. *Nature* 371:750.
7. Anderson, G.L., J. Williams, and R. J. Hille. 1992. The purification and characterization of arsenite oxidase from *Alcaligenes faecalis*, a molybdenum-containing hydroxylase. *Biol. Chem.* 267:23674-23682.
8. Santini, J.M., L.I. Sly, R.D. Schnagl, and J.M. Macy. 2000. A new chemolithotrophic arsenite-oxidizing bacterium isolated from a gold mine: phylogenetic, physiological, and preliminary biochemical studies. *Appl. Environ. Microbiol.* 66:92-97.
9. Silver, S., L.T. Phung, and B.P. Rosen. 2002. Arsenic metabolism: resistance, reduction, and oxidation. In *Environmental Chemistry of Arsenic*; Frankenberger, W. T. Jr. Ed.; Marcel Dekker: New York, pp. 247-272.
10. Stolz, J.F., and R.S. Oremland. 1999. Bacterial respiration of arsenic and selenium. *FEMS Microbiol. Rev.* 23:615-627.
11. Salmassi, T.M., K. Venkateswaren, M. Satomi, K.H. Nealson, D.K. Newman, and J.G. Hering. 2002. Oxidation of arsenite by *Agrobacterium albertimagni*, AOL15, sp. nov., isolated from Hot Creek, California. *Geomicrobiol. J.* 19:53-66.
12. Ellis, P.J., T. Conrads, R. Hille, and P. Kuhn. 2001. Crystal structure of the 100 kDa arsenite oxidase from *Alcaligenes faecalis* in two crystal forms at 1.64 angstrom and 2.03 angstrom. *Structure.* 9:125-132

13. Gihring, T.M., and J.F. Banfield. 2001. Arsenite oxidation and respiration by a new *Thermus* isolate. *FEMS Microbiol. Let.* 204:335-340.
14. Newman, D.K., D. Ahmann, and F.M.M. Morel. 1998. A brief review of microbial arsenate respiration. *Geomicrobiol. J.* 15:255-268.
15. Niggemyer, A., S. Spring, E. Stackebrandt, and R.F. Rosenzweig. 2001. Isolation and characterization of a novel As(V)-reducing bacterium: Implications for arsenic mobilization and the genus *Desulfitobacterium*. *Appl. Environ. Microbiol.* 67:5568-5580.
16. Huber, R., M. Sacher, A. Vollmann, H. Huber, and D. Rose. 2000. Respiration of arsenate and selenate by hyperthermophilic archaea. *System. Appl. Microbiol.* 23:305-314.
17. Jones, C.A., H.W. Langner, K. Anderson, T.R. McDermott, and W.P. Inskeep. 2000. Rates of microbially mediated arsenate reduction and solubilization. *Soil Sci. Soc. Am. J.* 64:600-608.
18. Macur, R.E., J.T. Wheeler, T.R. McDermott, and W.P. Inskeep. 2001. Microbial populations associated with the reduction and enhanced mobilization of arsenic in mine tailings. *Environ. Sci. Technol.* 35:3676-3682.
19. Macy, J.M., J.M. Santini, B.V. Pauling, A.H. O'Neill, and L.I. Sly. 2000. Two new arsenate/sulfate-reducing bacteria: mechanisms of arsenate reduction. *Arch. Microbiol.* 173:49-57.
20. Cervantes, C., G. Ji, J.L. Ramirez, and S. Silver. 1994. Resistance to arsenic compounds in microorganisms. *FEMS Microbiol. Rev.* 15:355-367.
21. Diorio, C., J. Cai, J. Marmor, R. Shinder, and M.S. DuBow. 1995. An *Escherichia coli* chromosomal *ars* operon homolog is functional in arsenic detoxification and is conserved in gram-negative bacteria. *J. Bacteriol.* 177:2050-2056.
22. Silver, S., K. Budd, K.M. Leahy, W.V. Shaw, D. Hammond, R.P. Novick, G.R. Willsky, M.H. Malamy, and H. Rosenberg. 1981. Inducible plasmid-determined resistance to arsenate, arsenite and antimony(III) in *Escherichia coli* and *Staphylococcus aureus*. *J. Bacteriol.* 146:983-996.
23. Butcher, B.G., S.M. Deane, and D.E. Rawlings. The chromosomal arsenic resistance genes of *Thiobacillus ferrooxidans* have an unusual arrangement and confer increased arsenic and antimony resistance to *Escherichia coli*. *Appl. Environ. Microbiol.* 66:1826-1833.

24. Cai, J., K. Salmon, and M.S. DuBow. 1998. A chromosomal *ars* operon homologue of *Pseudomonas aeruginosa* confers increased resistance of to arsenic and antimony I *Escherichia coli*. *Microbiol.* 144:2705-2713.
25. Neyt, C., M. Iriarte, V.H. Thi, and G.R. Cornelis. 1997. Virulence and arsenic resistance in *Yersinia*. *J. Bacteriol.* 179:612-619.
26. Sato, T., and Y. Kobayashi. 1998. The *ars* operon in the skin element of *Bacillus subtilis* confers resistance to arsenate and arsenite. *J. Bacteriol.* 180:1655-1661.
27. Jackson, C.R., and S.L. Dugas. 2003. Phylogenetic analysis of bacterial and archaeal *arsC* gene sequences suggests an ancient, and common origin for arsenate reductase. *BMC Evol. Biol.* 3:18-28.
28. Cullen, W.R., and K.J. Reimer. 1989. Arsenic speciation in the environment. *Chem. Rev.* 89:713-764.
29. Sohrin, Y., M. Matsui, M. Kawashima, M. Hojo, and H. Hasegawa. 1997. Arsenic biogeochemistry affected by eutrophication in Lake Biwa, Japan. *Environ. Sci. Technol.* 31:2712-2720.
30. Osborne, F.H., and H.L. Ehrlich. 1976. Oxidation of arsenite by a soil isolate *Alcaligenes*. *J Appl. Bacteriol.* 41:295-305.
31. Jones, C. A., W.P. Inskeep, J.W. Bauder, and K.E. Keith. 1999. Arsenic solubility and attenuation in soils of the Madison River basin, Montana: Impacts of long-term irrigation. *J. Environ. Qual.* 28:1314-1320.
32. Nimick, D.A. 1998. Arsenic hydrogeochemistry in an irrigated river valley: A reevaluation. *Ground Water.* 36:743.
33. Angle, J.S., S.P. McGrath, and R.L. Chaney. 1991. New culture medium containing ionic concentrations of nutrients similar to concentrations found in the soil solution. *Appl. Environ. Microbiol.* 57:3674-3676.
34. Skerman, V.B.D. 1967. A guide to the identification of the genera of bacteria. The Williams and Wilkins Co.: Baltimore, MD.
35. Newman, D.K., T.J. Beveridge, and F.M.M. Morel. 1997. Precipitation of arsenic trisulfide by *Desulfotomaculum auripigmentum*. *Appl. Environ. Microbiol.* 63:2022-2028.
36. Amann, R.I., W. Ludwig, and K.H. Schleifer. 1995. Phylogenetic identification and in situ detection of individual cells without cultivation. *Microbiol. Rev.* 59:143-169.

37. Ferris, M.J., G. Muyzer, and D.M. Ward. 1996. Denaturing gradient gel electrophoresis profiles of 16S rRNA-defined populations inhabiting a hot spring microbial mat community. *Appl. Environ. Microbiol.* 62:340-346.
38. Altschul, S.F., T.L. Madden, A.A. Schaffer, J. Zhang, Z. Zhang, W. Miller, and D.J. Lipman. 1997. Gapped BLAST and PSI-BLAST: a new generation of protein database search programs. *Nucleic Acid Res.* 25:3389-3402.
39. Inskeep, W.P., T.R. McDermott, and S. Fendorf. 2002. Arsenic (V)/(III) cycling in soils and natural waters: chemical and microbiological processes, p. 183-215. *In* W. T. Frankenberger, Jr. (ed.), *Environmental Chemistry of Arsenic*. Marcell Dekker, Inc., New York, N.Y.
40. Macur, R.E., T.R. McDermott, and W.P. Inskeep. 2000. Microbially mediated arsenic cycling in a contaminated soil. 2000 Annual Meetings Abstracts of the Soil Science Society of America: Madison, WI.
41. Langner, H.W., W.P. Inskeep, H.M. Gaber, W.L. Jones, B.S. Das, and J.M. Wraith. 1998. Pore water velocity and residence time effects on the degradation of 2,4-D during transport. *Environ. Sci. Technol.* 32:1308-1315.
42. Holm, T.R., and C.D. Curtiss. 1989. A comparison of oxidation-reduction potentials calculated from the As(V)/As(III) and Fe(III)/Fe(II) couples with measured platinum-electrode potentials in groundwater. *J. Contam. Hydro.* 5:67-81.
43. Suzuki, M.T., and S.J. Giovannoni. 1996. Bias caused by template annealing in the amplification of mixtures of 16S rRNA genes by PCR. *Appl. Environ. Microbiol.* 62:625-630.
44. Mukhopadhyay, R., B.P. Rosen, L.T. Phung, and S. Silver. 2002. Microbial arsenic: from geocycles to genes and enzymes. *FEMS Microbiol. Rev.* 26:311-325.
45. Borst, P., and D.R. Greaves. 1987. Programmed gene rearrangements altering gene expression. *Science.* 235:658-667.
46. Campo, N., M.L. Daveran-Mingot, K. Leenhouts, P. Ritzenthaler, and P. Le Bourgeois. 2002. Cre-loxP recombination system for large genome rearrangements in *Lactococcus lactis*. *Appl. Environ. Microbiol.* 68:2359-2367.
47. Jumas-Bilak, E., S. Michaux-Charachon, G. Bourg, M. Ramuz, and A. Allardet-Servent. 1998. Unconventional genomic organization in the alpha subgroup of the Proteobacteria. *J. Bacteriol.* 180:2749-2755.

48. Mavingui, P., M. Flores, X. Guo, G. Da ´vila, X. Perret, W.J. Broughton, and R.J. Palacios. 2002. Dynamics of genome architecture in *Rhizobium* sp. strain NGR234. *Bacteriol.* 184:171-176.
49. Oremland, R.S., and J.S. Stolz. 2003. The ecology of arsenic. *Science.* 300:939-944.

## CHAPTER 4

LINKING GEOCHEMICAL PROCESSES WITH MICROBIAL COMMUNITY  
ANALYSIS: SUCCESSIONAL DYNAMICS IN AN ARSENIC-RICH ACID-  
SULFATE-CHLORIDE GEOTHERMAL SPRINGIntroduction

Source waters of geothermal springs are generally far from thermodynamic equilibrium with respect to earth-surface conditions, resulting in thermal and chemical energy gradients that drive a variety of abiotic and microbially mediated reactions. Many chemical constituents present in geothermal waters undergo abiotic reactions including oxidation reactions with  $O_2$ , and release of oversaturated constituents via degassing or precipitation. Many of the oxidation-reduction processes important in geochemical cycling are also catalyzed by microorganisms, where reduced species such as  $H_2$ ,  $H_2S$ ,  $S^0$ ,  $Fe(II)$  and  $As(III)$  may serve as electron donors for energy conservation, and oxidized species such as  $O_2$ ,  $NO_3^-$ ,  $SO_4^{2-}$ , and  $As(V)$  may be reduced during respiration. In addition, potentially toxic trace elements such as As may be transformed by microbial processes associated with detoxification rather than energy conservation (1). In many cases, the relative importance of abiotic and biotic processes varies for specific constituents as a function of temperature and distance down gradient from spring discharge, creating numerous unique thermal and geochemical environments that serve as niches for possible microbial colonization.

The source waters of ASC geothermal springs located in the Norris Geyser Basin of Yellowstone National Park (YNP) contain variable concentrations of reduced chemical

species including  $H_2$ ,  $H_2S$ , As(III) and Fe(II) in a background solution containing millimolar levels of  $Na^+$ ,  $SO_4^{2-}$  and  $Cl^-$  (2-4). The combination of high temperature, low pH (~3), high sulfide, high As(III) and elevated levels of other trace elements such as B create an extreme environment where chemolithoautotrophs dependent on inorganic constituents for energy generation and  $CO_2$  as a C source constitute the dominant primary producers (4, 5). Microorganisms adapted to these unique and extreme geothermal environments may exhibit metabolic strategies that are quite different than those used by many of the microorganisms in culture (e.g., 5-7). Consequently, considerable effort has recently focused on describing novel 16S rDNA sequences and or isolates from extreme environments, as well as the ecology and geochemistry of these unusual habitats (e.g., 4-9).

Recent molecular and geochemical characterization of a representative ASC thermal spring (Dragon Spring) in Norris Basin showed that microbial mat communities changed dramatically with distance down the outflow channel correlating with major changes in aqueous and solid phase geochemistry (4, 9). While no As(III) oxidation was observed within the  $S^0$  depositional zone (0 - 3 m), *in situ* microbial oxidation of As(III) to As(V) occurred at rates faster than ever reported for natural waters immediately down gradient (4 - 5 m, half-lives ~ 0.6 min, 4, 10). Results from electron microscopy (SEM/EDAX), x-ray diffraction (XRD) and x-ray photoelectron spectroscopy (XPS) showed that the microbial mats in this region were composed of an x-ray amorphous hydrous ferric oxide (HFO) phase containing 0.6 - 0.7 mole ratio As:Fe, among the highest As contents observed in naturally occurring HFO's (11, 12). Phylogenetic analysis of 16S rDNA cloned from these microbial mat communities suggested that

*Hydrogenobaculum*, *Desulfurella*, *Acidimicrobium ferrooxidans*, and *Meiothermus*-like populations were important organisms inhabiting the different microenvironments within the spring (9). In addition, six archaeal 16S rDNA sequences were identified that exhibited poor matches (mean similarity ~ 90 %) to currently known sequences from hydrothermal vents and terrestrial hot springs. Consequently, it was difficult to infer the potential role of these novel organisms in mat development and or geochemical cycling. More generally, direct links between microbial populations and the unique chemical processes occurring in geothermal springs has been limited (8).

Examination of microbial and geochemical changes occurring during reestablishment of microbial mats following disturbance has served as a useful tool for elucidating the function of individual microbial populations in hot springs (13, 14). For example, Ferris et al. (14) used molecular techniques to assess changes in cyanobacterial populations after microbial mat removal. The apparent physiology and ecological role of specific populations was determined by coupling molecular information with measurements of O<sub>2</sub> production/consumption and <sup>14</sup>CO<sub>2</sub> partitioning over time. In the current study, a similar strategy was used to identify microbial populations associated with geochemical cycling of H<sub>2</sub>, S, As and Fe in an acidic geothermal spring. Specifically, the objectives of this study were to, (i) correlate the distribution of bacterial and archaeal sequences in time and space with changes in temperature and geochemical energy gradients occurring throughout the outflow channel of an ASC geothermal spring, (ii) identify microorganisms responsible for rapid rates of *in situ* As(III) oxidation, and (iii) determine the microorganisms and processes responsible for the formation of As-rich HFO mats. These objectives were addressed by monitoring changes in aqueous and solid

phase geochemistry, and 16S rDNA sequence distribution occurring during microbial colonization and mat establishment in a newly formed discharge channel. The suite of complementary analyses included 16S rDNA molecular fingerprinting using denaturing gradient gel electrophoresis (DGGE) and subsequent 16S rDNA sequence analysis, along with a variety of chemical, microscopic, and spectroscopic techniques.

### Materials and Methods

#### Site Description and Sampling Procedures

The acid-sulfate-chloride (ASC) geothermal spring selected for this study, referred to as Succession Spring (44° 43' 75.7" N. Latitude, 110° 42' 74.7" W. Longitude), is geochemically typical of many ASC springs found in the Hundred Springs Plain of Norris Geyser Basin, Yellowstone National Park. On July 18, 2001, discharge water from this small spring (source pool approximately 17 cm in diameter and 3 cm deep in the center, flow rate  $\sim 7$  liter  $\text{min}^{-1}$ ) was redirected into a new channel through siliceous sandy parent material characteristic of Norris Basin. The new channel was approximately 9 cm wide, a maximum of 1 cm deep, and extended approximately 15 m before mixing with runoff from adjacent springs. Immediately after redirecting the flow, a series of glass slides (1 x 4 x 50 mm) were placed in the new channel 0, 2, 4, 8, and 12 m from the spring source pool to serve as surfaces for growth of microbial mats and deposition of solid phases. Chemical and microbial changes were evaluated at ten dates from July 18 through October 29, 2001. At each sampling date, two sets of glass slides were removed from the channel, placed in 15 mL sterile tubes, and immediately frozen (placed on dry ice until storage at -80 °C). The slides were subsequently utilized for

physical, chemical, and molecular characterization of adhering microbial mats and solid phases (described below). At the same dates, aqueous samples were collected from positions 0, 2, 4, 6, 8, 12, and 14 m from the source pool and used for a suite of chemical analyses.

### Aqueous Phase Chemistry

At each sampling date, *in situ* measurements of temperature and temperature-compensated pH were made with a Mettler Toledo MA130 portable pH meter fitted with a Mettler Toledo IP67 NTC electrode and calibrated using pH 1.68 and 4.01 buffers. Samples used for aqueous phase analysis were withdrawn from selected positions in the spring using a 20 mL syringe. Total dissolved sulfide (15) was analyzed by aliquoting a 7.5 mL subsample into a glass test tube containing 0.5 mL diamine sulfuric acid reagent and immediately adding 4 drops of FeCl<sub>3</sub> reagent. The tube was slowly inverted once, and after 4 min, 1.6 mL of 3.8 M (NH<sub>4</sub>)<sub>2</sub>HPO<sub>4</sub> was added. Absorbance (664 nm) was measured in the laboratory within 30 h of sampling. Total Fe and Fe(II) in 5 mL filtered (0.22 μm) aliquots were analyzed on site using the FerroZine method (16). Absorbance of the FerroZine-Fe(II) complex was measured at 562 nm within 1 h of sampling. Ion chromatography (IC) was used to determine the concentration of predominant anions (F<sup>-</sup>, Cl<sup>-</sup>, SO<sub>4</sub><sup>2-</sup>, NO<sub>3</sub><sup>-</sup>, CO<sub>3</sub><sup>2-</sup>, AsO<sub>4</sub><sup>3-</sup>) within 1 h of sampling [Dionex DX500 Chromatography System, 25 L injection loop, AS16-4 mm ion exchange column (Dionex Corp., Sunnyvale, CA), eluant gradient of 20 to 50 % 100 mM NaOH]. Total As was also determined with IC using samples pretreated with KMnO<sub>4</sub> to oxidize As(III) to As(V). Selected aqueous samples were analyzed for Na, K, Ca, Mg, Fe, Si, Al, B, S, P, As, Cd,

Cr, Cu, Mn, Ni, Pb, Sb, Se, and Zn using inductively coupled plasma atomic emission spectrometry (ICP-AES). Values for total As determined using ICP were consistently within 10 % of values measured with IC. Dissolved organic C (DOC) was measured with a DC-80 carbon analyzer (Tekmar-Dohrmann, Cincinnati, OH) after acidifying to 70 mM  $\text{H}_3\text{PO}_4$  and purging with  $\text{O}_2$  for 5 min to remove dissolved carbonate species. Colorimetric analysis of  $\text{NH}_4^+$ -N was performed with a Lachat auto analyzer. Aqueous  $\text{H}_2$  was measured within 18 h after completely filling 72 mL serum bottles with source water and capping. Prior to analysis, serum bottles (stored at 4 °C) were brought to room temperature (21 °C) and a known volume of liquid was removed and replaced with an equal volume of  $\text{N}_2(\text{g})$ . After the sample was shaken for 40 min., 1 mL of headspace was removed and injected into a Carle Series 100 AGC gas chromatograph (Carle Chromatography, Tulsa, OK) equipped with a molecular sieve 13X 80/100 column and thermal conductivity detector (carrier gas: argon @ 30 mL  $\text{min}^{-1}$ , 50 °C). Concentrations of dissolved  $\text{H}_2$  were calculated using a Henry's law constant of  $7.5 \times 10^{-4}$  M/atm derived from  $\Delta G_{\text{rxn}}^0$  values (5). Dissolved  $\text{O}_2$  was measured at the site using a FOXY system (USB2000-FL, USB-LS-450, FOXY-R fiber optic probe, Ocean Optics, Inc., Dunedin, FL) with temperature compensation.

#### Characterization of Solid-Phases

Microbial mats and solid phases deposited on the glass slides were examined with a JEOL 6100 scanning electron microscope (SEM) equipped with an energy-dispersive x-ray spectrometer (EDS) within 22 h of sample collection (incident electron beam = 19 keV). The glass slides were placed on Al-stubs and coated with Au prior to analysis using

a cryostage attachment to retain microbial cell integrity. Total elemental composition of selected mat/solid phase samples was determined using a four acid heat treatment followed by elemental analysis with ICP-AES. The mineralogies of several samples were evaluated by drying the sample at 60 °C and preparing a random powder mount. X-ray diffraction data were collected at the Stanford Synchrotron Radiation Laboratory in collaboration with Drs S. Fendorf and B. Bostick (12). The amount of oxalate-extractable Fe was determined by extracting 0.1 g solid phase in 30 mL of 0.175 M NH<sub>4</sub>-oxalate / 0.1 M oxalic acid at pH 3 in the dark for 2 h (17).

#### Molecular Analysis of Microbial Communities

Total DNA was extracted from microbial mats formed on glass slides and from sand adjacent to the stream using the FastDNA SPIN Kit for Soil (Bio 101, Vista, CA). Polymerase chain reactions (PCR) using the total DNA extracts targeted specific regions within the 16S rRNA gene of the domains bacteria and archaea. One primer set was designed to capture a 322 bp segment within the domain *Bacteria* using Bac1070 forward (*E. coli* positions 1055-1070) paired with Univ1392 reverse-GC (*E. coli* positions 1392-1406; 9). To facilitate analysis by denaturing gradient gel electrophoresis (DGGE), the reverse primer incorporated a 40 bp GC-rich clamp (18). A second primer set was designed to capture a 461 bp region within the domain *Archaea*, utilizing the forward primer Arc931f, and the reverse primer Univ1392 reverse-GC as described above (9). The 50 µL PCR mixtures contained 10 mM Tris-HCl (pH 8), 50 mM KCl, 0.1 % Triton X-100, 4.0 mM MgCl<sub>2</sub>, 800 µM dNTP's, 0.5 µM of each primer, 1.25 U *Taq* DNA polymerase (Promega, Madison, WI), and 1-5 µL template DNA (2-20 ng). Thermal

cycler protocol was 94 °C for 4 min, 25 - 35 cycles of 94 °C, 54 °C and 72 °C each for 55 sec, and a final 7 min extension period at 72 °C. Negative control reactions (no template) were routinely performed to insure purity.

Denaturing gradient gel electrophoresis (DGGE) was used to separate 16S rRNA gene fragments following a method modified from Ferris et al. (18). PCR products (~ 90 ng per lane) were loaded onto gels consisting of 8% acrylamide and a 40 - 70% denaturing gradient of urea/formamide. The gels were electrophoresed at 60 V at 60 °C for 17 h using a DCode System (Bio-Rad, Hercules, CA) and stained with SYBR Green II (Molecular Probes, Eugene, OR) for 30 min prior to photography using UV transillumination. DGGE bands were purified by stabbing with a sterile pipet tip and rinsing the tip in molecular biology grade water, which was then used as template for PCR. The position and purity of PCR amplified band stabs were checked using DGGE, and if necessary, the process was repeated until pure bands were obtained. Prior to sequencing, DNA was purified using a Microcon PCR centrifugal filter kit (Millipore Corp. Bedford, MA). Bands were sequenced by PCR amplification using primers 1070 forward for bacteria and 931 forward for archaea and 1392 reverse (without the GC clamp). The sequencing reaction was performed using an ABI Prism BigDye Terminator Cycle Sequencing Ready Reaction Kit (Perkin-Elmer, Foster City, CA) and the samples were processed on an ABI Prism 310 capillary sequencer (Perkin-Elmer). Sequencher 3.1.1 software (Gene Codes Corporation, Ann Arbor, MI) was used to align and edit the resultant sequences which were then compared with sequences found in the GenBank database using BLAST (19).

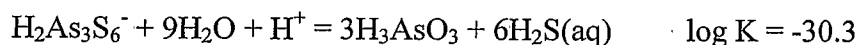
### Thermodynamic Calculations

Microorganisms residing in the ASC springs of Norris can, in theory, derive energy from a wide variety of inorganic chemical reactions. Possible electron donors present at significant concentrations in acidic geothermal springs of Norris Basin include  $H_2$ ,  $H_2 S^\circ$ ,  $S_2O_3^{2-}$ ,  $S^\circ$ , As(III), and Fe(II). Potential electron acceptors include,  $S^\circ$ ,  $SO_4^{2-}$ ,  $O_2$ , As(V), Fe(III) and  $NO_3^-$ . The free energies ( $\Delta G_{rxn}$ ,  $kJ\ mol^{-1}$ ) of several potentially important redox couples were calculated using the familiar expression:

$$\Delta G_{rxn} = \Delta G_{rxn}^\circ + RT \ln(Q_{rxn})$$

where standard state free energies of reaction ( $\Delta G_{rxn}^\circ$ ) as a function of temperature were obtained from Amend and Shock (5), and temperature corrected activities of chemical species used in the reaction quotient ( $Q_{rxn}$ ) were calculated with the aqueous equilibrium model, Visual MINTEQ (20), using measured values of chemical constituents at the spring source. Values of  $\Delta G_{rxn}^\circ$  not available in the literature were calculated using temperature corrected standard free energies of formation ( $\Delta G_f^\circ$ ) for constituents measured in the spring (5). Temperature corrected values of  $\Delta G_{rxn}^\circ$  and  $\Delta G_f^\circ$  were provided at specific temperatures by Amend and Shock (5, e.g., 45, 55, 70, and 85 °C), and the values at 85 °C (within 7 °C of the source) were used for calculations of  $\Delta G_{rxn}$ . This approximation resulted in deviations to  $\Delta G_{rxn}$  no greater than 3  $kJ\ mol^{-1}$  compared to fitted values of  $\Delta G_{rxn}^\circ$  and  $\Delta G_f^\circ$  that corresponded to minimum temperatures measured at the source (77 °C). Visual MINTEQ was also used to estimate saturation indices [ $\log(\text{ion activity product (IAP)} / \text{solubility product (K}_{sp}))$ ] for various solid phases at spring temperatures. Solubility constants for  $As_2S_3$  (orpiment) and  $As_2S_3$  (amorphous) were based on constants derived from Eary (21) and Webster (22) and further adopted by

Nordstrom and Archer (23). Important equilibrium reactions and aqueous species used for calculating saturation indices of  $\text{As}_2\text{S}_3$  phases were:



The enthalpy ( $\Delta H_f^\circ$ ) for  $\text{H}_2\text{As}_3\text{S}_6^-$  was estimated using the van't Hoff expression and  $\Delta G_{\text{rxn}}^\circ$  values provided by Eary (21). The  $\text{AsS}(\text{OH})(\text{SH})^-$  complex, found to be important in As(III)-sulfide solutions was also included in the equilibrium calculations (24).

## Results and Discussion

### Aqueous Temperature and Chemistry

Temperature values declined exponentially with distance down gradient, averaging 79.2 °C at the source and 48.3 °C at 14 m, consequently, hyperthermophilic to moderately thermophilic temperature regimes were represented along the 14 m stream gradient. The temperatures varied approximately 10 °C at any given distance down the outflow channel during the study (Fig. 4.1A). Some of this temperature variation is a result of variation in spring discharge rates, and although discharge rates were generally consistent over short time-frames (days - weeks), they varied from approximately 5 L  $\text{min}^{-1}$  on day 14 to a maximum of 9 L  $\text{min}^{-1}$  on day 103 d. The increase in flow rate observed in this study is consistent with previous observations by Fournier (25). The pH values were relatively consistent over the sampling period but showed a slight decline down gradient, where pH values averaged  $3.10 \pm 0.07$  at the source and decreased to  $2.97 \pm 0.08$  by 14 m. The decline in pH may be due to a combination of factors including evaporation and formation of amorphous HFO. Concentrations of selected chemical

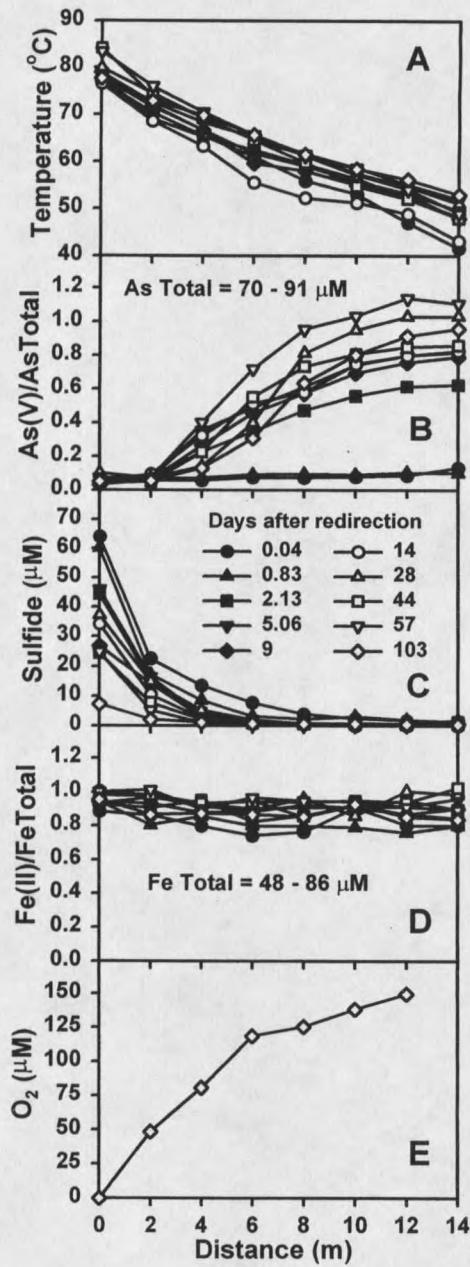


Figure 4.1. Selected aqueous geochemical constituents measured at different sampling dates are shown as a function of distance from the source of Succession Spring.

Table 4.1. Concentrations of selected chemical constituents measured in Succession Spring source water sampled 103 days after spring redirection (Oct. 29, 2001).

Cations and Anions	Concentration ( $\mu\text{M}$ )	Weak Acids/Bases	Concentration ( $\mu\text{M}$ )
$\text{Na}^+$	12,532	Si	4,819
$\text{K}^+$	954	DIC <sup>b</sup>	1,763
Ca	116.7	B	651
Al	108.7	As	70.1
Fe	86.1	$\text{NH}_4^+$	44.9
Mg	9.4	DOC <sup>c</sup>	41.0
Zn	2.1	S(-II)	7.4
Mn	0.65	P	0.9
$\text{Cl}^-$	13,342	$\text{H}_2(\text{aq})$	0.017
$\text{SO}_4^{2-}$	1,331		
$\text{F}^-$	174.9	Charge Difference <sup>d</sup>	3.0 %
$\text{NO}_3^-$	24.4	Ionic Strength <sup>d</sup>	0.0165 M

<sup>a</sup> Undetected elements with method detection limits in parenthesis: Se (<4  $\mu\text{M}$ ); Ni, (<0.9  $\mu\text{M}$ ); Sb, Pb, Cr (<0.6  $\mu\text{M}$ ); Cd, Cu, (<0.2  $\mu\text{M}$ ). <sup>b</sup> Dissolved inorganic C. <sup>c</sup> Dissolved organic C. <sup>d</sup> Charge difference and ionic strength calculated using the chemical equilibrium modeling program Visual MINTEQ (20).

constituents (Table 1) measured in the source water of Succession Spring yield a computed ionic strength (Visual MINTEQ) of 16.5 mM, comprised primarily of  $\text{Na}^+$ ,  $\text{H}^+$ ,  $\text{Cl}^-$ ,  $\text{SO}_4^{2-}$ ,  $\text{K}^+$  and dissolved inorganic carbon (DIC).

#### Aqueous Chemistry of Arsenic

The total soluble As concentration at the source ranged from 70-90  $\mu\text{M}$ , considerably higher ( $\sim 3\text{X}$ ) than adjacent springs in Norris Basin that have been the subject of recent geochemical investigations (4, 12). Arsenite was the predominant species of As in Succession Spring source water [nearly 100% As(III)] and no signs of As(III) oxidation were observed from 0 to 14 m down gradient of the source during the first two sampling dates (0.04 and 0.83 d; Fig. 4.1B). After 2 d, however, significant oxidation of As(III) to As(V) was detected, and by 14 m down gradient, 62 % of the total As was in the form of As(V). The fraction of As(III) oxidized generally continued to increase over the duration of the study, and by day 57, 100 % of the initial As(III) was oxidized by 12 m. Apparent *in situ* rate constants ( $k$ ) for the oxidation of As(III) as a function of distance were determined by fitting As(III) concentrations to the first-order rate equation  $[\text{As(III)}] = [\text{As(III)}_0]e^{-kt}$ . The calculated As(III) oxidation rate constants (e.g.,  $5.0 \text{ min}^{-1}$  at 11 m on day 103, corresponding to a half-life of 0.14 min, Fig. 4.2) are some of the highest ever observed for a natural system (4, 11). Furthermore, As(III) oxidation occurred over a wide range of temperatures and geochemical conditions suggesting that multiple microorganisms may have been responsible for As(III) oxidation during succession.

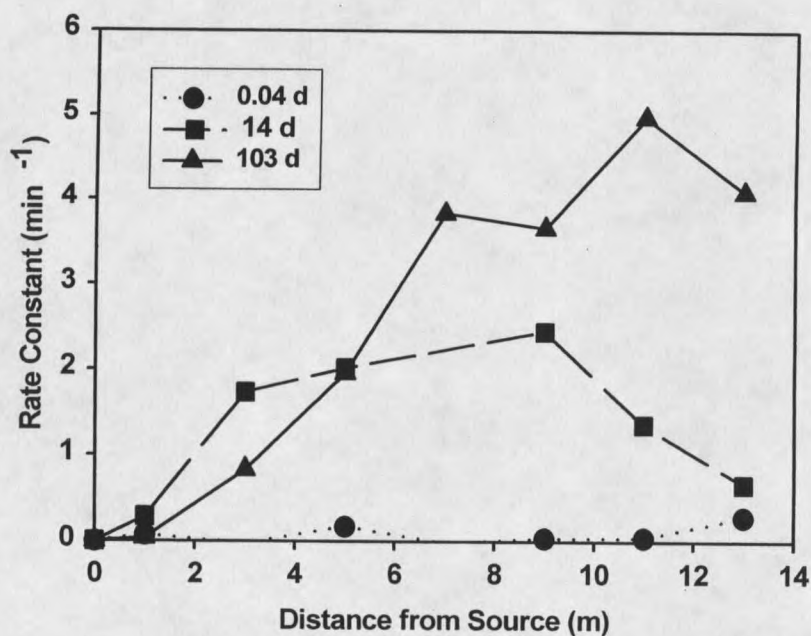


Figure 4.2. Pseudo first-order rate constants ( $k$ ) for the oxidation of As(III) based on measured values of As species are shown as a function of distance from the source of Succession Spring.

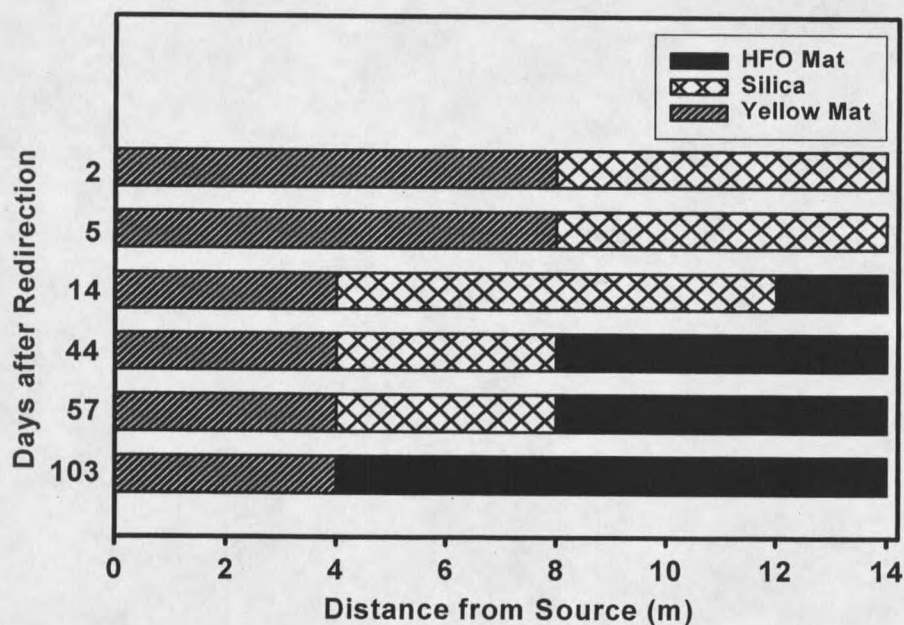


Figure 4.3. Chronological progression of yellow and HFO mats, and silica precipitates in Succession Spring during the time of the study.

### Sulfur Species

Concentrations of dissolved sulfide decreased to detection limits of approximately  $1 \mu\text{M}$  after 10 m at all sampling events (Fig. 4.1C). Apparent first-order rate constants for the disappearance of  $\text{H}_2\text{S}(\text{aq})$  (predominant species of dissolved sulfide at pH 3) ranged from  $5.7$  to  $10 \text{ min}^{-1}$  (corresponding to half-lives of 0.12 to 0.07 min) with maximum  $k$  values occurring nearest the source. These values are very close to maximum rate constants describing As(III) oxidation (Fig. 4.2), suggesting a close inverse relationship between  $\text{H}_2\text{S}$  disappearance and As(III) oxidation. However, despite fluctuating sulfide concentrations at the spring source ranging from  $8$  to  $64 \mu\text{M}$ , no changes in the  $\text{H}_2\text{S}(\text{aq})$  disappearance profiles were observed prior to or during microbial mat formation, suggesting that abiotic pathways including degassing of  $\text{H}_2\text{S}(\text{aq})$  and or oxidation to  $\text{S}^\circ$  and thiosulfate upon oxygenation (26) make important contributions to the disappearance of dissolved sulfide. Further, under acidic conditions, thiosulfate rapidly disproportionates to  $\text{S}^\circ$  and sulfite, and sulfite in turn rapidly oxidizes to sulfate (26). The lack of detectable thiosulfate and sulfite using ion chromatography may be explained by the transient nature of these compounds at this pH ( $\sim 3.0$ ). The rapid abiotic oxidation of  $\text{H}_2\text{S}(\text{aq})$  is consistent with  $\text{S}^\circ$  depositional patterns as a function of time and distance (discussed below). In addition, the oxidation of  $\text{H}_2\text{S}$  to  $\text{SO}_4^{2-}$  could not be quantified due to the high background levels of  $\text{SO}_4^{2-}$  ( $\sim 1.3 \text{ mM}$ ) relative to  $\text{H}_2\text{S}$  ( $< 0.07 \text{ mM}$ ). Modeling of aqueous chemical speciation using Visual MINTEQ predicted that  $\text{H}_2\text{As}_3\text{S}_6^-$  is the dominant species of dissolved sulfide at the source (e.g.,  $> 85 \%$  of total dissolved S(-II) on day 2). Consequently, the predicted predominance of this species may have significant implications for the toxicity and bioavailability of sulfide in this zone of the spring.

### Dissolved Inorganic C

Concentrations of DIC measured in the source water ranged from 1.0 – 2.3 mM over the study period. As with  $\text{H}_2\text{S}(\text{aq})$ , a rapid decline in DIC as a function of distance from the source was observed, typically decreasing to  $< 0.1$  mM (detection limit) by 12 m. The rapid decline in  $\text{H}_2\text{CO}_3^\circ(\text{aq})$  with distance is attributed primarily to degassing of  $\text{CO}_2(\text{aq})$ , which like  $\text{H}_2\text{S}(\text{aq})$  is favored at low pH. The source waters are more than 100 times oversaturated with respect to the  $\text{pCO}_2(\text{g})$  assumed for atmospheric conditions. Consequently, there is a significant disequilibrium with respect to atmospheric  $\text{CO}_2$  that drives degassing. Another potential sink for  $\text{CO}_2$  is fixation via autotrophic organisms, although first-order fits of the data do not show any trends or changes in rate constants that would be attributable to the time course of microbial mat development (data not shown).

### Soluble Fe, $\text{H}_2$ , and $\text{O}_2$ Profiles

Concentrations of total soluble Fe ( $\text{Fe}_{\text{ts}}$ ) varied from 48 to 87  $\mu\text{M}$  during the study (Fig. 4.1D), and no measurable losses of  $\text{Fe}_{\text{ts}}$  were observed down gradient (Fig. 4.1D). Furthermore, the predominant valence of Fe was Fe(II), comprising 80 - 100 % of the  $\text{Fe}_{\text{ts}}$  over the course of the study. No consistent changes in Fe(II):Fe(III) ratios were noted as a function of time or distance down gradient. Under these geochemical conditions (i.e. pH = 3), Fe(II) is actually thermodynamically favored relative to Fe(III). As expected, rapid ingassing of  $\text{O}_2$  occurred as with distance. Concentrations of dissolved  $\text{O}_2$  on day 103 (Fig. 4.1E) were below detection limits at the source ( $< 0.08$   $\mu\text{M}$ ) and gradually increased to saturation levels by 12 m (measured value = 150  $\mu\text{M}$ ; predicted saturation @ 55 °C and

2195 m elevation = 144  $\mu\text{M}$ ). Finally,  $\text{H}_2(\text{aq})$  concentrations of the source water have been measured several times since the original study in 2001 and found to range from 15 - 100 nM, consistent with  $\text{H}_2(\text{aq})$  levels measured in other ASC springs in Norris Basin (unpublished data, and, personal communication, Dr. John Spears).

#### Characterization of Microbial Mats and Associated Solid Phases

One of the primary goals of this study was to describe the distribution of microorganisms as a function of geochemical and thermal gradients. Towards this end, visible and microscopic observations of solid phase deposition and microbial mat development were coupled with corresponding changes in aqueous chemistry and 16S rDNA sequence distribution occurring after spring redirection. The first obvious change in solid phase deposition and microbial community development occurred within 2 d, when yellow solid phase began to line the channel floor from 0 to 8 m (Fig. 4.3 and Fig. 4.4A). Electron micrographs and elemental analysis (EDAX) of the yellow solid phase revealed several types of  $\text{S}^0$  ( $> 92$  atom % S) morphologies including spheres and rhombohedral crystals (Fig. 4.5). In some cases, the  $\text{S}^0$  spheres appear to serve as nucleation sites for growth of orthorhombic crystals (Fig. 4.5C). Spheres and rhombohedrals of  $\text{S}^0$  have been previously reported in volcanic areas (27). Electron micrographs also demonstrated evidence of initial stages of microbial colonization by day 2 where several rods and filaments ( $\sim 0.7 \mu\text{m}$  diameter) can be seen on orthorhombic  $\text{S}^0$  surfaces. The role of these early colonizers in formation and deposition of the  $\text{S}^0$  phase was not clear, given that the majority of  $\text{S}^0$  phases did not reveal any surface-attached microorganisms corresponding to the time frame necessary to deposit this phase. Rather,

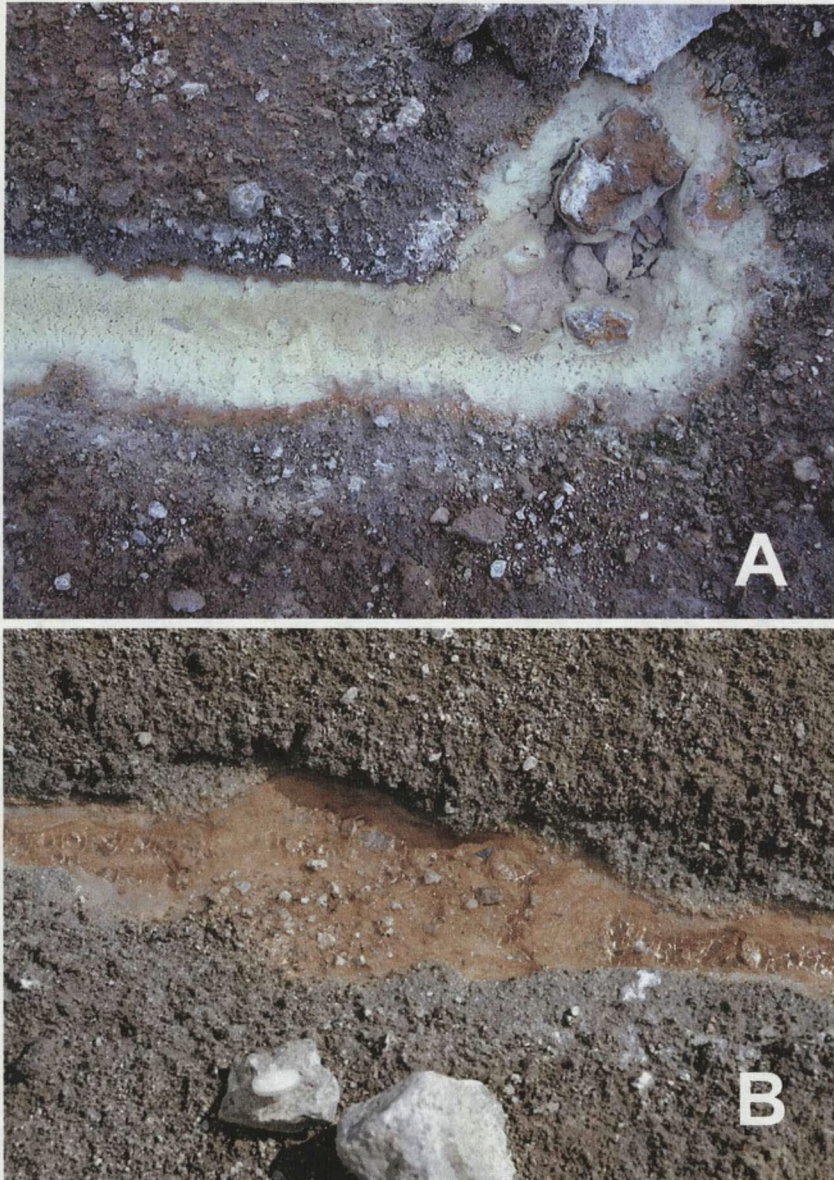


Figure 4.4. Photographs of Succession Spring 57 days after redirection of flow (Sept 13, 2001). The streambed at and immediately downstream of source exhibiting yellow mat composed predominantly of  $S^{\circ}$  is shown in panel A. The As-rich HFO mat  $\sim 10$  m downstream from source is shown in panel B.

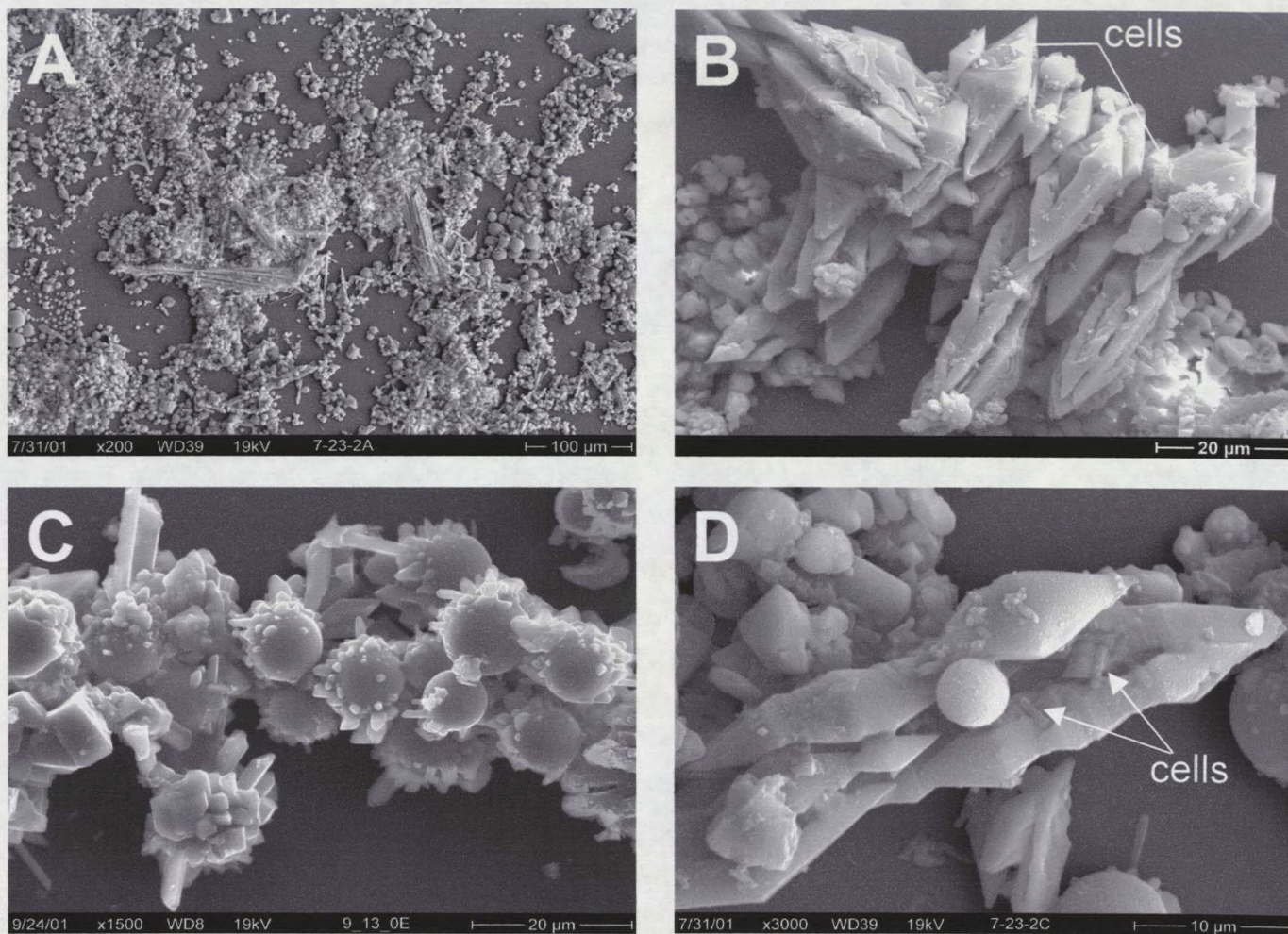


Figure 4.5. SEM images of yellow mat obtained using cryostage mount. Panel A shows 200X magnification of mat that had developed during the first 5 days after spring redirection. Higher magnification images in panels B – D reveal rhombohedrals and spheres, and crystals protruding from spheres, all composed predominantly of  $S^{\circ}$  based on EDAX. Note the presence of rods and filaments (cells) on the mineral surfaces in panels B and D.

the rapid deposition of elemental  $S^{\circ}$  was attributed primarily to  $O_2(g)$  ingassing followed by kinetically favored abiotic oxidation of  $H_2S$  to  $S^{\circ}$  (26). The length of the  $S^{\circ}$  depositional zone gradually decreased during the course of the study and retreated to 4 m by day 103 (Fig. 4.3). The decrease in length of the yellow mat correlated with a corresponding decline in source water  $H_2S(aq)$  concentrations (Fig. 4.1C). During the study period, concentrations of  $H_2S(aq)$  at the lower boundary of the  $S^{\circ}$  zone were consistently between 0.5 to 2  $\mu M$ , suggesting that concentrations  $> 2 \mu M$  are required to effectively support the formation of  $S^{\circ}$  at these temperatures. The corresponding temperature range defining the  $S^{\circ}$  depositional zone was approximately 57 - 80  $^{\circ}C$  (Fig. 4.1A, Fig. 4.3).

Several spheres (5 to 20  $\mu m$  dia.) composed of  $As_2S_3$  (As:S mole ratios averaged 0.61) were observed on glass slides retrieved from the 0 m position on day 2. Thermodynamic calculations using temperature corrected constants in Visual MINTEQ, predicted that the source water was significantly undersaturated with respect to amorphous  $As_2S_3$  and orpiment [ $\log(IAP/K_{sp})$  for  $As_2S_{3(am)} = -8.5$  and  $As_2S_{3(orp)} = -7.6$ ]. These predictions are consistent with the fact that  $As_2S_3$  phases were not observed as a predominant phase in this zone on day 2, and were not observed throughout the remainder of the study. Aside from the  $As_2S_3$  phases observed on day 2, no other As containing solid phases were detected in the  $S^{\circ}$  depositional zone despite the high concentration of As in the source water.

### Fe Successional Changes

The first visual and microscopic (SEM/EDAX) evidence of an arsenic-rich hydrous ferric oxide (HFO) mat occurred by 14 d in the lower reaches of the outflow channel (12 - 14 m). During the next 89 d, the upper boundary of HFO deposition gradually progressed upstream, reaching 4 m by day 103 (Fig 4.3). SEM/EDAX observations of the brown solid phase samples obtained during initial stages of formation (14 d at 12 m, Fig. 4.6A and B) showed clusters of cells with raspberry-like appearance similar to the coalescing spherules of amorphous As(V)-Fe(III)-O observed in acid mine drainage by Morin et al. (11). Surfaces adjacent to cell clusters were also encrusted with the textured As-Fe-O solid phase. Deposition of SiO<sub>2</sub> phases also occurred in this zone, but these solid phases did not contain Fe or As and were not associated with cellular morphology. Thus, the origin of the As-rich HFO phase was apparently biogenic, its appearance correlating in time and space with direct evidence of microbial colonization. The biogenesis of this mat is also supported by thermodynamic calculations, indicating that Fe(II) is stable under these conditions. In addition, filtered (0.22 μm) source water incubated at spring temperatures confirmed that spontaneous oxidation of Fe(II) does not occur over time scales necessary to control formation of these mats (data not shown). Furthermore, previous studies have shown that abiotic oxidation of Fe(II) at low pH is extremely slow (28). Currently, the specific mechanism by which these associated organisms may catalyze HFO mineralization is unknown and can only be inferred from phylogenetic analysis of populations detected in the brown mat using molecular methods (discussed below).

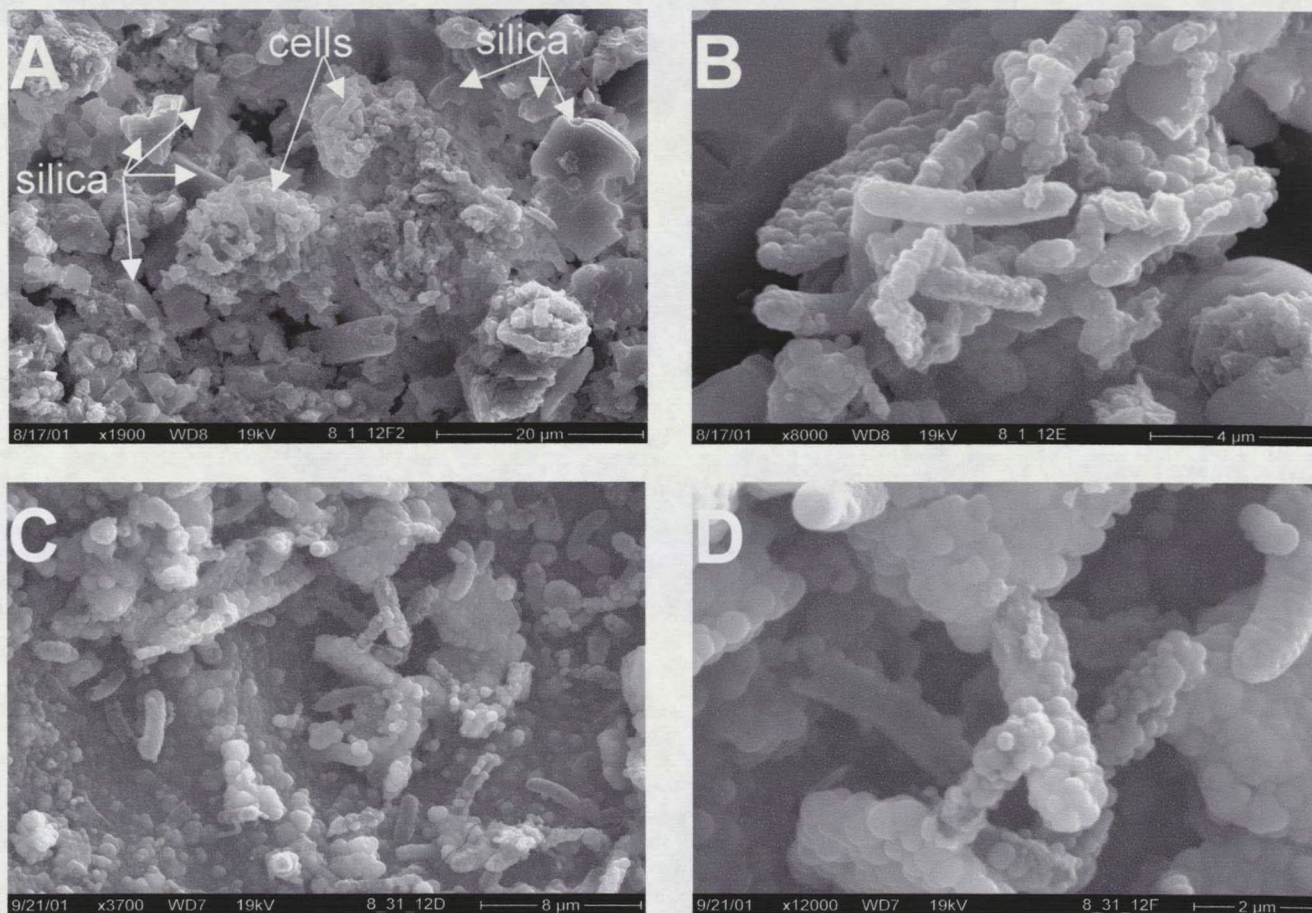


Figure 4.6. Scanning electron micrographs (cryostage mount) of HFO mat formed in Succession Spring. Arrows in panel A, point to clusters of cells that are coated with an As-Fe-O mineral phase as determined by EDAX. Minerals immediately surrounding cell clusters are composed predominantly of silica. Panel B shows higher magnification image (8,000X) of cell cluster with raspberry-like textured surfaces characteristic to the As-rich HFO solid phase. Panels C and D show mature brown mat with nearly all surfaces comprised of As-Fe-O.

Maturation of HFO microbial mats in Succession Spring was characterized by coverage of all surfaces with As-rich HFO (Fig. 4.6C and D), including numerous  $\sim 1 \mu\text{m}$  diameter rodshaped cells. EDAX of cells and surfaces encrusted with HFO showed mole ratios of As:Fe ranging from 0.60 to 0.74, similar to those observed in adjacent ASC springs (4, 12) and very close to maximum values of 0.68 observed in synthetic solutions where 2-line ferrihydrite was precipitated in the presence of As(V) (29). Total dissolution analysis yielded an average molar As:Fe ratio of 0.69, and essentially 100 % of this phase was extractable with  $\text{NH}_4$ -oxalate (pH 3, 17). The lability of this phase in oxalate was consistent with x-ray diffraction showing two broad Bragg peaks at d-spacings characteristic of 2-line ferrihydrite (data not shown). To our knowledge, these phases contain the highest As contents observed in naturally occurring HFO (4, 11, 12). While compositionally similar, HFO mats in three adjacent ASC springs, Succession, Dragon, and Beowulf Springs, exhibit considerable variability in micromorphology. Specifically, no filaments were observed in Succession Spring by day 103 while the HFO mats of Dragon and Beowulf were comprised of an extensive network of filaments, the formation of which are generally associated with flowing water (e.g., 30). The relatively short duration of successional observations in the current study (103 d) may explain the predominance of rods versus filaments.

Irregularly shaped silica phases were observed at all positions within the outflow channel throughout the study period (Fig. 4.6A, B). The formation of these phases is consistent with aqueous chemical speciation indicating the waters are over saturated with respect to amorphous silica and quartz, resulting in temperature corrected saturation indices ( $\log [IAP/K_{sp}]$ ) of 0.3 for  $\text{SiO}_{2(\text{am})}$  and 1.3 for  $\text{SiO}_{2(\text{quartz})}$ . Synchrotron XRD has

revealed that Si phases formed under these conditions are more similar to opal-CT rather than quartz (12). Silica phases observed early in the study (2 d, SEM/EDAX) were free of surface coatings, however, within the HFO depositional zone, SiO<sub>2</sub> phases became encrusted with As-rich HFO after 14 d.

#### Microbial Populations Detected in Parent Material

Fingerprints of microbial communities located at five positions in the stream channel were obtained at seven sampling dates using PCR amplification and denaturing gradient gel electrophoresis (DGGE) of 16S rDNA fragments. Sequence analysis of DGGE bands and subsequent comparisons to sequences within GenBank showed that on day 0.8, amplifiable sequences from the stream channel corresponded to sequences from *Comamonas*, *Alcaligenes*, and *Pseudomonas*-like organisms (Fig 4.7). The detection of these bacteria at all sampling positions (0-12 m) immediately after redirecting stream flow suggested that these organisms were residents of the siliceous sandy parent material and were not associated with subsequent geochemical processes. This scenario is supported by the fact that (i) these populations were detected in nonthermal sand control samples collected adjacent to the stream channel, (ii) the three bands gradually diminished over time and completely disappeared after 14 days, and (iii) these organisms are not known to have thermophilic near relatives.

#### Initial Colonization by *Hydrogenobaculum*-like Organisms

The first microorganisms to colonize the stream channel after spring redirection were closely related to *Hydrogenobaculum* sp. (> 98 % similarity; accession no

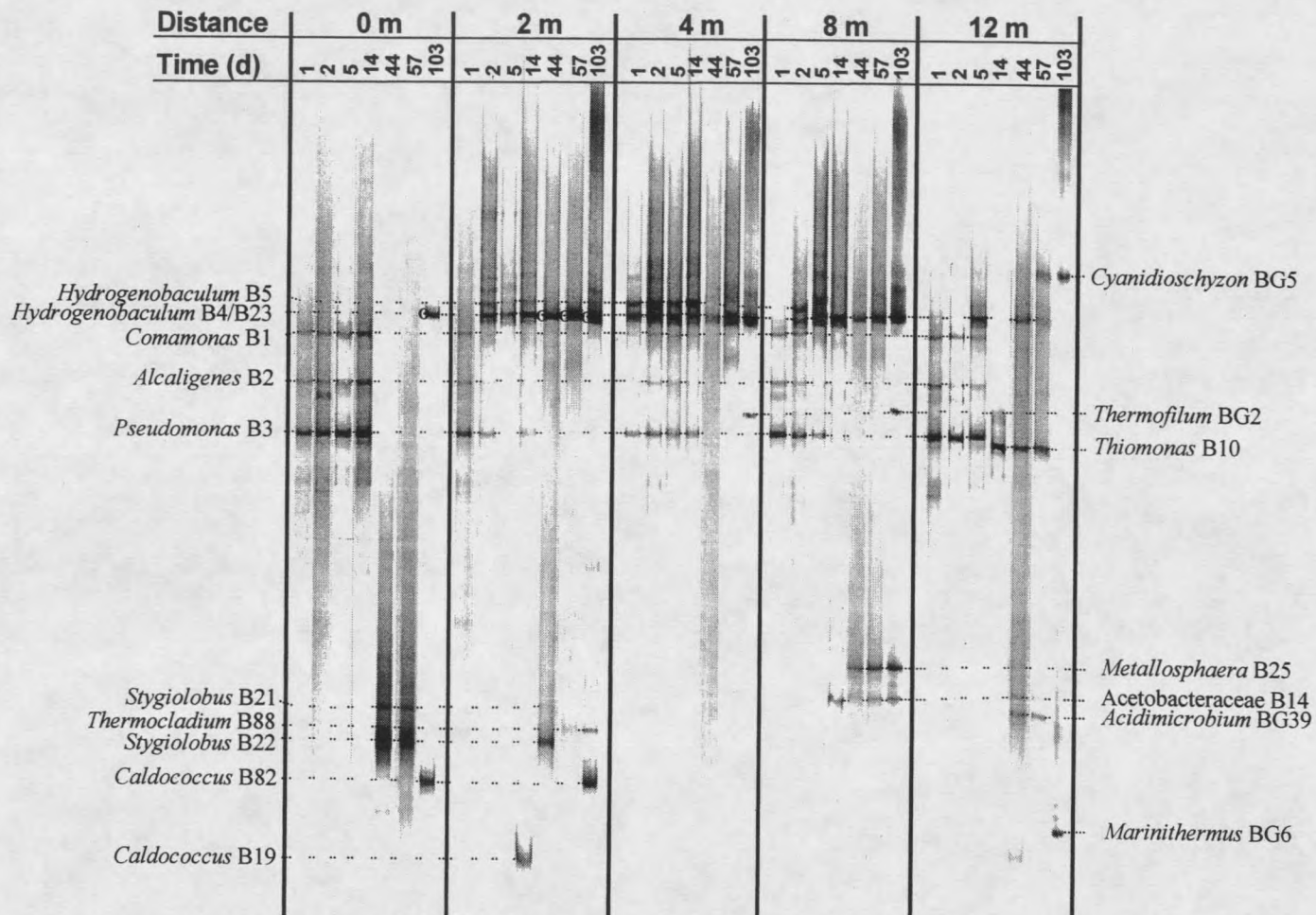


Figure 4.7. Denaturing gradient gel (40–70 %) of 16S rDNA fragments obtained by amplification of Succession Spring DNA using universal bacterial primers. DNA was extracted from glass slides that were removed at selected sampling dates. The image is a composite of lanes from gels that were run at different times during the study. Lanes from different gels were aligned based on position of bands with identical sequences. Names of nearest GenBank matches to band sequences are designated and dashed lines show comigrating bands. Bands marked with an o indicate sequences that correspond to B23.



Table 4.2. Accession numbers for partial 16S rDNA sequences obtained from Succession Spring and, percent sequence similarity and characteristics of nearest cultivated GenBank neighbors<sup>a</sup>.

Accession Number	DGGE Band Number	-----Nearest Cultured GenBank neighbor <sup>a</sup> -----			
		Percent Similarity		Phylogenetic Group	Characteristics of Cultured Organisms
AY191870	B23	98.6	<i>Hydrogenobaculum</i> sp. NOR3L3B	Aquificales	microaerophilic, chemolithotrophic, H <sub>2</sub> -oxidizer
AY191871	B5	99.1	<i>Hydrogenobaculum</i> sp. NOR3L3B	Aquificales	microaerophilic, chemolithotrophic, H <sub>2</sub> -oxidizer
AY191873	B156	99.6	<i>Hydrogenobaculum</i> sp. NOR3L3B	Aquificales	microaerophilic, chemolithotrophic, H <sub>2</sub> -oxidizer
AY191869	B4	99.5	<i>Hydrogenobaculum</i> sp. NOR3L3B	Aquificales	microaerophilic, chemolithotrophic, H <sub>2</sub> -oxidizer
AY191874	B182	99.5	<i>Hydrogenobaculum</i> sp. NOR3L3B	Aquificales	microaerophilic, chemolithotrophic, H <sub>2</sub> -oxidizer
AY191883	B22	98.3	<i>Stygiolobus azoricus</i>	Crenarchaeota	obligately anaerobic, chemolithotrophic, H <sub>2</sub> -oxidizer, S-reducer
AY191887	B168	96	<i>Stygiolobus azoricus</i>	Crenarchaeota	obligately anaerobic, chemolithotrophic, H <sub>2</sub> -oxidizer, S-reducer
AY191882	B21	97.7	<i>Stygiolobus azoricus</i>	Crenarchaeota	obligately anaerobic, chemolithotrophic, H <sub>2</sub> -oxidizer, S-reducer
AY191881	B19	99.0	<i>Caldococcus noboribetus</i>	Crenarchaeota	anaerobic, heterotrophic
AY191885	B82	97.6	<i>Caldococcus noboribetus</i>	Crenarchaeota	anaerobic, heterotrophic

Table 4.2 Continued.

AY191890	B185	95.8	<i>Caldisphaera lagunensis</i>	Crenarchaeota	anaerobic, heterotrophic, S-reducer
AY191886	B88	98.6	<i>Thermocladium modestius</i>	Crenarchaeota	anaerobic-microaerophilic, obligately heterotrophic, S-reducer
AY191892	BG2	89.3	<i>Thermofilum pendens</i>	Crenarchaeota	anaerobic, S-reducer
AY191880	B14	99.1	Acetobacteraceae Y008	$\alpha$ Proteobacteria	heterotrophic, Fe-reducer
AY191894	BG11	89.1	<i>Aeropyrum pernix</i> OH1	Crenarchaeota	aerobic, heterotrophic
AY191884	B25	98.1	<i>Metallosphaera prunae</i>	Crenarchaeota	obligate aerobe, facultative chemolithoautotrophic, Fe-oxidizer
AY191879	B10	98.1	<i>Thiomonas</i> sp. Ynys3	$\beta$ Proteobacteria	aerobic, Fe-oxidizer, autotrophic S <sub>2</sub> O <sub>3</sub> -oxidizer
AY191899	BG39	98.5	<i>Acidimicrobium</i> sp. Y0018	Actinobacteria	aerobic-anaerobic, Fe(II)-oxidizer, Fe(III)-reducer
AY191888	B179	96.7	<i>Acidisphaera rubrifaciens</i>	$\alpha$ Proteobacteria	aerobic, heterotrophic, contains bacteriochlorophyll
AY191889	BG6	90.7	<i>Marinithermus hydrothermalis</i>	Deinococcus- Thermus	obligately aerobic, heterotrophic
AY191895	BG12	92.3	Planctomycete strain 567	Planctomycete	nonthermophilic
AY191902	BG5	100	<i>Cyanidioschyzon merolae</i> <i>chloroplast</i>	Rhodophyta	phototrophic

<sup>a</sup>The nearest GenBank neighbor was determined by comparing partial 16S rDNA sequences of DGGE bands to sequences in the GenBank database using BLAST (Altschul et al., 1997).

AJ320225; 30). Three different *Hydrogenobaculum* sequence types (B4, B5, and B182) were observed within 1-2 days at positions 2, 4, or 8 m (Fig. 4.7, 4.8). With time, *Hydrogenobaculum*-like sequences were detected at all sampling positions (0 - 12 m) in the stream, representing the only genus that was so widely distributed across thermal and geochemical gradients (Fig. 4.7, 4.8.). The sequence of a hyperthermophilic population, designated B23, was detected on day 103 at 0 - 2 m where anaerobic conditions and significant levels of H<sub>2</sub> and H<sub>2</sub>S persist. Another population represented by band B156 was detected only at 4 m, possibly a function of reduced thermal or H<sub>2</sub>S tolerance, or dependence on low levels of O<sub>2</sub>. The population corresponding to sequence B4 was detected at positions from 2 to 12 m and appeared to be displaced from the 2 m position by the hyperthermophilic population (B23) after 14 d. It is possible that the *Hydrogenobaculum*-like populations detected at the lower positions of the stream channel (B4 and B182) were adapted to aerobic conditions and depleted levels of H<sub>2</sub> and H<sub>2</sub>S. The differential detection of these highly related sequences (> 98 % similarity to each other; Table 2) across the thermal and geochemical gradients of the stream channel suggests that the populations represented by these sequences are capable of a variety of physiologies and are adapted to different microenvironments. The observations also suggest that these closely related populations originally descended from a common ancestor and may have adapted to different thermal and geochemical niches along the stream channel (31). The presence of different *Hydrogenobaculum* -like sequences was also observed in Dragon Spring, where molecular analysis revealed 16 different populations (operational taxonomic units using RFLP analysis) at two sampling locations (9). However, observations from the current study clearly document the distribution of

different *Hydrogenobaculum* -like populations as a function of temperature and geochemical conditions.

The nearest cultivated relative to all of the *Hydrogenobaculum* -like populations detected in this study is *Hydrogenobaculum* sp. strain NOR3L3B (> 98 % similarity; accession no. AJ320225; 30). This isolate was cultivated from a 91°C spring in Norris Basin, further demonstrating the thermotolerance and versatility of this closely related group. *Hydrogenobaculum* sp. strain NOR3L3B and two other close relatives, *H. acidophilium* isolated from a Japanese solfataric field (> 97 % similarity to all *Hydrogenobaculum* -like populations detected, accession no. D16296, 32), and *Hydrogenobaculum* sp. strain H55 isolated from *Dragon Spring* (> 97 % similarity to all *Hydrogenobaculum* -like populations detected, accession no. AY268103, 33) are all autotrophic, acidothermophilic, microaerobes that utilize H<sub>2</sub> as an energy source. In addition, *H. acidophilium* requires S<sup>0</sup> for growth.

### Hyperthermophiles

The source waters of Succession Spring are considerably warmer than geochemically similar adjacent ASC springs, and ranged from 77 – 84 °C during this study. Microorganisms growing at these temperatures are considered hyperthermophiles and currently there is limited information about the distribution, diversity, and function of these extremophiles in natural systems (8, 34). Microbial colonization of surfaces immediately adjacent to the spring source (0 m) was first detected 14 d after redirection (Fig. 4.7, 4.8). The first colonizers at the source were *Stygiolobus* -like populations, where three different *Stygiolobus* -like sequences (B21, B22, and B168) were detected at

0 and 2 m, each with 96 – 98 % similarity to *Stygiolobus azoricus* (accession no. X90480, 35). Members of this genus are obligately anaerobic chemolithotrophs, which can couple the oxidation of H<sub>2</sub> to the reduction of S<sup>0</sup> and have an optimal growth temperature of about 80° C. Consequently, phylogenetic inference is consistent with the position of these populations near the source of the spring where high temperatures and significant levels of H<sub>2</sub> and S<sup>0</sup> persist. Dominant populations detected at 2 m on day 14 and at 0 m after day 14 included *Caldococcus*, *Caldisphaera*, and *Thermocladium* -like members of the Crenarchaeota, and a *Hydrogenobaculum*-like population (Fig. 4.7, 4.8; Table 4.2). Two populations with close 16S rDNA matches to the hyperthermophile *Caldococcus noboribetus* (bands B19 and B82, 97 - 99 % similarity, accession no. D85038, 36), were detected at 0 - 2 m. Although the availability of S<sup>0</sup> is not essential for *Caldococcus noboribetus* (the only member of this genus that has been characterized), it is required for rapid growth and may be important for competitiveness (36). Two other 16S sequences detected near the spring source most closely matched sequences of isolates previously characterized as obligate heterotrophs. One of these sequences (B185) was 95 % similar to the sequence of *Caldisphaera lagunensis*, an anaerobe-microaerobe whose optimal growth at 75° C and pH 3.7 was promoted by S<sup>0</sup> as an electron acceptor (accession no. AB087499, 37). The sequence of band (B88) was 98 % similar to the sequence of the S<sup>0</sup> respiring heterotroph, *Thermocladium modestius*, currently the only characterized species of *Thermocladium* (accession no. AB005296, 38). Comigrating DGGE bands representing this population were detected over a wide range of positions in the stream (0 – 8 m), suggesting that this genus has broader tolerance to temperature and O<sub>2</sub> compared to *Stygiolobus* and *Caldococcus*. This is supported by characteristics of *T. modestius*,

which has an optimal growth range between 60 and 80 °C and is tolerant of low levels of O<sub>2</sub>, whereas *Stygiolobus* and *Caldococcus* are adapted to higher temperatures and strict anaerobic conditions.

#### Formation of HFO Microbial Mats

The first visual and microscopic evidence of HFO phases occurred at 12 m on day 14 (49 °C) and correlated with the detection of bands B10 and BG39 (Fig. 4.7 and 4.8) whose sequences are closely related to *Thiomonas* sp. strain Ynys3 (98 % similar to band B10, accession no. AF387303, 39) and *Acidimicrobium* sp. (98 % similar to band BG39, accession no. AY140240, 40). The fact that close relatives of these populations have been shown to oxidize Fe(II) and their detection in the spring coincided with HFO biomineralization, suggests that these populations were important in the initial formation of As-rich HFO microbial mats. The detection of populations closely related to known Fe-oxidizers provides another line of evidence that HFO formation was not simply a result of passive Fe(II) oxidation and nucleation processes. A *Metallosphaera*-like population (band B25, 98 % similarity to *Metallosphaera prunae*, accession no. X90482, 41) was detected in the HFO mat after the mat had progressed upstream to 8 m on day 44. The mean temperature at 8 m was ~ 58 °C (Fig. 4.1), just above the minimum temperature (55 °C) required for growth of the Fe-oxidizing *Metallosphaera prunae* (41). Thus, it is likely that the *Metallosphaera* -like population was involved in HFO mat formation in a warmer region of the spring channel, as opposed to the *Thiomonas* -like population that was always detected at < 57 °C. The genus *Metallosphaera* is composed of thermophilic, aerobic, facultative chemolithoautotrophs capable of growth on S<sup>0</sup>,

Fe(II) or sulfidic ores such as pyrite (41, 42). *Thiomonas* are also aerobic, facultative chemolithotrophs capable of utilizing reduced S forms as electron donors and are capable of mixotrophic growth as well (39, 43). Interestingly, *Acidimicrobium* sp. strain Y0018 (98 % similar to band BG39, 40) isolated from Frying Pan Spring in Norris Basin was shown to be capable of dual Fe metabolisms; it could both oxidize Fe(II) under aerobic conditions and reduce Fe(III) under anaerobic conditions. Thus, phylogenetic inference suggests that the close relative of *Acidimicrobium* sp. (strain Y0018) detected in Succession Spring (BG39) may be relevant to Fe transformations in both anaerobic and aerobic zones of the HFO mat. Several other organisms detected in the HFO depositional zone may also be associated with Fe cycling. The sequence of band B14 was detected at 8 m on day 14 and was 99 % similar to the sequence of an Fe(III)-reducing Acetobacteraceae strain Y008 obtained from Frying Pan Spring in Norris Basin (accession no. AY140238, 40). In addition, the sequence of band B179 detected in the HFO zone (12 m) on day 103 was 96 % similar to the sequence of an aerobic bacteriochlorophyll producing *Acidisphaera rubrifaciens* (accession no. D86512, 44) isolated from acidic hot springs in Japan and >94 % similar to the sequence from *Acidiphilium cryptum* strain JF-5 that was capable of reducing Fe(III) (accession no. Y18446, 45).

#### Novel Microorganisms

Several archaeal and bacterial sequences (band numbers BG2, BG6, BG11, and BG12) detected in the spring after 14 d exhibited poor matches to sequences from previously characterized isolates (< 92 %; Table 2). For example, the closest sequence

match to band BG2 (2 - 8 m) was from *Thermofilum pendens* (89 % similarity, accession no. X14835, 46), a Crenarchaeote isolated from a solfataric hot spring in Iceland. The sequence of band BG11 detected at 8 m on day 103 exhibited only 89 % similarity to the sequence of its closest cultivated relative, *Aeropyrum pernix* strain OH1 (accession no. AB078015), a hyperthermophilic Crenarchaeote isolated from a neutral pH hot spring in southwestern Japan (47). Band BG6, detected at 12 m on day 103 most closely matched the sequence from *Marinithermus hydrothermalis*, an aerobic heterotroph isolated from a deep sea hydrothermal vent (90 % similar, accession no. AB079382, 48). Finally, band BG12 was only 92 % similar to the sequence from a nonthermophilic planctomycete strain 567 (accession no. AJ231172, 49) isolated from Lake Heidensee in Germany. Consequently, very limited insight regarding the metabolisms of these microorganisms is possible due to the poor sequence similarities to cultivated organisms. The microorganisms represented by these sequences are likely members of novel genera and possibly novel families or orders of acidothermophiles whose physiologies can only be inferred from the environments in which they were detected. Recent efforts to clone 16S rDNA from ASC springs and soils in Norris Basin revealed many sequences similar to bands BG2, BG11, and BG12 (> 98 %, e.g. accession nos. AF325186, AF391991, AF391976), suggesting that related microorganisms represented by these sequences are widespread throughout Norris Geyser basin.

The sequence of band BG5 detected at 12 m on day 103 was 100 % similar to the sequence of chloroplast DNA in *Cyanidioschyzon merolae* (accession no. AB002583, 50). The Cyanidiales have been characterized as red algae that live in high salt environments with temperatures ranging from 37 – 45 °C and pH between 1 and 2 (51).

### Microbially Mediated As(III) Oxidation

Oxidation of As(III) to As(V) from 2 – 8 m was initially detected 2 days after spring redirection (Fig. 4.1), and correlated with the appearance of three *Hydrogenobaculum*-like populations (bands B4, B5, and B182; Fig. 4.7, 4.8). *Hydrogenobaculum* sp. strain H55 (accession no. AY268103, 33), a close relative of these *Hydrogenobaculum*-like populations (> 97 % similarity), can rapidly oxidize As(III) under microaerophilic conditions, apparently for detoxification purposes (33). By 14 d, *in situ* As(III) oxidation rates were significant from 3 – 9 m and declined at distances > 9 m. However, As(III) oxidation rates continued to increase after 14 d corresponding to the development of HFO mats, and maximum rates were observed at 9 – 13 m on day 103 (Fig. 4.2 and 4.3, half-life = 0.14 min at 11 m). A *Thiomonas* -like population detected in the HFO mat was closely related to two *Thiomonas* sp. strains (97 % similarity to band B10, accession nos. AJ549219 and AJ549220, 52) shown to oxidize As(III) via an apparent detoxification mechanism. *Hydrogenobaculum* -like populations were also detected in the HFO mat after 14 d (Fig. 4.7, 4.8). Currently, these *Thiomonas* and *Hydrogenobaculum* -like populations were the only populations detected in the spring whose near relatives have demonstrated the ability to oxidize As(III). It is expected however, that all organisms present in the As-rich microbial mats of Succession Spring possess some type of As resistance mechanism or may utilize As for energy conservation. In addition, because arsenate is a structural analogue of orthophosphate, organisms residing in the lower reaches of the stream where waters have high As(V):P ratios (As(V):P at 12 m ~ 40:1), may utilize highly selective P uptake systems as a mechanism for As(V) resistance (53).

The fact that As(III) oxidation was not observed between 0 and 2 m may be explained by significant H<sub>2</sub>S concentrations (> 2 μM) within this zone. Previous work has shown that addition of H<sub>2</sub>S (60 μM) to cultures of *Hydrogenobaculum* sp. strain H55 resulted in immediate and complete inhibition of As(III) oxidation (33). The mechanism by which H<sub>2</sub>S inhibits biotic oxidation of As(III) may be due to O<sub>2</sub> scavenging by H<sub>2</sub>S, and/or inhibition of enzymes responsible for As(III) oxidation (33). Alternatively, the populations present at 0 – 2 m may lack the ability to oxidize As(III). Abiotic reduction of As(V) to As(III) via H<sub>2</sub>S may also contribute to the As(III) observed within the H<sub>2</sub>S(aq) zone (54), however, previous work suggests that under spring conditions, abiotic reduction of As(V) is too slow to significantly alter As(III):As(V) ratios given the short residence times from 0 – 4 m (33).

#### Energetics and Primary Production

The source waters of Succession Spring contain concentrations of H<sub>2</sub>, H<sub>2</sub>S, Fe(II), and As(III) that are capable of driving primary production. In addition, SO<sub>4</sub><sup>2-</sup>, NO<sub>3</sub><sup>-</sup>, and Fe(III) are present at significant concentrations across the length of the stream and may be important electron acceptors for respiration. Other potential electron acceptors include S<sup>0</sup>, which was deposited near the source, and O<sub>2</sub> and As(V), whose concentrations increase as waters flow down gradient. Combinations of these electron donors and acceptors can serve to drive energy conserving reactions for a diversity of microorganisms. To assess the energy available to microorganisms, the Gibbs free energies ( $\Delta G_{\text{rxn}}$ ) for several oxidation-reduction reactions were predicted using temperature corrected thermodynamic equilibrium constants in conjunction with

temperature corrected predicted activities of constituents measured at the source (Table 3). The energy available per mole of electron transferred was greatest for reactions with  $H_2$ , followed in order by  $S^\circ$  (oxidation to  $SO_4^{2-}$ ), As(III),  $H_2S$  (oxidation to  $S^\circ$ ), Fe(II) and  $NH_4^+$ . Consequently, organisms dependent on  $H_2$  would be expected to proliferate near the source of the spring where reactions with  $H_2$  are the most energetically favorable. This prediction is consistent with known physiology of *Stygiolobus* and *Hydrogenobaculum*-like populations (B21, B22, B168, B4, and B23) detected near the spring source (0 – 2 m), suggesting that they utilize  $H_2$  as an energy source (32, 55). The second most energetically favorable reaction in the source waters is the oxidation of  $S^\circ$  to  $SO_4^{2-}$ . *Hydrogenobaculum*-like populations were the only organisms detected near the source that have close relatives known to oxidize  $S^\circ$  or  $H_2S$  for energy conservation (*H. acidophilum*, 32). Conversely, members of the genus *Stygiolobus* are known to utilize  $S^\circ$  as an electron acceptor rather than an electron donor. The characteristics of closest cultivated relatives to *Caldococcus*, *Caldisphaera*, and *Thermocladium* -like populations detected near the source suggests that these populations are anaerobic heterotrophs that utilize  $S^\circ$  as an electron acceptor. The predicted physiology of these *Caldococcus*, *Caldisphaera*, and *Thermocladium* -like populations was consistent with the fact that they live in anaerobic  $S^\circ$  mats and waters that have significant concentrations of DOC (~ 40  $\mu M$ ). Recent measurements of  $H_2(aq)$  down stream from the source of Succession Spring and several other ASC springs show rapid depletion of  $H_2(aq)$  with distance down gradient (G. Ackerman, unpublished data). Thus, down gradient of the  $S^\circ$  depositional zone where electron donors  $H_2S$ ,  $S^\circ$ , and  $H_2$  are depleted, As(III) and Fe(II) are still present at sufficient levels to drive primary production (Fig. 4.1). For example, closest

Table 4.3. Predicted Gibbs free energies ( $\Delta G_{\text{rxn}}$ ) for reactions potentially used by chemolithotrophic organisms in the outflow channel of Succession Spring. All calculations were based on temperature corrected equilibrium constants and predicted activities of constituents (Visual MINTEQ) measured at 0 m on day 103.

Reaction <sup>a</sup>	$\Delta G_{\text{rxn}}$ (kJ mol electron <sup>-1</sup> ) <sup>b</sup>
$\text{H}_2(\text{aq}) + 0.5\text{O}_2(\text{aq}) = \text{H}_2\text{O}$	-91
$\text{H}_2(\text{aq}) + 2\text{Fe}^{+3} = 2\text{Fe}^{+2} + 2\text{H}^+$	-64
$\text{H}_2(\text{aq}) + 0.25\text{NO}_3^- + 0.5\text{H}^+ = 0.25\text{NH}_4^+ + 0.75\text{H}_2\text{O}$	-61
$\text{H}_2(\text{aq}) + \text{S}^\circ = \text{H}_2\text{S}(\text{aq})$	-18
$\text{H}_2(\text{aq}) + \text{H}_2\text{AsO}_4^- + \text{H}^+ = \text{H}_3\text{AsO}_3^\circ + \text{H}_2\text{O}$	-16
$\text{H}_2(\text{aq}) + 0.25\text{SO}_4^{-2} + 0.5\text{H}^+ = 0.25\text{H}_2\text{S}(\text{aq}) + \text{H}_2\text{O}$	-10
$\text{H}_2\text{S}(\text{aq}) + 0.5\text{O}_2(\text{aq}) = \text{S}^\circ + \text{H}_2\text{O}$	-73
$\text{H}_2\text{S}(\text{aq}) + 2\text{Fe}^{+3} = 2\text{Fe}^{+2} + 2\text{H}^+ + \text{S}^\circ$	-46
$\text{H}_2\text{S}(\text{aq}) + \text{NO}_3^- + 2\text{H}^+ = \text{NH}_4^+ + \text{S}^\circ + 1.5\text{O}_2$	-12
$\text{H}_2\text{S}(\text{aq}) + \text{H}_2\text{AsO}_4^- + \text{H}^+ = \text{H}_3\text{AsO}_3^\circ + \text{S}^\circ + \text{H}_2\text{O}$	2
$\text{S}^\circ + 1.5\text{O}_2(\text{aq}) + \text{H}_2\text{O} = \text{SO}_4^{-2} + 2\text{H}^+$	-84
$\text{S}^\circ + 0.75\text{NO}_3^- + \text{H}_2\text{O} + 2\text{H}^+ = \text{SO}_4^{-2} + 0.75\text{NH}_4^+$	-76
$\text{S}^\circ + 6\text{Fe}^{+3} + 4\text{H}_2\text{O} = 6\text{Fe}^{+2} + \text{SO}_4^{-2} + 8\text{H}^+$	-57
$\text{S}^\circ + 3\text{H}_2\text{AsO}_4^- + \text{H}^+ + \text{H}_2\text{O} = 3\text{H}_3\text{AsO}_3^\circ + \text{SO}_4^{-2}$	-9
$\text{H}_3\text{AsO}_3^\circ + 0.5\text{O}_2(\text{aq}) = \text{H}_2\text{AsO}_4^- + \text{H}^+$	-75
$\text{H}_3\text{AsO}_3^\circ + 2\text{Fe}^{+3} + \text{H}_2\text{O} = \text{H}_2\text{AsO}_4^- + 2\text{Fe}^{+2} + 3\text{H}^+$	-47
$\text{H}_3\text{AsO}_3^\circ + 0.25\text{NO}_3^- + 0.25\text{H}_2\text{O} = \text{H}_2\text{AsO}_4^- + 0.5\text{H}^+ + 0.25\text{NH}_4^+$	-45
$\text{Fe}^{+2} + 0.25\text{O}_2(\text{aq}) + \text{H}^+ = \text{Fe}^{+3} + 0.5\text{H}_2\text{O}$	-27
$\text{Fe}^{+2} + 0.125\text{NO}_3^- + 1.25\text{H}^+ = \text{Fe}^{+3} + 0.125\text{NH}_4^+ + 0.375\text{H}_2\text{O}$	3
$\text{NH}_4^+ + 2\text{O}_2(\text{aq}) = \text{NO}_3^- + 2\text{H}^+ + \text{H}_2\text{O}$	-27

<sup>a</sup> Reactions written in terms of predominant species at spring conditions.

<sup>b</sup> Concentration of  $\text{O}_2(\text{aq})$  was assumed to be 0.08  $\mu\text{M}$  for these calculations.

cultivated relatives of the *Metallosphaera* -like population detected in the HFO mat have been shown to oxidize Fe(II) for energy conservation, suggesting that this population (B25) may also utilize Fe(II) as an electron donor during respiration (41, 42). The Succession Spring environment also appears favorable for As(III)-oxidizing chemolithotrophs, however, phylogenetic association to known chemolithotrophic As(III) oxidizers is not insightful because only a few bacteria capable of chemolithotrophic growth on As(III) have been reported (56-58).

#### Microbial Species Distribution and Community Development

One of the primary challenges in environmental microbiology is to determine distribution patterns and ecological role of microbial populations as a function of geochemical environment. The Succession Spring environment represents a relatively simple model system that facilitated the study of sequence distribution along thermal and geochemical gradients. The function of specific microbial populations was inferred by monitoring the development of microbial communities and coincident changes in geochemistry after spring redirection. The initial establishment of chemolithotrophic microorganisms dependent on H<sub>2</sub> near the spring source followed by the development of a more complex community, which included heterotrophs, was supported by both phylogenetic inference to sequences detected in the spring and thermodynamic predictions based on spring geochemistry. For example, initial colonization by chemolithotrophic *Hydrogenobaculum* and *Stygiolobus* -like populations was followed by appearance of heterotrophic *Caldococcus*, *Caldisphaera*, and *Thermocladium*-like organisms. Additionally, development of the As-rich HFO mat in a zone depleted in H<sub>2</sub>,

S<sup>0</sup>, and H<sub>2</sub>S and rich in Fe(II) was attributed to *Thiomonas*, *Acidimicrobium*, and *Metallosphaera*-like populations whose closest cultivated relatives were Fe(II)-oxidizers. Several bacterial and archaeal sequences detected in the HFO mat following initial colonization were not closely related to 16S rDNA sequences from previously characterized organisms, and currently their physiology can only be inferred from the geochemical environments which they occupy. Continuing work on ASC springs in Norris Basin will utilize the geochemical and phylogenetic information gained from this study to design enrichment environments for isolating and characterizing these uncultured unique microorganisms. Defining linkages among specific organisms and geochemical processes mediating Fe and As speciation continues to be the focus of future work on ASC springs in YNP.

## REFERENCES CITED

1. Silver, S. 1996. Bacterial Resistances to toxic metal ions-a review. *Gene* 176:9-19.
2. Ball, J.W., R.B. McCleskey, D.K. Nordstrom, J.M. Holloway, and P.L. Verplanck. 2002. Water-chemistry data for selected springs, geysers, and streams in Yellowstone National Park, Wyoming 1999-2000. USGS, Boulder, CO.
3. Stauffer, R.E., E.A. Jenne, and J.W. Ball. 1980. Chemical studies of selected trace elements in hot-spring drainages of Yellowstone National Park. United States Government Printing Office, Washington D.C.
4. Langner, H.W., C.R. Jackson, T.R. McDermott, and W.P. Inskeep. 2001. Rapid oxidation of arsenite in a hot spring ecosystem, Yellowstone National Park. *Environ. Sci. Technol.* 35:3302-3309.
5. Amend, J.M. and E.L. Shock. 2001. Energetics of overall metabolic reactions of thermophilic and hyperthermophilic Archaea and Bacteria. *FEMS Microbiol. Rev.* 25:175-243.
6. Huber, R., H. Huber, and K.O. Stetter. 2000. Towards the ecology of hyperthermophiles: biotopes, new isolations strategies and novel metabolic properties. *FEMS Microbiol. Rev.* 24:615-623.
7. Horikoshi, K. and W.D. Grant. 1999. Extremophiles, microbial life in extreme environments. John Wiley & Sons Inc., New York.
8. Reysenbach, A.L. and E.L. Shock. 2002. Merging genomes with geochemistry in hydrothermal ecosystems. *Science* 296:1077-1082.
9. Jackson, C. R., H.W. Langner, J. Donahoe-Christiansen, W.P. Inskeep, and T.R. McDermott. 2001. Molecular analysis of microbial community structure in an arsenite-oxidizing acidic thermal spring. *Environ. Microbiol.* 3:532-542.
10. Wilkie, J.A. and J.G. Hering. 1998. Rapid oxidation of geothermal arsenic(III) in streamwaters of the Eastern Sierra Nevada. *Environ. Sci. Technol.* 32:657-662.
11. Morin, G., F. Juillot, C. Casiot, O. Bruneel, J.C. Personné, F. Elbaz-Poulichet, M. Leblanc, P. Ildefonse, and G. Calas. 2003. Bacterial formation of tooeleite and mixed arsenic(III) or arsenic(V) - iron (III) gels in the Carnoulès acid mine drainage, France. A XANES, XRD, and SEM study. *Environ. Sci. Technol.* 37:1705-1712.

12. Inskeep, W.P., R.E. Macur, G. Harrison, B.C. Bostick, and S. Fendorf. 2003. Microbial mineralization of As(V)-hydrous ferric oxyhydroxide mats in an acid-sulfate chloride geothermal spring of Norris Geyser Basin, Yellowstone National Park. *Geochim. et Cosmochim. Acta*. In Press.
13. Brock, T. D. and M.L. Brock. 1969. Recovery of a hot spring community from a catastrophe. *J. Phycol.* 5:75-77.
14. Ferris, M.J., S.C. Nold, N.P. Revsbech, and D.M. Ward. 1997. Population structure and physiological changes within a hot spring microbial mat community following disturbance. *Appl. Environ. Microbiol.* 63:1367-1374.
15. APHA. 1989. Iron. p.100-106. *In* LS. Clesceri, A.E. Greenberg, and R.R. Trussell (ed.) Standard methods for the examination of water and wastewater. American Public Health Association, Washington, D.C.
16. To, T.B., D.K. Nordstrom, K.M. Cunningham, J.W. Ball, and R.B. McCleskey. 1999. New method for the direct determination of dissolved Fe(III) concentration in acid mine waters. *Environ. Sci. Technol.* 33:807-813.
17. Loeppert, R.H. and W.P. Inskeep. 1996. Iron. p.639-664. *In* D.L. Sparks (ed.) Methods of soil analysis. Part 3. Chemical methods. SSSA book series no. 5. Soil Science Society of America and American Society of Agronomy, Madison, WI.
18. Ferris, M.J., G. Muyzer, and D.M. Ward. 1996. Denaturing gradient gel electrophoresis profiles of 16S rRNA-defined populations inhabiting a hot spring microbial mat community. *Appl. Environ. Microbiol.* 62:340-346.
19. Altschul, S.F., T.L. Madden, A.A. Schäffer, J. Zhang, Z. Zhang, W. Miller, and D.J. Lipman. 1997. Gapped BLAST and PSI-BLAST: a new generation of protein database search programs. *Nucleic Acid Res.* 25:3389-3402.
20. Allison, J.D., D.S. Brown, and K.J. Novo-Gradac. 1991. MINTEQA2/PRODEFA2, a geochemical assessment model for environmental systems: Version 3.0 User's Manual. Environmental Research Laboratory, Office of Research and Development, USEPA, Athens, Georgia.
21. Eary, L.E. 1992. The solubility of amorphous As<sub>2</sub>S<sub>3</sub> from 25 to 90°C. *Geochim. Cosmochim. Acta* 56:2267-2280.
22. Webster, J.G. 1990. The solubility of As<sub>2</sub>S<sub>3</sub> and speciation of As in dilute and sulphide-bearing fluids at 25 and 90°C. *Geochim. Cosmochim. Acta* 54:1009-1017.

23. Nordstrom, D.K. and D.G. Archer. 2002. Arsenic thermodynamic data and environmental geochemistry. p.1-25. *In* A.H. Welch and K.G. Stollenwerk (ed.) Arsenic in ground water. Kluwer Academic publishers, Boston.
24. Helz, G.R., J.A. Tossell, J.M. Charnock, R.A.D. Pattrick, D.J. Vaughan, and C.D. Garner. 1995. Oligomerization in As(III) sulfide solutions: theoretical constraints and spectroscopic evidence. *Geochim. Cosmochim. Acta* 59:4591-4604.
25. Fournier, R.O. 1989. Geochemistry and dynamics of the Yellowstone National Park hydrothermal system. *Ann. Rev. Planet. Sci.* 17:13-53.
26. Xu, Y., M.A.A. Schoonen, D.K. Nordstrom, K.M. Cunningham, and J.W. Ball. 1998. Sulfur geochemistry of hydrothermal waters in Yellowstone National Park: I. The origin of thiosulfate in hot spring waters. *Geochim. Cosmochim. Acta* 62:3729-3743.
27. Kostov, I. and R.I. Kostov. 1999. Crystal Habits of Minerals. Prof. Marin Drinov Academic Publishing House & Pensoft Publishers, Sofia, Bulgaria.
28. Nordstrom, D.K. and G. Southam. 1997. Geomicrobiology of sulfide mineral oxidation. p.361-390. *In* Geomicrobiology: Interactions between Microbes and Minerals, Rev. Mineral.
29. Waychunas, G.A., B.A. Rea, C.C. Fuller, and J.A. Davis. 1993. Surface chemistry of ferrihydrite: Part 1. EXAFS studies of the geometry of coprecipitated and adsorbed arsenate. *Geochim. Cosmochim. Acta* 57:2251-2269.
30. Eder, W. and R. Huber. 2002. New isolates and physiological properties of the *Aquificales* and description of *Thermocrinis albus* sp.nov. *Extremophiles* 6:309-318.
31. Ward D.M., M.J. Ferris, S.C. Nold, and M.M. Bateson. 1998. A natural view of microbial biodiversity within hot spring cyanobacterial mat communities. *Microbiol Mol Biol Rev.* 62:1353-1370.
32. Shima, S. and K.I. Suzuki. 1993. *Hydrogenobacter acidophilus* sp. nov., a thermoacidophilic, aerobic, hydrogen-oxidizing bacterium requiring elemental sulfur for growth. *Int. J. System. Bacteriol.* 43:703-708.
33. Donahoe-Christiansen, J. 2002. Arsenite oxidation by a *Hydrogenobaculum* sp. isolated from Yellowstone National Park. Master of Science. Montana State University-Bozeman.
34. Stetter, K.O., G. Fiala, G. Huber, R. Huber, and A. Segerer. 1990. Hyperthermophilic microorganisms. *FEMS Microbiol. Rev.* 75:117-124.

35. Fuchs, T., H. Huber, S. Burggraf, and K.O. Stetter. 1996. 16S rDNA-based phylogeny of the archaeal order sulfolobales and reclassification of *Desulfurolobus ambivalens* as *Acidianus ambivalens* comb. nov. *System. Appl. Microbiol.* 19:56-60.
36. Aoshima, M., Y. Nishibe, M. Hasegawa, A. Yamagishi, and T. Oshima. 1996. Cloning and sequencing of a gene encoding 16s ribosomal RNA from a novel hyperthermophilic archaeobacterium NC12. *Gene* 180:183-187.
37. Itoh, T., K.I. Suzuki, P.C. Sanchez, and T. Nakase. 2003. *Caldisphaera lagunensis* gen. nov., sp. nov., a novel thermoacidophilic crenarchaeote isolated from a hot spring at Mt. Maquiling, Philippines. *Int. J. System. Evol. Microbiol.* 53:1149-1154.
38. Itoh, T., K.I. Suzuki, and T. Natase. 1998. *Thermocladium modestius* gen. nov., sp. nov., a new genus of rod-shaped, extremely thermophilic crenarchaeote. *Int. J. Syst. Bacteriol.* 48:879-87.
39. Dennison, F., A.M. Sen, K.B. Hallberg, and D.B. Johnson. 2001. Biological versus abiotic oxidation of iron in acid mine drainage waters: an important role for moderately acidophilic, iron-oxidising bacteria. p.493-501. *In* V.T. Ciminelli and O. Garcia Jr. (ed.) *Biohydrometallurgy: Fundamentals, technology, and sustainable development, Part B.* Elsevier Science B.V., Amsterdam, Netherlands.
40. Johnson, D.B., N. Okibe, and F.F. Roberto. 2003. Novel thermo-acidophilic bacteria isolated from geothermal sites in Yellowstone National Park: physiological and phylogenetic characteristics. *Arch. Microbiol.* 180:60-68.
41. Fuchs, T., H. Huber, K. Teiner, S. Burggraf, and K.O. Stetter. 1995. *Metallosphaera prunae* sp. nov., a novel metal-mobilizing, thermoacidophilic *Archaeum*, isolates from a uranium mine in Germany. *System. Appl. Microbiol.* 18:560-566.
42. Peebles, T.L. and R.M. Kelly. 1995. Bioenergetic response of the extreme thermoacidophile *Metallosphaera sedula* to thermal and nutritional stress. *Appl. Environ. Microbiol.* 61:2314-2321.
43. Moreira, D. and R. Amils. 1997. Phylogeny of *Thiobacillus cuprinus* and other mixotrophic Thiobacilli: proposal for *Thiomonas* gen. nov. *Int. J. System. Bacteriol.* 47:522-528.
44. Hiraiishi, A., Y. Matsuzawa, T. Kanbe, and N. Wakao. 2000. *Aciaisphaera rubrifaciens* gen. nov., sp. nov., an aerobic bacteriochlorophyll-containing bacterium isolated from acidic environments. *Int. J. System. Evol. Microbiol.* 50:1539-1546.

45. Kusel, K., T. Dorsch, G. Acker, and E. Stackebrandt. 1999. Microbial reduction of Fe(III) in acidic sediments: isolation of *Acidiphilium cryptum* JF-5 capable of coupling the reduction of Fe(III) to the oxidation of glucose. *Appl. Environ. Microbiol.* 65:3633-3640.
46. Kjems, J., H. Leffers, T. Olesen, H. Ingelore, and R.A. Garrett. 1990. Sequence, organization and transcription of the ribosomal RNA operon and the downstream tRNA and protein genes in the archaeobacterium *Thermofilum pendens*. *System. Appl. Microbiol.* 13:117-127.
47. Nomura, N., Y. Morinaga, T. Kogishi, E.J. Kim, Y. Sako, and A. Uchida. 2002. Heterogeneous yet similar introns reside in identical positions of the rRNA genes in natural isolates of the archaeon *Aeropyrum pernix*. *Gene* 295:45-50.
48. Sako, Y., S. Nakagawa, K. Takai, and K. Horikoshi. 2003. *Marinithermus hydrothermalis* gen. nov., sp. nov., a strictly aerobic, thermophilic bacterium from a deep-sea hydrothermal vent chimney. *Int. J. System. Evol. Microbiol.* 53:59-65.
49. Gripenburg, U., N. Ward-Rainey, S. Mohamed, H. Schlesner, H. Marxsen, F.A. Rainey, E. Stackebrandt, and G. Auling. 1999. Phylogenetic diversity, polyamine pattern and DNA base composition of members of the other *Planctomycetales*. *Int. J. System. Bacteriol.* 49:689-696.
50. Ohta, N., M. Matsuzaki, O. Misumi, S. Miyagishima, H. Nozaki, K. Tanaka, T. Shin-i, Y. Kohara, and T. Kuroiwa. 2003. Complete sequence and analysis of the plastid genome of the unicellular red algae *Cyanidioschyzon*. *DNA Res.* 10:67-77.
51. Yoon, H.S., J.D. Hackett, G. Pinto, and D. Bhattacharya. 2002. The single, ancient origin of chromist plastids. *Proc. Nat. Acad. Sci.* 99:15507-15512.
52. Bruneel, O., J.C. Personné, C. Casiot, M. Leblanc, F. Elbaz-Poulichet, B.J. Mahler, A. Le Flèche, and P.A.D. Grimont. 2003. Mediation of arsenic oxidation by *Thiomonas* sp. in acid-mine drainage (Carnoulès, France). *J. Appl. Microbiol.* 95:492-499.
53. Cervantes, C., G. Ji, J.L. Ramirez, and S. Silver. 1994. Resistance to arsenic compounds in microorganisms. *FEMS Microbiol. Rev.* 15:355-367.
54. Rochette, E.A., B.C. Bostick, G. Li, and S. Fendorf. 2000. Kinetics of arsenate reduction by dissolved sulfide. *Environ. Sci. Technol.* 34:4714-4720.
55. Segerer, A.H., A. Trincone, M. Gahrtz, and K.O. Stetter. 1991. *Stygiolobus azoricus* gen. nov., sp. nov., represents a novel genus of anaerobic, extremely thermoacidophilic archaeobacteria of the order *Sulfolobales*. *Int. J. Syst. Bacteriol.* 41:495-501.

56. Ilyaletdinov, A.N. and S.A. Abdrashitova. 1981. Autotrophic oxidation of arsenic by a culture of *Pseudomonas arsenitoxidans*. Mikrobiologiya 50:197-204.
57. Santini, J.M., L.I. Sly, R.D. Schnagl, and J.M. Macy . 2000 . A new chemolithoautotrophic arsenite-oxidizing bacterium isolated from a gold mine: Phylogenetic, physiological, and preliminary biochemical studies . Applied and Environmental Microbiology 66:92-97.
58. Santini, J.M., L.I. Sly, A. Wen, D. Comrie, P. De Wulf-Durand, and J.M. Macy. 2002. New arsenite-oxidizing bacteria isolated from Australian gold mining environments-phylogenetic relationships. Geomicrobiol. J. 19:67-76.

## CHAPTER 5

2,4-D CONCENTRATION DRIVEN SHIFTS IN SOIL MICROBIAL  
POPULATIONS ASSOCIATED WITH 2,4-D DEGRADATION  
UNDER BATCH AND TRANSPORT CONDITIONSIntroduction

The commonly used herbicide, 2,4-dichlorophenoxyacetic acid (2,4-D), is rapidly degraded by a variety of microorganisms in different soil environments (e.g., 1-5). Development of a comprehensive understanding of the microbial diversity associated with 2,4-D degradation in soil has been difficult due to the limitations of specific methods used to identify and characterize relevant populations. For example, researchers have often used traditional cultivation techniques, such as most-probable-number (MPN) and direct plating using 2,4-D as the sole C source, in order to obtain 2,4-D degrading populations for further characterization. While obtaining pure cultures is often beneficial for describing the metabolic capabilities of microorganisms that reside in soil, traditional cultivation approaches may not capture the 2,4-D degrading organisms important in actual soil physical-chemical environments. Furthermore, different isolation strategies may yield microbial populations with different 2,4-D catabolic traits (6). Consequently, cultivation-independent approaches that focus on phylogenetic (16S rDNA) and functional gene analysis are important tools for assessing populations and pathways responsible for 2,4-D degradation in soils.

Molecular techniques have been used in several studies to examine the diversity of 2,4-D degrading microorganisms as a function of 2,4-D application rate. Community

level response in three different soils was evaluated using Random Amplified Polymorphic DNA (RAPD) analysis and community DNA cross-hybridization (7). These techniques however, did not detect any quantitative changes in soil community structure after application of 10 mg 2,4-D kg<sup>-1</sup>. Ka et al. (8) studied the microbial diversity of 2,4-D degradation using *tfdA* as a functional gene probe. They showed that increases in 2,4-D application rate (0 – 100 mg kg<sup>-1</sup>) selected for organisms which hybridized to *tfdA* probes. Reduced complexity of southern blot patterns generated from digested soil DNA blotted with a universal 16S rRNA probe suggested that overall community diversity was also reduced at higher 2,4-D concentrations. However, analysis of 2,4-D degrader diversity using *tfdA* genes is complicated by the fact that many 2,4-D degrading bacteria do not carry *tfd* genes (4), and conversely, many bacteria harboring *tfdA* are not capable of 2,4-D degradation (9). Nonetheless, the study by Ka et al. (8) showed that 2,4-D concentration plays an important role in the selection of specific 2,4-D degrading populations.

The hydrodynamic environment may also be an important factor controlling the selection and abundance of specific 2,4-D degrading microorganisms in soils. Transport studies using soil columns have shown that apparent rate constants describing 2,4-D degradation varied significantly between batch and transport environments, and that a single rate constant determined under batch conditions was grossly inadequate for predicting the degradation, fate, and mobility of 2,4-D under transport conditions (10, 11). Although the specific cause for the disparity between degradation rates was not resolved, one possible explanation is that different hydrologic environments may result in

selection of different 2,4-D degrading microorganisms with different intrinsic degradation capabilities.

The primary focus of this study was to observe changes in soil microbial community structure as a function of 2,4-D concentration and hydrodynamic environment (batch versus transport conditions). Both cultivation-independent and cultivation-dependent methods were employed to accomplish this goal. Molecular analysis of 16S rDNA fragments was used in combination with traditional isolation methods, MPN determination in solution culture and direct plating to overcome biases associated with the use of specific techniques alone (6, 12) and to provide a robust assessment of microbial diversity associated with 2,4-D degradation.

### Materials and Methods

#### Soil

The surface horizon of an Amsterdam silt loam (fine-silty, mixed Typic Haploboroll) was collected near Bozeman, Montana, in November 1997 and in May 1999 for use in two replicate experiments (Exp. 1 and Exp. 2). This agricultural soil, typically seeded to small grains, had received regular applications of 1 to 2 kg ha<sup>-1</sup> y<sup>-1</sup> of 2,4-D over the past 25 years with exception of the last 5 y in which no pesticides were applied. After collection, the soil was air dried to 15 % moisture content (w/w) prior to storage at 4 °C. The soil used in Exp. 1 contained 1.2 % organic C (13), 29.0 mg kg<sup>-1</sup> NO<sub>3</sub>-N, 29.8 mg kg<sup>-1</sup> Olsen-P, 10 % sand, 60 % silt and 30 % clay. The 1:2 pH and electrical conductivity were 6.4 and 0.18 dS m<sup>-1</sup>, respectively.

Enrichment of 2,4-D Degrading Microorganisms  
Under Batch Conditions

The degradation of 2,4-D was evaluated during soil enrichments in 125 mL gas-tight batch reaction flasks as a function of 2,4-D application rate. Reagent grade and uniformly  $^{14}\text{C}$ -ring-labeled 2,4-D (Sigma Chemical Co. St. Louis, MO) were dissolved in nutrient media (1 mL) and added to 50 g of soil (dry wt.) to yield a final concentration of 0, 10, 100 or 500 mg 2,4-D  $\text{kg}^{-1}$  and  $4.33 \times 10^4$  Bq  $\text{kg}^{-1}$  of  $^{14}\text{C}$ -2,4-D. All treatments received nutrient media which was formulated to provide a 110:10:1:1 C:N:P:S ratio, based on the amount of C added to the 500 mg 2,4-D  $\text{kg}^{-1}$  treatment (217 mg C  $\text{kg}^{-1}$ ). The media contained  $\text{NH}_4\text{NO}_3$  (12 mM),  $\text{KH}_2\text{PO}_4$  (1.13 mM),  $\text{K}_2\text{HPO}_4$  (1.13 mM),  $\text{NH}_4\text{SO}_4$  (2.0 mM),  $\text{H}_2\text{SO}_4$  (0.5 mM), KOH (0.25 mM),  $\text{MgCl}_2$  (0.05 mM),  $\text{CaCl}_2$  (0.05 mM),  $\text{FeCl}_2$  (2.5  $\mu\text{M}$ ) supplemented with 50  $\mu\text{L L}^{-1}$  of micronutrient solution (14). All batch experiments were conducted under unsaturated conditions with soil water contents ranging between 17 and 23 % (w/w,  $\sim 40$  % of saturation) and under continuous humidified air flow (2 mL  $\text{min}^{-1}$ ) venting through 0.5 M NaOH to trap  $^{14}\text{CO}_2$ . The trap solutions were changed periodically and one mL aliquots were analyzed for  $^{14}\text{CO}_2$  using scintillation analysis (Packard Tricarb CA2200 scintillation counter, Meriden, CT). After termination of the experiments (61-128 d, depending on treatments), subsamples of soil were used for molecular analysis, MPN determinations, and isolation of 2,4-D degrading bacteria. In addition, 1 g subsamples were combusted in a biological oxidizer (Model OX-300; R.J. Harvey Inst. Corp., Hillsdale, NJ) for analysis of residual  $^{14}\text{C}$ . Mass balance calculations based on  $^{14}\text{CO}_2$  evolved plus residual  $^{14}\text{C}$  yielded C recoveries ranging from 84.3 to 103.8 %. Each treatment was performed in duplicate or triplicate. The whole

experiment (referred to as Exp. #2) was repeated at 0, 10 and 500 mg 2,4-D kg<sup>-1</sup> using soil collected from the same location 1.5 y after the initial collection.

#### Enrichment of 2,4-D Degrading Microorganisms Under Transport Conditions

The development of 2,4-D degrading microbial communities was also studied under unsaturated transport conditions using polycarbonate columns (length = 275 mm, diameter = 35 mm) packed with a mixture of 5% soil (collected May, 1999) and 95 % autoclaved quartz sand (40-200 mesh, Fluka, Milwaukee, WI) to a bulk density of 1.15 g cm<sup>-3</sup>. The column apparatus was autoclaved prior to packing. Autoclaved influent was supplied to the top of the columns with a continuous flow pump set to deliver 1.55 mL h<sup>-1</sup> (pore water velocity = 6.6 mm h<sup>-1</sup>). To insure thorough aeration and maintain unsaturated flow within the columns, a peristaltic pump was attached to the bottom end cap and set to draw 100 mL h<sup>-1</sup> filter sterilized air (~ 0.7 mmole O<sub>2</sub> h<sup>-1</sup>) through the soil/sand matrix and nylon mesh screen at the bottom end cap. Nutrient media solution (ratios of C:N:P:S = 110:10:1:1 as described above) applied to the top of the columns percolated through the soil/sand matrix gravimetrically and exited the bottom of the columns along with the air stream. The volumetric water content ( $\theta_v$ ) of the soil/sand mixture was maintained at 0.24 cm<sup>3</sup> cm<sup>-3</sup> (~ 42 % of saturation). The input solution contained 276 mg 2,4-D L<sup>-1</sup> (10 mM C) with  $9.0 \times 10^4$  Bq L<sup>-1</sup> of <sup>14</sup>C-2,4-D. Mass balance was evaluated as a function of time by analyzing both total <sup>14</sup>C in column effluent and mineralized <sup>14</sup>C-2,4-D exiting the column as <sup>14</sup>CO<sub>2</sub> (0.5 M NaOH base trap) using liquid scintillation counting. Upon termination (22 d), the soil/sand matrix was mixed and subsamples used for molecular analysis and bacterial isolation. Total residual <sup>14</sup>C in the subsamples was measured by

combusting 1.0 g in a biological oxidizer, followed by liquid scintillation counting. Mass balance calculations for two replicate columns based on  $^{14}\text{C}$  eluted,  $^{14}\text{CO}_2$  evolved, and residual  $^{14}\text{C}$  yielded recoveries of 72.5 and 82.1%.

#### Enumeration and Isolation of 2,4-D Degrading Microorganisms

MPN determinations of 2,4-D degrading populations were performed after completion of batch experiments. A series of MPN tubes containing 5 mL of MMO basal salts medium (15), 100 mg 2,4-D  $\text{L}^{-1}$  and  $\sim 1.0 \times 10^5$  Bq  $\text{L}^{-1}$  of ring labeled  $^{14}\text{C}$ -2,4-D were inoculated with 10-fold serially diluted soil suspensions (50 mM phosphate, pH 7.0). Five sets of tubes per treatment replicate were incubated for 3 wks, then assayed for 2,4-D degradation by liquid scintillation. Tubes were scored positive when residual radioactivity of the suspension was less than  $5 \times 10^4$  Bq  $\text{L}^{-1}$  (half of the initial radioactivity).

Two methods were used to isolate 2,4-D degrading populations. In the first method, aliquots from the two most dilute positive MPN tubes from each microcosm replicate were plated onto R2A agar medium (Difco, Detroit, MI) supplemented with 100 mg 2,4-D  $\text{L}^{-1}$ . Selected colonies were streaked onto R2A agar containing 100 mg 2,4-D  $\text{L}^{-1}$ , restreaked for purification, then checked for 2,4-D degrading ability using the same protocol as described for the MPN method. In the second method, isolates were obtained by direct plating of serially diluted soil suspensions onto R2A agar plates (9). Colonies were picked from the most dilute colony-containing plates and tested for their ability to degrade 2,4-D in solution media as described above. By using both the MPN and direct

plating techniques, more than 100 isolates from each batch treatment and 50 isolates from the column experiment were obtained and tested for 2,4-D degradation.

#### Nucleic Acid Extraction and 16S rDNA Sequence Analysis

DNA was extracted from soils and isolates using the FastDNA SPIN Kit for Soil (Bio 101, Vista, CA) following the supplier's instructions. A 322 bp region within the 16S rRNA gene was amplified using the 1070 forward primer targeting the domain *Bacteria* (*E. coli* positions 1055-1070), and the 1392 reverse-GC primer targeting a universally conserved region (*E. coli* positions 1392-1406; 16). The 5' end of the reverse primer contained a 40 bp GC-rich clamp to facilitate analysis by denaturant gradient gel electrophoresis (DGGE; 16). PCR mixtures (50  $\mu$ L) contained 1-5  $\mu$ L template DNA (2-20 ng), 10 mM Tris-HCl (pH 8), 50 mM KCl, 0.1 % Triton X-100, 4.0 mM MgCl<sub>2</sub>, 200  $\mu$ M each dNTP, 0.5  $\mu$ M of each primer, and 1.25 U *Taq* DNA polymerase (Promega, Madison, WI). The thermal cycler protocol was 94 °C for 4 min, 30 cycles of 94 °C, 55 °C and 72 °C each for 45 sec, and a final 7 min extension period at 72 °C. DNA was quantified by electrophoresis in 3% agarose gels run with a Low DNA Mass Ladder (Gibco BRL, Grand Island, NY), stained with ethidium bromide, and photographed using UV transillumination. The amplified DNA fragments were analyzed by DGGE using a method modified from Muyzer et al. (17). PCR products were resolved using the DCode System (Bio-Rad, Hercules, CA) with gels consisting of 8% acrylamide and a 40 - 70% denaturing gradient of urea/formamide and electrophoresed at 60 V and 60 °C for 17 h. DGGE gels were stained with SYBR Green II (Molecular Probes, Eugene, OR) for 25 min and photographed using UV transillumination.

Selected DGGE bands were stabbed with a sterile pipette tip, rinsed in DNAase-free molecular biology grade water and used as template for PCR amplification and subsequent sequencing reactions. The cycle of stabbing, PCR, and DGGE was repeated until pure bands were obtained. Products were purified with a QIAquick PCR Purification Kit (Qiagen Inc., Valencia, CA) and sequenced using an ABI Prism BigDye Terminator Cycle Sequencing Ready Reaction Kit as described by the manufacturer (Perkin-Elmer, Foster City, CA). The DNA products were processed using an ABI Prism 310 capillary sequencer (Perkin-Elmer) and the resultant sequences aligned using Sequencher 3.1.1 (Gene Codes Corporation, Ann Arbor, MI). Phylogenetic information was obtained by comparing the nucleotide sequences with sequences found in the GenBank database using BLAST (18).

#### PCR Amplification and Sequencing of Near-Full Length 16S rRNA Genes

Genomic DNA extracted from each of the isolates was used as template for PCR. Primers for the initial PCR consisted of the *Bacteria*-specific primer Bac8 forward and the universal primer Univ1492 reverse. The amplified products were purified with a QIAquick PCR Purification Kit and used in a series of sequencing reactions with primers Bac8 forward, Univ1492 reverse, and internal primers derived from the probes described by Amann et al. (19). Sequencing reactions and analysis were conducted as described above. The resultant near-full length 16S rDNA sequences for the 2,4-D degrading isolates have been submitted to GenBank and assigned the accession numbers AY238498 – AY238507.

### PCR Amplification and Sequencing of *tfdA* Genes

The presence and diversity of *tfdA* genes in total bacterial DNA preparations from each of our isolates was examined by PCR amplification and sequencing using primers designed from consensus regions in the *tfdA* gene of *Ralstonia eutropha* JMP134 (pJP4) and *Burkholderia* strain RASC (9). The PCR reaction mixture included 2-20 ng of isolate DNA (1-5  $\mu$ L) and 0.5  $\mu$ M each of the forward and reverse primers. Other PCR ingredients as well as thermal cycler settings, and sequencing protocol were as described above with the exception of using an annealing temperature of 53° C. Comparisons of resultant sequences with sequences in the GenBank database were performed using BLAST (18) and the *tfdA* sequences were submitted to GenBank under the accession numbers AY238492-AY238497.

## Results and Discussion

### 2,4-D Degradation Under Batch and Transport Conditions

Repeated applications of 2,4-D to batch soil microcosms resulted in subsequent periods of rapid 2,4-D mineralization for all treatments (Fig. 5.1). An acclimation period of one to several 2,4-D applications was required prior to attaining repeatable cycles of rapid degradation. The first application of 2,4-D in the 10 mg kg<sup>-1</sup> treatment did not result in appreciable 2,4-D mineralization, possibly due to the sorption of 2,4-D by organic matter resulting in reduced bioavailability (20). Degradation of 2,4-D commenced about 4 d after initial application of 100 mg kg<sup>-1</sup>, while an even longer lag phase of more than 20 d was observed with the 500 mg kg<sup>-1</sup> treatment. The protracted lag phase observed for

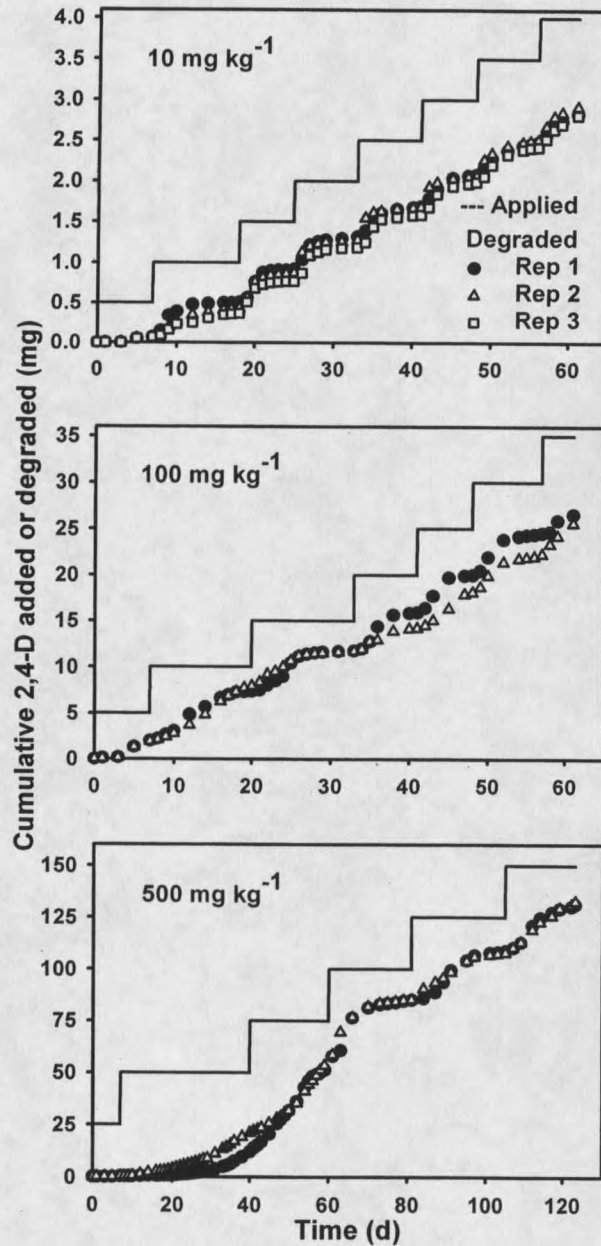


Figure 5.1. Degradation of 2,4-D in Exp. 1 measured as cumulative <sup>14</sup>CO<sub>2</sub> evolved from soil microcosms treated with repeated applications of 2,4-D. Vertical portions of the application curves indicate times when 0.5, 5.0, or 25.0 mg of 2,4-D were applied to the 10, 100, or 500 mg kg<sup>-1</sup> treatments, respectively.

the highest 2,4-D application rate suggested that there was significant selective pressure for microorganisms capable of degrading high concentrations of 2,4-D. The duplicate batch experiment conducted using a different soil sample from the same field site (Exp. #2) resulted in similar degradation patterns (data not shown). For all batch treatment replicates, more than 67 % of the total 2,4-D applied had been mineralized at the time of final sampling based on measurements of  $^{14}\text{CO}_2$  evolved.

Degradation of 2,4-D was also studied under transport conditions using replicate soil columns. Analysis of column effluent from both replicates indicated that nearly all of the applied 2,4-D was removed from solution by either sorption or degradation after 5 d (Fig. 5.2). After 22 d,  $62 \pm 5$  % of the total 2,4-D applied had been mineralized based on measurements of  $^{14}\text{CO}_2$  evolved.

#### MPN Determinations

Population densities of 2,4-D degrading microorganisms in batch microcosms were estimated using the MPN approach in liquid culture (Fig. 5.3). Linear regression analysis of the data showed that a high correlation existed between the numbers of 2,4-D-degraders measured by MPN and the 0, 10, and 100 mg 2,4-D  $\text{kg}^{-1}$  application rates ( $r^2 = 0.999$ ). A highly linear relationship ( $r^2 = 1.00$ ) between numbers of 2,4-D degraders (measured by MPN) and 2,4-D application rates ranging between 0 and 100 mg  $\text{kg}^{-1}$  was also observed by Ka et al. (8). In the current study, numbers of 2,4-D degraders measured by MPN reached a plateau with the 100 mg  $\text{kg}^{-1}$  application (Fig. 5.3). Using MPN estimates of cell numbers and maximum rates of 2,4-D degradation determined from maximum slopes of the curves shown in Figure 5.1, degradation rates calculated on a per

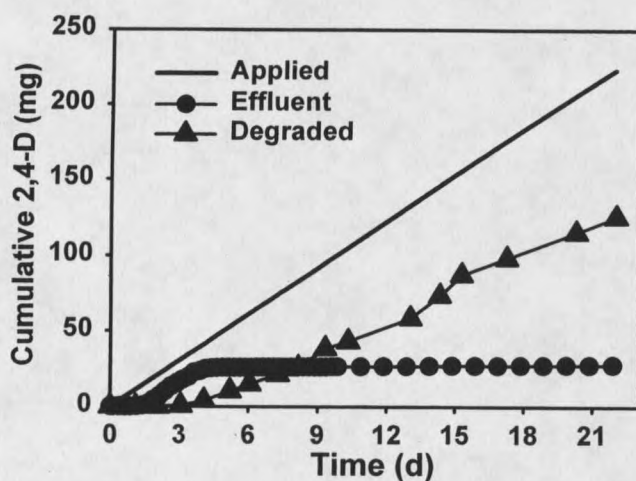


Figure 5.2. Cumulative 2,4-D applied, degraded, and recovered in the effluent from one of the replicate unsaturated soil/sand columns receiving 276 mg 2,4-D L<sup>-1</sup>.

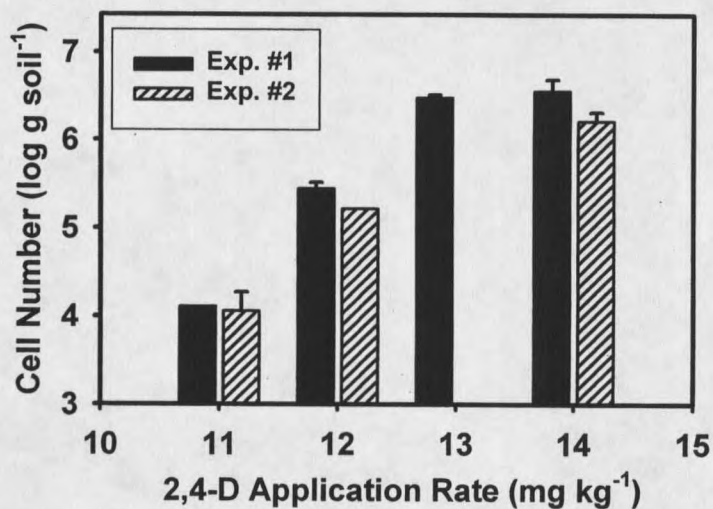


Figure 5.3. Numbers of 2,4-D degrading bacteria in batch soil microcosms treated with increasing rates of 2,4-D. Bars represent standard errors of treatment means measured using the MPN approach in liquid culture for replicate Exp. #1 and Exp. #2.

cell basis were determined to be 0.31, 0.35, and 0.93  $\text{pg min}^{-1} \text{ cell}^{-1}$  for the 10, 100, and 500  $\text{mg kg}^{-1}$  treatments, respectively.

### 2,4-D Degrading Isolates

A total of 73 2,4-D degrading isolates were obtained from the batch and column enrichments: 27 isolates were obtained from MPN tubes and 46 by direct plating of serial soil dilutions on non-selective R2A agar media (Table 5.1). The 2,4-D degrading isolates were grouped by migration of 16S rDNA fragments in DGGE gels, reducing the total number of different isolates to 10 (Table 5.1). Comparison of near-full length 16S rRNA sequences to sequences in the GenBank database revealed that the closest phylogenetic neighbor to the only 2,4-D degrading bacterium isolated from the 0  $\text{mg kg}^{-1}$  batch treatment was *Variovorax paradoxus*. Closest neighbors to isolates obtained from the 10  $\text{mg kg}^{-1}$  treatment belong to the genera *Variovorax*, *Achromobacter*, *Mesorhizobium*, *Arthrobacter*, *Bradyrhizobium*, and *Burkholderia*, which represented the most diverse group of isolates obtained from any of the batch or column treatments. Only one population, a *Bradyrhizobium*-like bacterium, was obtained from the 100  $\text{mg kg}^{-1}$  treatment, due in part to the limited attempts to obtain isolates from this treatment (i.e., the 100  $\text{mg kg}^{-1}$  treatment was only performed in Exp. 1 and the MPN approach was the only method used to retrieve isolates from this treatment). Characteristic to the *Bradyrhizobium* genus, this isolate grew much slower compared to other 2,4-D degrading isolates. Three related isolates (> 95.6 % similar in near full-length 16S rDNA sequence) were obtained from the 500  $\text{mg kg}^{-1}$  batch treatment, all with closest GenBank neighbors corresponding to *Burkholderia* sp. Comparison of isolates obtained from batch

TABLE 5.1. Phylogenetic affiliation of isolates cultivated from batch and column enrichments, and of prominent 16S rDNA bands obtained from the enrichments using DGGE. Isolates and corresponding DGGE bands were obtained from the treatments indicated with checkmark (✓). The specific method used to acquire isolates is indicated with an X. GenBank accession numbers for *tfdA* genes amplified from 2,4-D degrading isolates are provided.

Isolate no. (Accession no.)	DGGE Band no. <sup>a</sup> (Accession no.)	-----Nearest GenBank Neighbor-----  Species	% Identity	-----Treatment-----				Isolation		<i>tfdA</i> Accession no.	
				--Batch (mg/kg)---				---- Method ----			
				0	10	100	500	Column	MPN	Direct Plating	
55 (AY238498)		<i>Variovorax</i> sp.	99.4	✓	✓			✓	X	X	AY238494
92 (AY238499)	92	<i>Achromobacter</i> sp.	98.6		✓				X		AY238495
98 (AY238500)		<i>Mesorhizobium</i> sp.	100		✓				X		
108 (AY238501)		<i>Arthrobacter ramosus</i>	99.2		✓				X	X	
110 (AY238502)		<i>Arthrobacter oxydans</i>	99.6		✓				X		
1 (AY238503)		<i>Bradyrhizobium</i> sp.	98.3		✓	✓			X		
54 (AY238504)	54	<i>Burkholderia graminis</i>	99.8		✓		✓	✓	X	X	AY238496
13 (AY238505)		<i>Burkholderia</i> sp.	99.4				✓		X		AY238492
14 (AY238506)	14	<i>Burkholderia</i> sp.	97.2				✓		X		AY238493
80 (AY238507)	80	<i>Ralstonia campinensis</i>	99.7					✓		X	AY238497
DGGE bands with no corresponding isolates											
	2 (AY238508)	<i>Burkholderia</i> sp.	100				✓				
	3 (AY238509)	<i>Swingsiella fulva</i>	99.7				✓	✓			
	4 (AY238510)	<i>Swingsiella fulva</i>	99.3				✓				
	5 (AY238511)	<i>Methylobacterium extorquens</i>	99.7					✓			

<sup>a</sup> Band numbers correspond to DGGE band numbers in Figures 5.4 and 5.5, and those listed with a corresponding isolate are identical within the region sequenced.

treatments at 10 and 500 mg kg<sup>-1</sup> suggested a significant reduction in diversity of cultivated 2,4-D degrading populations at high 2,4-D concentrations, where the selection of *Burkholderia*-like organisms was favored.

Two 2,4-D degrading organisms were isolated via direct plating from column enrichments and their closest relatives were *Burkholderia graminis* and *Ralstonia campinensis* (Table 5.1). The *B. graminis*-like isolate obtained from column enrichments was identical (based on full length 16S rDNA) to one of the isolates obtained from the 10 and 500 mg kg<sup>-1</sup> batch microcosms. In addition, these *B. graminis* and *R. campinensis*-like isolates were 98.3 and 99.7 % identical respectively, to *B. terricola* and *R. campinensis* strains that became dominant members of the microbial community after 2,4-D amendment of Belgian soils (21, 22).

#### Molecular Analysis of Bacteria Selected Under Batch Conditions

Effects of 2,4-D concentration on microbial community structure were examined using PCR amplification and subsequent separation of 16S rDNA fragments with DGGE. Reproducible DGGE band profiles from replicate 0 mg kg<sup>-1</sup> treatments exhibited numerous 16S bands suggesting that many populations were present in soil not treated with 2,4-D. Visual inspection of 16S banding patterns did not reveal significant changes in community structure at 10 mg 2,4-D kg<sup>-1</sup>, with exception of a band appearing in one replicate of Exp. 2 (Fig. 5.4B), which comigrated with a 2,4-D degrading *B. graminis*-like isolate (band 54). At 100 mg 2,4-D kg<sup>-1</sup>, at least two bands increased in intensity for both replicates of Exp. 1 (bands 2 and 54 in Fig. 5.4A) indicating that selection pressure exerted by 2,4-D was significant at this concentration. These bands were purified and

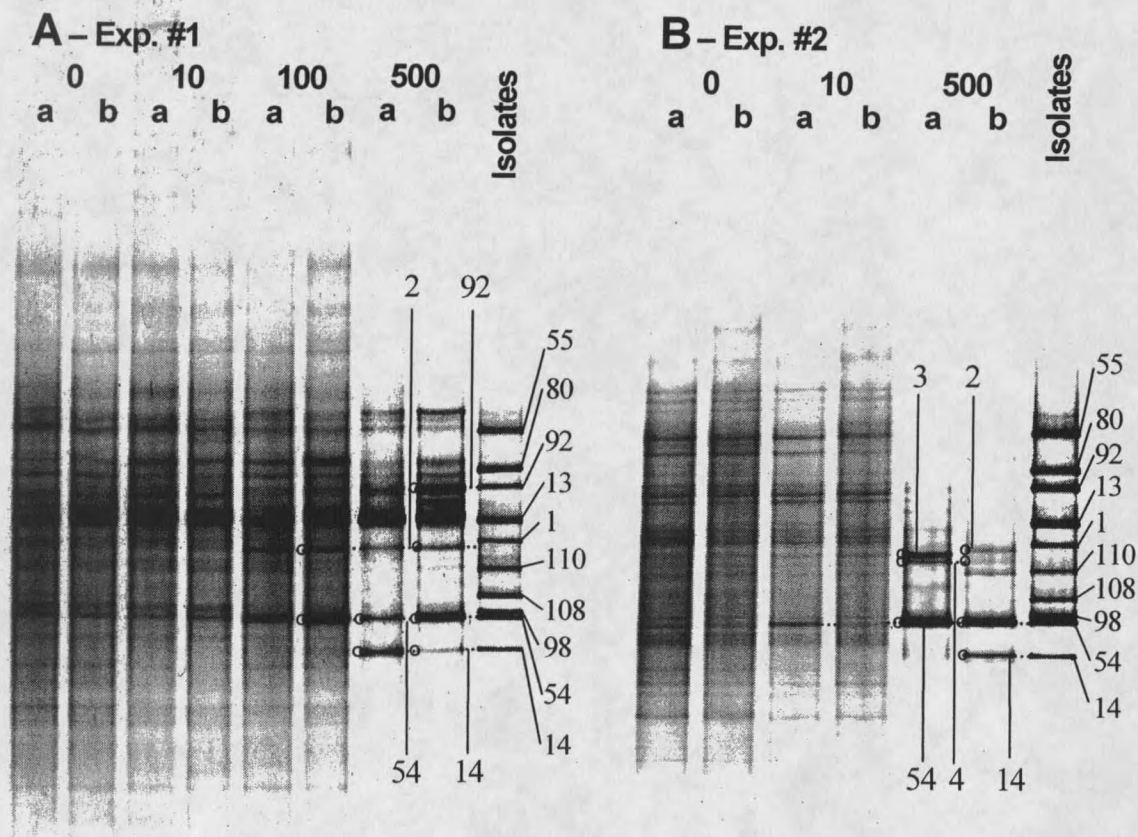


Figure 5.4. Denaturing gradient gel (40–70 %) of PCR-amplified 16S rDNA fragments from batch soil treatments receiving 0, 10, 100, or 500 mg 2,4-D kg<sup>-1</sup> (replicates a and b), and ladders of 2,4-D degrading isolates that were obtained during this study (see Table 5.1). Gradient gels A and B are results from Exp. #1 and Exp. #2 respectively, differing with regard to the use of soil inoculum that was collected from the same field site one and a half years apart. Isolate bands are numerically labeled at the right of each gel. Sequenced bands are designated with ○ and comigrating bands are delineated with dashed lines and numbered.

sequenced, then compared to isolate sequences and sequences in the GenBank database. Bands 2 and 54 were found to be 100 and 99.8 % similar, respectively, to sequences of *Burkholderia* sp. and *Burkholderia graminis* deposited in GenBank (Table 5.1). Interestingly, the sequence of band 2 was identical to *tfdA* harboring, 2,4-D degrading *Burkholderia* isolates obtained from a Michigan soil (3). In addition, band 54 comigrated with, and its DNA sequence was 100 % identical to the 2,4-D degrading *B. graminis*-like isolate obtained from the 10 and 500 mg 2,4-D kg<sup>-1</sup> treatments. Conversely, no isolate corresponding to band 2 was obtained in the current study.

The addition of 500 mg 2,4-D kg<sup>-1</sup> to batch enrichments resulted in significant changes in microbial community structure as evidenced by a reduction in the total number of 16S bands and increased intensity of several prominent bands compared to treatments at 0, 10 and 100 mg 2,4-D kg<sup>-1</sup> (Fig. 5.4A, B). The 16S sequences of prominent bands 14, 54, and 92 in Exp. 1 showed 97.2, 99.8 and 98.7 % similarity, respectively, to *Burkholderia* sp., *Burkholderia graminis*, and *Achromobacter xylosoxidans* sequences deposited in GenBank (Table 5.1), and were 100 % identical to three of the 2,4-D degrading isolates obtained from batch enrichments. Band 2, representing a 16S sequence 100 % similar to a 2,4-D degrading *Burkholderia* sp. (described above), was also observed in the 500 mg kg<sup>-1</sup> treatment. In addition, the 16S rDNA fragment from one of the 2,4-D degrading *Burkholderia* sp.-like isolates comigrated with a prominent band (band 13) present in nearly all of the Exp. 1 treatments. However, we were unable to purify and sequence this band from the experimental treatments. DGGE profiles of the 500 mg kg<sup>-1</sup> treatment from Exp. 2 also exhibited reduced band diversity compared to treatments at 0 and 10 mg 2,4-D kg<sup>-1</sup>. Two

bands (3 and 4) observed only in Exp. 2 were closely related to a *Swingsiella fulva* (Table 5.1). Although the band profiles observed at 500 mg 2,4-D kg<sup>-1</sup> in Exp. 2 (Fig. 5.4) were not identical to Exp. 1, bands 14 and 54 (corresponding to *Burkholderia sp.* and *B. graminis*-like isolates) were prominent in both experiments. These observations indicate that many of the populations enriched at the higher 2,4-D concentrations were *Burkholderia*-like, which are considered fast growing and very competitive at high substrate concentrations (23).

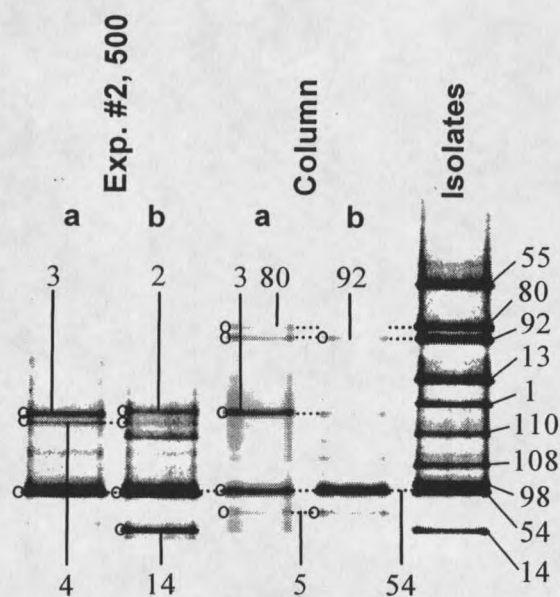


Figure 5.5. DGGE fingerprints of microbial communities assembled in soil columns receiving 276 mg 2,4-D L<sup>-1</sup> (replicate columns a and b) compared to profiles from the 500 mg kg<sup>-1</sup> treatment of Exp. #2 and 2,4-D degrading isolates (see Table 5.1). Isolate bands are numerically labeled at the right of the gel. Sequenced bands are designated with ○ and comigrating bands are delineated with dashed lines and numbered.

Molecular Analysis of Bacteria Selected  
Under Transport Conditions

16S rDNA fingerprints of bacterial communities enriched under transport conditions suggest strong selection pressure, similar to the reduced diversity observed in the 500 mg kg<sup>-1</sup> batch treatments of Exp. 2, which used the same soil inoculum (Fig. 5.5). In fact, the most prominent band consistently present in replicates of both the column and batch experiments (band 54, Fig. 5.5) was 100 % identical to the *B. graminis*-like 2,4-D degrading isolate. This was the only isolate obtained from both batch and column treated soils. The apparent predominance of this population in both the batch and transport treatments suggests that high concentrations of 2,4-D in either environment exert a strong selection pressure towards fast growing microorganisms, and that its competitiveness was not influenced by different physiochemical factors associated with each of these environments. Several bands were observed in column experiments that were not detected in batch vessels, including bands 5 and 80 (Fig. 5.5). No isolate was obtained that matched band 5 (99.7 % identical to *Methylobacterium extorquens*), however, band 80 comigrated with the 2,4-D degrading isolate (100 % identical) representing a *Ralstonia campinensis*-like population. The *R. campinensis*-like isolate was obtained only from column treatments, consequently, this population may be more adapted to transport environments. Conversely, bands 2, 4 and 14, representing *Burkholderia* and *Swingsiella*-like populations, were only observed under batch conditions. Although these results generally support the conclusion that different 2,4-D degrading communities are enriched under transport versus batch conditions, these distinctions were not entirely clear due to observed variability between treatment replicates. However, these results provide

evidence that differences in degradation behavior between batch and transport conditions may result from the selection of different bacterial populations, and that modeling efforts incorporating degradation rate terms determined under batch conditions should consider the possibility that different microbial populations may be present under transport conditions. Factors that may be important to selection of bacterial populations in transport versus batch environments include solute residence time and diffusional processes sensitive to pore water velocity, both of which affect the availability of 2,4-D and other nutrients important for microbial growth (11).

#### *tfdA* Harboring Isolates

Amplification of *tfdA* genes using primers designed from conserved regions of *tfdA* in pJP4 of *R. eutropha* strain JMP134 and *Burkholderia* strain RASC (9) generated products of the expected size for six of the ten 2,4-D degrading isolates. Sequencing of the PCR products revealed *tfdA* genes in the *B. graminis* and *R. campinensis*-like isolates that were identical to each other and 99 % identical to the sequence in *R. eutropha* strain JMP134 (accession no. M16730; designated type I *tfdA* by 24). The *tfdA* sequences found in the *V. paradoxus*, *Achromobacter xylosoxidans* and two *Burkholderia*-like isolates, 13 and 14, were identical to each other and 99 % identical to *tfdA* in *Burkholderia cepacia* (accession no. AF029344; type III *tfdA*). Currently, three groups of *tfdA* sequences are recognized, type I, II, and III, and intermediate sequences between these groups, except for minor bp differences have not been found (24). These observations suggest that the rate of horizontal transfer of *tfdA* genes among microorganisms is relatively high compared to the rate at which mutations may accumulate. Furthermore, the fact that six

isolates obtained in this study harbored either *tfdA* type I or type III genes with identical gene sequences, suggests that horizontal transfer of *tfdA* had recently occurred among these bacteria. Other studies have reported the conjugative transfer of plasmids encoding 2,4-D degradative genes to *Burkholderia* and *Ralstonia*-like populations after amendment with 2,4-D (21, 22, 25, 26).

No PCR product was observed from amplification of our slow-growing *Bradyrhizobium sp.*-like isolate using the *tfdA* primer set. However, the 16S rDNA sequence of this isolate was 97.4 % identical to a slow-growing, 2,4-D-degrading *Bradyrhizobium sp.* strain HW13 cultivated from a pristine buried Hawaiian soil (1). And recently, a novel 2,4-D catabolic pathway has been elucidated in this bacterium, encoding a very different 2,4-D dioxygenase, CadA, used in the first step of 2,4-D degradation (27). One possible explanation for the lack of *tfdA* product from our 2,4-D degrading *Bradyrhizobium*-like isolate is that it may carry *cad* type rather than *tfd* 2,4-D catabolic genes.

#### Diversity of 2,4-D Degrading Bacteria

In this study both cultivation-dependent and cultivation-independent methods were used to provide an in depth description of the microbial diversity associated with 2,4-D degradation in soil. A wide range of 2,4-D concentrations was used in these experiments (0 – 500 mg kg<sup>-1</sup>), encompassing application rates commonly used in agriculture (1 – 10 mg kg<sup>-1</sup>), and those often used for isolation of 2,4-D degraders (≥ 100 mg kg<sup>-1</sup>). Results from molecular analysis of 16S rRNA genes using DGGE showed that band profiles from the 10 mg 2,4-D kg<sup>-1</sup> treatment were essentially identical to profiles

from the 0 mg 2,4-D kg<sup>-1</sup> treatment. In contrast, cultivation efforts using MPN and direct plating indicated that the broadest diversity of 2,4-D degrading isolates was present in the 10 mg 2,4-D kg<sup>-1</sup> treatment. Evidently, the failure of DGGE to detect differences in microbial communities present in the 0 and 10 mg 2,4-D kg<sup>-1</sup> treatments was a consequence of the high apparent diversity of bacteria present in these treatments and/or insufficient 2,4-D concentrations to stimulate apparent increases in numbers of 2,4-D degrading organisms. Significant shifts in DGGE profiles were observed in soils treated with 100 and 500 mg 2,4-D kg<sup>-1</sup>, and sequencing of prominent bands revealed that the bacterial communities selected in these treatments were enriched in *Burkholderia*, *Achromobacter*, and *Swingsiella* type populations. Cultivation of 2,4-D degrading bacteria from these treatments yielded predominantly *Burkholderia* type populations.

Interestingly, 16S rDNA sequences of the 2,4-D degrading *B. graminis* and *R. campinensis*-like isolates obtained from the column treatments were close matches to 2,4-D degrading isolates obtained from a Belgium agricultural soil (> 98.3 % identity; 21, 22). DGGE profiles of the Belgian soil amended with 100 mg 2,4-D kg<sup>-1</sup> and an introduced pEMT1 donor *Pseudomonas* strain revealed significant shifts toward transconjugants that included *B. graminis* and *R. campinensis*-like populations. Studies by Newby et al. (25, 26) using soil from Arizona also showed that conjugation plays an important role in the selection of primarily *Burkholderia* and *Ralstonia* type 2,4-D degraders at high 2,4-D concentrations. Consequently, transfer of 2,4-D catabolic genes via conjugation may have been involved in the selection of 2,4-D degrading populations in the current study as well. The presence of identical type I *tfdA* sequences in both *B. graminis* and *R. campinensis*-like isolates supports this hypothesis.

Results from this study showed that shifts in the community structure of 2,4-D degrading bacteria occur at concentrations as low as  $10 \text{ mg 2,4-D kg}^{-1}$ , and that above this concentration, communities shift towards less diverse, faster-growing species that harbor *tfdA* genes. Additionally, results from this study showed that hydrodynamic environment influences the selection of 2,4-D degrading populations. Consequently, predictions of 2,4-D degradation under field transport conditions and at agriculturally relevant concentrations should utilize rate parameters derived from 2,4-D degrading populations selected under appropriate conditions.

## REFERENCES CITED

1. Kamagata, Y., R.R. Fulthorpe, K. Tamura, H. Takami, L.J. Forney, and J.M. Tiedje. 1997. Pristine environments harbor a new group of oligotrophic 2,4-dichlorophenoxyacetic acid-degrading bacteria. *Appl. Environ. Microbiol.* 63:2266-2272.
2. Fulthorpe, R.R., A.N. Rhodes, and J.M. Tiedje. 1996. Pristine soils mineralize 3-chlorobenzoate and 2,4-dichlorophenoxyacetate via different microbial populations. *Appl. Environ. Microbiol.* 62:1159-1166.
3. Tonso, N.L., V.G. Matheson, and W.E. Holben. 1995. Polyphasic characterization of a suite of bacterial isolates capable of degrading 2,4-D. *Microbial Ecol.* 30:1-22.
4. Ka, J.O., W.E. Holben, and J.M. Tiedje. 1994. Genetic and phenotypic diversity of 2,4-Dichlorophenoxyacetic Acid (2,4-D)-degrading bacteria isolated from 2,4-D-treated field soils. *Appl. Environ. Microbiol.* 60:1106-1115.
5. Sandmann, E., M.A. Loos, and L.P. Van Dyke. 1988. Microbial degradation of 2,4-dichlorophenoxyacetic acid in soil. *Rev. Environ. Contamin. Tox.* 101:1-53.
6. Dunbar, J., S. White, L. Forney. 1997. Genetic diversity through the looking glass: effect of enrichment bias. *Appl. Environ. Microbiol.* 63:1326-1331.
7. Xia, X., J Bollinger, and A. Ogram. 1995. Molecular genetic analysis of the response of three soil microbial communities to the application of 2,4-D. *Mol. Ecol.* 4:17-28.
8. Ka, J.O., P. Burauel, J.A. Bronson, W.E. Holben, and J.M. Tiedje. 1995. DNA probe analysis of microbial community selected in field by long-term 2,4-D application. *Soil Sci. Soc. Am. J.* 59:1581-1587.
9. Hogan, D.E., D.H. Buckley, C.H. Nakatsu, T.M. Schmidt, and R.P. Hausinger. 1997. Distribution of the *tfdA* gene in soil bacteria that do not degrade 2,4-dichlorophenoxyacetic acid (2,4-D). *Microbial Ecol.* 34:90-96.
10. Estrella, M.R., M.L. Brusseau, R.S. Maier, I.L. Pepper, P.J. Wierenga, and R.M. Miller. 1993. Biodegradation, sorption, and transport of 2,4-dichlorophenoxyacetic acid in saturated and unsaturated soils. *Appl. Environ. Microbiol.* 59:4266-4273.
11. Langner, H.W., W.P. Inskeep, H.M. Gaber, W.L. Jones, B.S. Das, and J.M. Wraith. 1998. Pore water velocity and residence time effects on the degradation of 2,4-D during transport. *Environ. Sci. Technol.* 32:1308-1315.

12. Suzuki, M.T. and S.J. Giovannoni. 1996. Bias caused by template annealing in the amplification of mixtures of 16S rRNA genes by PCR. *Appl. Environ. Microbiol.* 62:625-630.
13. Nelson, D.W. and L. E. Sommers. 1982. Total carbon, organic carbon and organic matter. In Page AL, ed, *Methods of Soil Analysis, Part 2, Chemical and Microbiological Properties*. American Society of Agronomy, Madison, WI, USA, pp 539-579.
14. Skerman, V.B.D. 1967. *A guide to the identification of the genera of bacteria*. Baltimore, The Williams and Wilkins Co.
15. Holben, W.E., B.M. Schroeter, V.G.M. Calabrese, R.H. Olsen, J.K. Kukor, V.O. Biederbeck, A.E. Smith, and J.M. Tiedje. 1992. Gene probe analysis of soil microbial populations selected by amendment with 2,4-Dichlorophenoxyacetic Acid. *Appl. Environ. Microbiol.* 58:3941-3948.
16. Ferris, M.J., G. Muyzer, and D.M. Ward. 1996. Denaturing gradient gel electrophoresis profiles of 16S rRNA-defined populations inhabiting a hot spring microbial mat community. *Appl. Environ. Microbiol.* 62:340-346.
17. Muyzer, G., E.C. de Waal, and A.G. Uitterlinden. 1993. Profiling of complex microbial populations by denaturing gradient gel electrophoresis analysis of polymerase chain reaction-amplified genes encoding for 16S rRNA. *Appl. Environ. Microbiol.* 59:695-700.
18. Altschul, S.F., T.L. Madden, A.A. Schaffer, J. Zhang, Z. Zhang, W. Miller, and D.J. Lipman. 1997. Gapped BLAST and PSI-BLAST: a new generation of protein database search programs. *Nucleic Acid Res.* 25:3389-3402.
19. Amann, R.I., W. Ludwig, and K.H. Schleifer. 1995. Phylogenetic identification and in situ detection of individual microbial cells without cultivation. *Microbiol. Rev.* 59:143-169.
20. Greer, L.E. and D.R. Shelton. 1992. Effect of inoculant strain and organic matter content on kinetics of 2,4-dichlorophenoxyacetic acid degradation in soil. *Appl. Environ. Microbiol.* 58:1459-1465.
21. Dejonghe, W., J. Goris, S. El Fantroussi, M. Hofte, P. De Vos, W. Verstraete, and E.M. Top. 2000. Effect of dissemination of 2,4-dichlorophenoxyacetic acid (2,4-D) degradation plasmids on 2,4-D degradation and on bacterial community structure in two different soil horizons. *Appl. Environ. Microbiol.* 2000 66:3297-304.

22. Goris J., W. Dejonghe, E. Falsen, E. De Clerck, B. Geeraerts, A. Willems, E.M. Top, P. Vandamme, and P. De Vos. 2002. Diversity of transconjugants that acquired plasmid pJP4 or pEMT1 after inoculation of a donor strain in the A- and B-horizon of an agricultural soil and description of *Burkholderia hospita* sp. nov. and *Burkholderia terricola* sp. nov. Syst. Appl. Microbiol. 25:340-52.
23. Friedrich, M., R.J. Grosser, E.A. Kern, W.P. Inskeep, and D.M. Ward. 2000. Effect of model sorptive phases on phenanthrene biodegradation: molecular analysis of enrichments and isolates suggests selection based bioavailability. Appl. Environ. Microbiol. 66:2703-2710.
24. McGowan, C., R. Fulthorpe, A. Wright, and J.M. Tiedje. 1998. Evidence for interspecies gene transfer in the evolution of 2,4-Dichlorophenoxyacetic acid degraders. Appl. Environ. Microbiol. 64:4089-4092.
25. Newby D.T., K.L. Josephson, and I.L. Pepper. 2000. Detection and characterization of plasmid pJP4 transfer to indigenous soil bacteria. Appl. Environ. Microbiol. 2000 66:290-296.
26. Newby, D.T., T.J. Gentry, and I.L. Pepper. 2000. Comparison of 2,4-dichlorophenoxyacetic acid degradation and plasmid transfer in soil resulting from bioaugmentation with two different pJP4 donors. Appl. Environ. Microbiol. 66:3399-3407.
27. Kitagawa, W., S. Takami, K. Miyauchi, E. Masai, Y. Kamagata, J.M. Tiedje, and M. Fukuda. 2002. Novel 2,4-Dichlorophenoxyacetic Acid degradation genes from oligotrophic *Bradyrhizobium* sp. strain HW13 isolated from a pristine environment. J. Bacteriol. 184:509-518.

## CHAPTER 6

## SUMMARY

The primary goal of my research was to identify and characterize the microbial populations responsible for transformations of As and 2,4-D in soils and waters. Chemical, spectroscopic, and microscopic techniques were used to characterize the aqueous and solid phase geochemistry of soils, mine tailings, and a geothermal spring. The potential role of specific microbial populations in these systems was examined using cultivation-independent molecular methods coupled with either cultivation and characterization of pure culture isolates, or inference of physiological characteristics from closely related cultured microorganisms. Four separate investigations were conducted using these approaches: two studies focused on As transformations in soils and mine tailings, one study focused on geochemical cycling in a thermal spring, and one study evaluated the fate of 2,4-D in soil systems.

The contaminants As and 2,4-D were used in these studies because of their classification as carcinogens, high risk for contaminating surface and ground waters, and because their chemistry in the environment is thought to be largely mediated by microorganisms. Arsenic is an acutely toxic metalloid, which accumulates in the environment via both natural and anthropogenic pathways. 2,4-D is a chlorinated aromatic compound utilized extensively throughout the world as a broadleaf herbicide. Understanding the processes that control the fate and transport of these contaminants is critical for intelligent management and restoration of the environment.

The microbial reduction of As(V) to As(III) and the subsequent effects on As mobilization in contaminated mine tailings was examined under transport conditions (Chapter 2). Column experiments were designed to observe relationships among pH (limed vs unlimed treatments), redox potential (Pt-electrode), and mobilization of As. The role of dominant microbial populations in the columns was determined using molecular analysis and traditional isolation methods. Liming increased pH values from approximately 4 to 8, resulting in a five-fold increase in total As eluted from sterile columns. Elution of As from limed columns was further enhanced by microbial activity. Arsenite was the predominant As species eluted from oxic, nonsterile columns. Conversely, in sterile treatments, As(V) was the predominant valence state in column effluent. Denaturing gradient gel electrophoresis (DGGE) coupled with sequence and phylogenetic analysis of 16S rRNA gene segments revealed that liming of the mine tailings stimulated specific *Caulobacter*, *Sphingomonas*, and *Rhizobium*-like populations. Pure culture isolates of these bacteria demonstrated the ability to rapidly reduce As(V) in aerated serum bottles. An intracellular As detoxification pathway was implicated in the reduction of As(V) by these isolates. Currently, nearest relatives of these organisms that have been shown to harbor homologs of As(V) reductase genes (*arsC*) include *Bradyrhizobium* and *Pseudomonas* species (1, 2). These results indicate that microbial reduction of As(V) in As-contaminated soils may occur under aerobic conditions over relatively short time scales, resulting in enhanced As mobilization.

The microbial populations responsible for the oxidation and reduction of As were also examined in unsaturated (aerobic) Madison River Valley soil treated with 75  $\mu\text{M}$

As(III) or 250  $\mu\text{M}$  As(V) (Chapter 3). Arsenite was rapidly oxidized to As(V) via microbial activity, whereas no apparent reduction of As(V) was observed in the column experiments. Eight aerobic heterotrophic bacteria with varying As redox phenotypes were isolated from the same columns. Three isolates, identified as *Agrobacterium tumefaciens*-, *Pseudomonas fluorescens*-, and *Variovorax paradoxus* -like organisms (based on 16S sequence), were As(III) oxidizers and all were detected in community DNA fingerprints generated by PCR coupled with DGGE. The five other isolates were identified (16S gene sequence) as *A. tumefaciens*, *Flavobacterium sp.*, *Microbacterium sp.*, and two *Arthrobacter sp.*-like organisms and shown to rapidly reduce As(V) under aerobic conditions. Although the two *A. tumefaciens* -like isolates exhibited opposite As redox activity, their 16S rDNA sequences (~1400 bp) were 100% identical. The results support the hypothesis that bacteria capable of either oxidizing As(III) or reducing As(V) coexist and are ubiquitous in soil environments, suggesting that the relative abundance and metabolic activity of specific microbial populations plays an important role in the speciation of inorganic As in soil pore waters.

The geothermal source waters of acid-sulfate-chloride (ASC) springs in Yellowstone National Park support microbial mats composed of diverse microorganisms thriving under conditions of low pH (~ 3), high temperatures, millimolar concentrations of  $\text{SO}_4^{2-}$  and  $\text{Cl}^-$ , and high levels of inorganic toxins including As. The study presented in Chapter 4 was conducted to further describe these unique biogeochemical systems and to elucidate which microbial populations were associated with the rapid rates of As(III) oxidation and the formation of As-rich, HFO mats. To accomplish these goals, flow from

a small ASC spring was redirected and monitored over 103 days for both aqueous and solid phase geochemistry. Successional changes in microbial communities colonizing the stream channel were monitored using DGGE and sequence analysis of 16S rDNA fragments. The rate of microbial As(III) oxidation was essentially 0 immediately after spring redirection. In conjunction with microbial mat development, As(III) oxidation increased to some of the highest rates observed in nature by day 103 (rate constant ( $k$ ) =  $5.0 \text{ min}^{-1}$ , half-life = 0.14 min at 11 m). The initial As(III) oxidation correlated with the appearance of three *Hydrogenobaculum*-like populations, which are all close relatives of a *Hydrogenobaculum*-like isolate (H55) shown to be capable of oxidizing As(III) (3). The formation of an As-rich HFO brown mat was correlated with the detection of *Thiomonas*, *Acidimicrobium*, and *Metallosphaera* -like populations. Phylogenetic inference and the geochemical environment in which these organisms were detected suggests that these three populations are Fe-oxidizers which actively form extracellular HFO crusts (4 - 6). Closely related *Thiomonas* sp. have also been shown to oxidize As(III) via an apparent detoxification mechanism (4). Several other 16S sequences detected in the HFO microbial mat were not closely related to previously characterized organisms (< 90 %). In such cases, limited insight is available to suggest potential function of these organisms *in situ* and their physiology can only be inferred from the chemical environment which they occupy.

The final study presented in this dissertation (Chapter 5), coupled the use of cultivation-independent molecular techniques with traditional isolation and enumeration methods to examine the effect of 2,4-D application rate on the diversity of 2,4-D

degrading bacteria under batch and transport conditions. Fingerprints of microbial communities established under increasing concentrations of 2,4-D (0 – 500 mg kg<sup>-1</sup>) in batch microcosms were obtained using DGGE of 16S rRNA gene segments. While a 2,4-D concentration of at least 100 mg kg<sup>-1</sup> was required to obtain apparent shifts in the community structure of batch microcosms, the greatest impact of 2,4-D concentration occurred in the 500 mg kg<sup>-1</sup> treatment, resulting in significantly reduced diversity of the dominant populations detected by DGGE. Sequence analysis of prominent DGGE bands revealed that the 2,4-D degrading community selected at high concentrations was predominantly composed of *Burkholderia*-like populations, which harbored homologs of *tfdA* genes of *Ralstonia eutrophus* JMP134 (type I) and *Burkholderia cepacia* (type III). Only three of the ten different 2,4-D degrading isolates obtained by cultivation using either liquid or agar media appeared to be dominant in the microcosms based on comparisons of DGGE band positions and DNA sequence analysis. DGGE profiles of bacterial communities assembled under transport conditions receiving 276 mg L<sup>-1</sup> 2,4-D resembled those enriched in batch microcosms treated with 500 mg kg<sup>-1</sup> 2,4-D. However, consistent differences in populations enriched in batch versus transport microcosms were observed, suggesting that modeling efforts incorporating degradation terms determined in batch culture must consider that variability in degradation behavior may result from the selection of different bacterial populations under transport conditions.

The four studies presented in chapters two through five showed that coupling molecular techniques with traditional cultivation and or chemical monitoring can be used to link microbial populations with their function in natural or enrichment environments.

These complimentary tools can be used for evaluating the role of specific microorganisms in natural or synthetic systems and for virtually any chemical process that microorganisms mediate. For example, bioreactors are used by industry to detoxify and transform chemicals. While many microorganisms may grow in bioreactors, only certain species may conduct the desired chemical transformation. Molecular analysis of community shifts in conjunction with chemical analysis can be used to elucidate which microbial populations are involved in the chemical transformation. Once important populations are identified, their isolation and characterization may lead to the development of more effective methods for maintaining their growth in the bioreactor.

Although 16S rDNA-based sequence analysis of soil and water samples can be used to identify relevant populations under different conditions, there are limitations to the application of this strategy. The potential problem lies in the use of 16S rRNA gene sequences alone to associate populations with specific functions. For example, the isolation of both As(III) oxidizing and As(V) reducing *A. tumefaciens* strains from the same soil column enrichment (Chapter 3) showed that the ability to either oxidize As(III) or reduce As(V) is variable even among strains with identical 16S sequences that proliferate under the same environmental conditions. Furthermore, although two *Pseudomonas fluorescens*-like isolates obtained from mine tailings (Chapter 2) and Madison River Valley soil (Chapter 3) were more than 99 % identical to each other at the 16S level, one isolate reduced As(V) while the other isolate oxidized As(III) under similar culture conditions. In another study, closely related (>99 % similarity) *Thiomonas* sp. strains (B1, B2, and B3) isolated from acid mine drainage exhibited different As(III)

oxidation capabilities (4). Because of such phenotypic variation within similar organisms, phylogenetic identification of microorganisms based on 16S rRNA sequence analysis may not be sufficient to predict the functions of specific bacterial populations. Thus, additional methods are needed to more precisely differentiate among physiologically distinct populations. One possible solution is to include the intragenic spacer (ITS) region along with the 16S rRNA gene in the sequencing effort. This region lies between the 16S and 23S rRNA genes and has greater sequence variability than the 16S (7). Thus, sequencing of the ITS region should improve the ability to differentiate among distinct populations (7). However, identification of populations using ITS-16S sequences may not be sufficient to identify functional attributes, especially if the functional genes of interest are rapidly transferred to some members of a population and not others (e.g., pJP4 transfer to microorganisms in 2,4-D amended soil, 8).

Elucidating the function and ecological role of specific populations within microbial communities is currently one of the central issues in environmental microbiology/microbial ecology. In general, ecological studies have been community oriented; i.e., measurable chemical transformations have been determined as a function of whole communities. The contribution of individual species to these processes has been difficult to access due to the inability to culture many members of the community, the difficulty in linking cultured isolates with dominant populations *in situ*, and the enormous diversity of microorganisms often observed in natural systems. The research presented in this dissertation was successful in overcoming these problems by working with model communities that were significantly less diverse than those in most natural systems.

Simple microbial communities allowed for the clear resolution of most DGGE bands and was likely one reason why many of the dominant populations could be easily isolated. This approach was taken so that we could begin to understand the relationship of specific organisms with their geochemical environment and their potential relationship with other cohabitating microorganisms.

Environmental microbiologists will rely on advanced molecular techniques to describe the function of specific populations in more complex systems. Bacterial Artificial Chromosomes (BACs) will continue to be used to directly link 16S rDNA sequences to functional genes in total community DNA (9). The key to the technique is that relatively large DNA inserts, > 300,000 kb can be stably maintained in *E. coli* transformants (10). The use of BACs for environmental analysis will become more feasible as the cost of sequencing declines due to the fact that a large amount of DNA sequence data is generated during analysis. Promising mRNA based techniques include high throughput sequence probing using microarrays (11), and fluorescent *in situ* hybridization (FISH) using highly sensitive probes and detection (12). Both these techniques rely on knowledge of gene sequences however, and will become more useful as the functions of novel genes are elucidated and the diversity of known genes are sequenced and added to databases.

Understanding patterns and similarities in complex biological systems as a function of geochemical environment continues to be an important thrust in environmental microbiology. The research presented in this dissertation serves as an important contribution to our knowledge of geochemical conditions that are associated

with the distribution, diversity, and divergence of genomes. These efforts also provide additional information on the usefulness of coupling geochemical analysis of environments with phylogenetic inference. Furthermore, geochemical and phylogenetic information obtained from Succession Spring in Yellowstone National Park will provide an important basis for developing cultivation strategies aimed at isolating novel microorganisms from this unique habitat.

## REFERENCES CITED

1. Kaneko, T., Y. Nakamura, S. Sato, K. Minamisawa, T. Uchiumi, S. Sasamoto, A. Watanabe, K. Idesawa, M. Iriguchi, K. Kawashima, M. Kohara, M. Matsumoto, S. Shimpo, H. Tsuruoka, T. Wada, M. Yamada, and S. Tabata. 2002. Complete genomic sequence of nitrogen-fixing symbiotic bacterium *Bradyrhizobium japonicum* USDA110. *DNA Res.* 9:189-197.
2. Diorio, C., J. Cai, J. Marmor, R. Shinder, and M.S. DuBow. 1995. An *Escherichia coli* chromosomal *ars* operon homolog is functional in arsenic detoxification and is conserved in gram-negative bacteria. *J. Bacteriol.* 177:2050-2056.
3. Donahoe-Christiansen, J. 2002. Arsenite oxidation by a *Hydrogenobaculum* sp. isolated from Yellowstone National Park. Master Thesis. Montana State University.
4. Bruneel, O., J.C. Personne, C. Casiot, M. Leblanc, F. Elbaz-Poulichet, B.J. Mahler, A. Le Fleche, and P.A.D. Grimont. 2003. Mediation of arsenic oxidation by *Thiomonas* sp. in acid-mine drainage (Carnoules, France). *J. Appl. Microbiol.* 95:492-499.
5. Johnson, D.B., N. Okibe, and F.F. Roberto. 2003. Novel thermo-acidophilic bacteria isolated from geothermal sites in Yellowstone National Park: Physiological and phylogenetic characteristics. *Arch. Microbiol.* 180:60-68.
6. Peeples, T.L., and R.M. Kelly. 1995. Bioenergetic response of the extreme thermoacidophile *Metallosphaera sedula* to thermal and nutritional stress. *Appl. Environ. Microbiol.* 61:2314-2321.
7. Ferris, M.J., M. Kuhl, A. Wieland, and D.M. Ward. 2003. Cyanobacterial ecotypes in different optical microenvironments of a 68° hot spring mat community revealed by 16S-23S rRNA internal transcribed spacer region variation. *Appl. Environ. Microbiol.* 69:2893-2898.
8. Newby, D.T., K.L. Josephson, and I.L. Pepper. 2000. Detection and characterization of plasmid pJP4 transfer to indigenous soil bacteria. *Appl. Environ. Microbiol.* 66:290-296.
9. Beja, O., M.T. Suzuki, E.V. Koonin, L. Aravind, A. Hadd, L.P. Nguyen, R. Villacorta, M. Amjadi, C. Garrigues, S.B. Jovanovich, R.A. Feldman, and E.F. DeLong. 2000. Construction and analysis of bacterial artificial chromosome libraries from a marine microbial assemblage. *Environ. Microbiol.* 2:516-529.
10. Zimmer R., and A.M.V. Gibbins. 1997. Construction and characterization of a large-fragment chicken bacterial artificial chromosome library. *Genomics.* 42:217-226.

11. Greer, C.W., L.G. Whyte, J.R. Lawrence, L. Masson, and R. Brousseau. 2001. Genomic technologies for environmental science. *Environ. Sci. Technol.* 35:364A-370A.
12. Bakermans, C. and E.L. Madsen. 2002. Detection in coal tar waste-contaminated groundwater of mRNA transcripts related to naphthalene dioxygenase by fluorescent in situ hybridization with tyramide signal amplification. *J. Microbiol. Methods.* 50:75-84.

MONTANA STATE UNIVERSITY - BOZEMAN



3 1762 10465608 5